

Cover Page



Universiteit Leiden



The following handle holds various files of this Leiden University dissertation:

<http://hdl.handle.net/1887/71375>

Author: Pomeran, M. van

Title: Through the magnifying glass: The effects of size and shape on the uptake, biodistribution and (eco)toxicity of nanoparticles

Issue Date: 2019-04-17

Through the magnifying glass

**The effects of size and shape on the uptake,
biodistribution and (eco)toxicity of nanoparticles.**

Marinda van Pomerén

©2019 Marinda van Pomerén

Through the magnifying glass: The effects of size and shape on the uptake, biodistribution and (eco)toxicity of nanoparticles.

Ph.D. thesis Leiden University, The Netherlands

ISBN: 978-94-6380-253-6

All rights reserved. No part of this thesis may be reproduced, stored in a retrieval system, or transmitted in any form or by any means, without the prior written permission of the copyright holder

Cover design: Marinda van Pomerén, original image by Lynn Ketchum, courtesy of Oregon State University

Photos: Marinda van Pomerén

Printed by: Proefschriftmaken.nl || www.proefschriftmaken.nl

Through the magnifying glass

**The effects of size and shape on the uptake,
biodistribution and (eco)toxicity of nanoparticles.**

Proefschrift

ter verkrijging van

de graad van Doctor aan de Universiteit Leiden,

op gezag van de Rector Magnificus prof. mr. C.J.J.M. Stolker,

volgens besluit van het College van Promoties

te verdedigen op woensdag 17 april 2019

klokke 15.00 uur

door

Marinda van Pomerén

Geboren te Amstelveen, Nederland

In 1989

Promotiecommissie:

Promotors: Prof. Dr. W.J.G.M. Peijnenburg

Prof. Dr. ir. M.G. Vijver

Overige leden: Prof. Dr. A. Tukker (Universiteit Leiden)

Prof. Dr. P.M. van Bodegom (Universiteit Leiden)

Prof. Dr. H.P. Spaink (Universiteit Leiden)

Dr. J. Legradi (Vrije Universiteit Amsterdam)

Dr. W.H. de Jong (RIVM)

Contents

Chapter 1	9
General Introduction	
Chapter 2	31
Exploring uptake and biodistribution of polystyrene (nano)particles in zebrafish embryos at different developmental stages	
Chapter 3	51
The biodistribution and immuno-responses of differently shaped non-modified gold particles in zebrafish embryos	
Chapter 4	75
A novel experimental and modelling strategy for nanoparticle toxicity testing enabling the use of small quantities	
Chapter 5	101
The impacts of interactions between TiO ₂ nanoparticles and differently dissolving nanoparticles on mixture toxicity	
Chapter 6	135
Discussion	
Summary	147
Samenvatting	151
Curriculum Vitae	153
Publication list	154
Acknowledgements	155

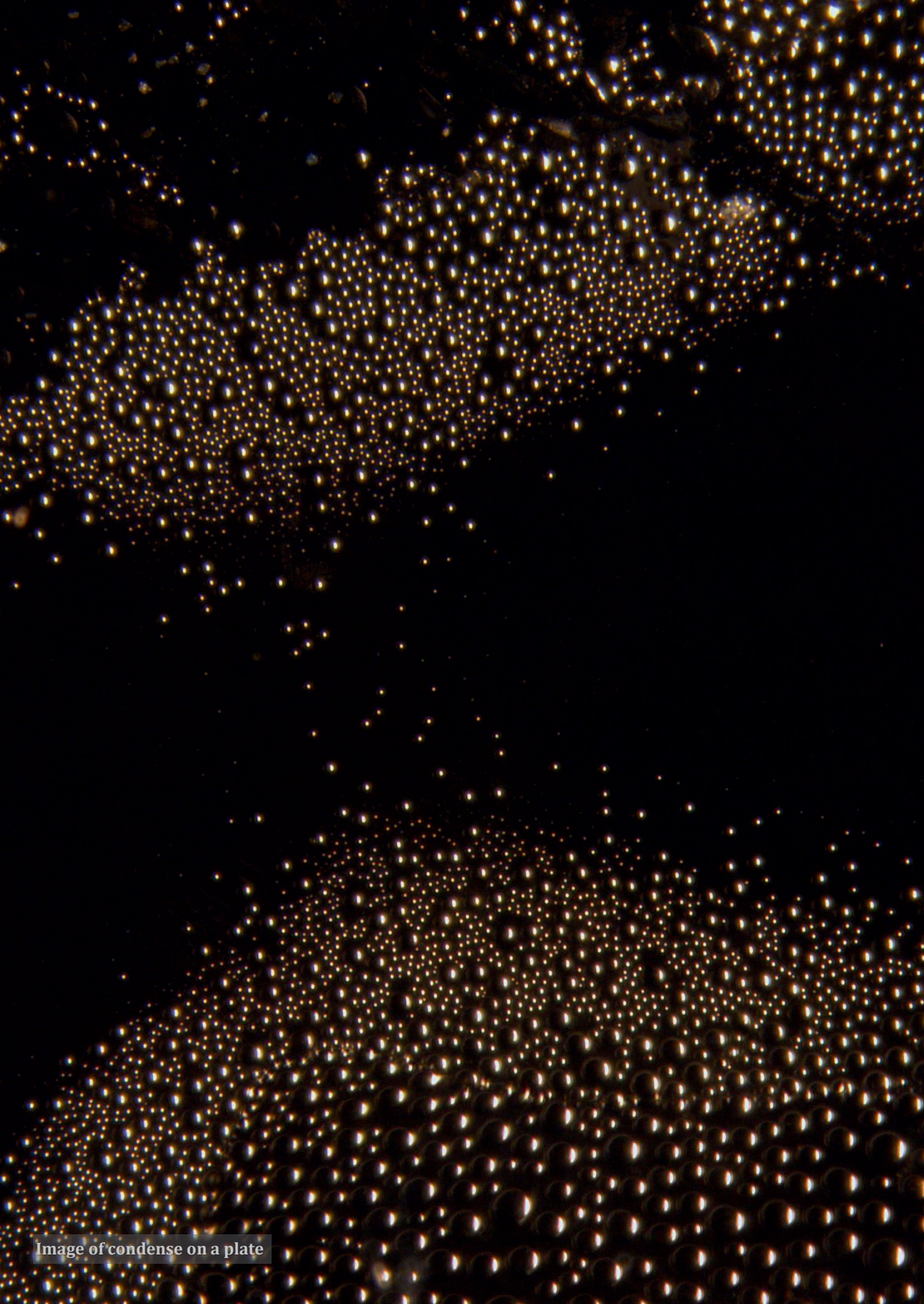


Image of condense on a plate

Chapter 1

General Introduction

Nanoparticles: what they are and where they come from

Nanomaterials have been present since the beginning of the Earth. Main sources of naturally occurring colloids (suspensions of nanoparticles) are dust of volcano eruptions and bush fires, and corrosion of river beddings and sea floors. In early civilization, men began to use these extraordinary and very small particles, without extensive knowledge about their characteristics. In the fourth century A.D. the ancient roman glass industry produced for instance the famous Lycurgus Cup: a ruby red cup colored with colloidal gold¹. In the 19th century, modern technologies such as microscopes allowed for the rise of the nanotechnology: the production of well-defined and well-characterized nanomaterials². Through the development of advanced techniques, the production of colloids started to become more sophisticated.

In nanotechnology, nanomaterials are defined as being materials that have one or more dimension within the 1 to 100 nm size range³. More specifically, if the nanomaterial has three dimensions within the nano range, it is classified as nanoparticle (NP)⁴. Although these definitions remained the same, different generations of nanotechnologies have been developed. The first generation of technologies (pre 2005) can be found on the market, with products containing particles either as individual nanomaterials or as mixtures with other materials. Examples of products are antibacterial socks (silver)⁵, sunscreen (titanium dioxide and zinc oxide)⁵ and solar cells (e.g. copper and silicon)⁶. Because they are widely used on the market, most research has been done and is still being done on these particles. Technologies developed from 2005 until 2010 are considered second generation: functional structures of products as based on nanoscale elements. The third generation technologies (2010-2015) start to layer their materials, making a combination of macro-, meso-, micro- and nano-scales. This can also be in a three-dimensional setting. Finally, the fourth generation (from 2015 onward) focuses on so called 'molecular manufacturing': multi-functionality and control of function at molecular level.⁵

Due to their unique properties, nanomaterials have gained interest from producers and entered the global market. Potentials that are ascribed to nanotechnology are: stronger, more efficient, cleaner and compact materials that allow for small yet complex products⁵. Currently, nanomaterials are used in numerous products, although exact numbers are lacking. In 2014, it was estimated that the market contains more than 13000 nano-based products⁷. The variety of products is large,

ranging from sunscreens and paint, to textiles, medicines, electronics and many more^{5,8,9}, covering many sectors.

With more and more nanotechnology entering the market, the amount of waste increases as well. Since most of the products are still in use, only an estimation can be made about the impact of all the nanomaterials in waste. The most important route from nanoparticles to the environment is via wastewater, with different types of nanoparticles released to water⁷. Man-made nanoparticles have already been detected in wastewater¹⁰ and waste leachate¹¹. With the fast growing nanotechnology, the amount of new and unknown materials that are introduced into the environment will increase concomitantly, which may lead to unpredictable long-term consequences on human and environmental health¹².

Nanoparticles in the aquatic environment

Once nanomaterials have entered the environment, a multitude of effects can occur. Nanoparticles are fairly small, and with decreasing size their surface to volume ratio increases rapidly (see Figure 1). Due to their large surface to volume ratio, the nanomaterial surface becomes more reactive in itself and to its contiguous environment¹³. However, the size of the particles can change over time. In the aquatic environment, non-stable metallic nanoparticles dissolve slowly over time, releasing ions to the environment while simultaneously the particle decreases in size¹⁴. On the other hand, agglomeration (loose clusters) and aggregation (irreversible clustering) processes result in an increase in size¹⁵.

Furthermore, with their relative large surface area, nanoparticles are prone to react with organic and inorganic materials. These interactions influence the stability of the particles in the water, which in turn influences whether the particles remain in the water column and thereby determining which type of organism faces the highest exposure. For instance, when particles sediment and settle down, bottom dwellers are much more exposed than organisms that live at the water surface.

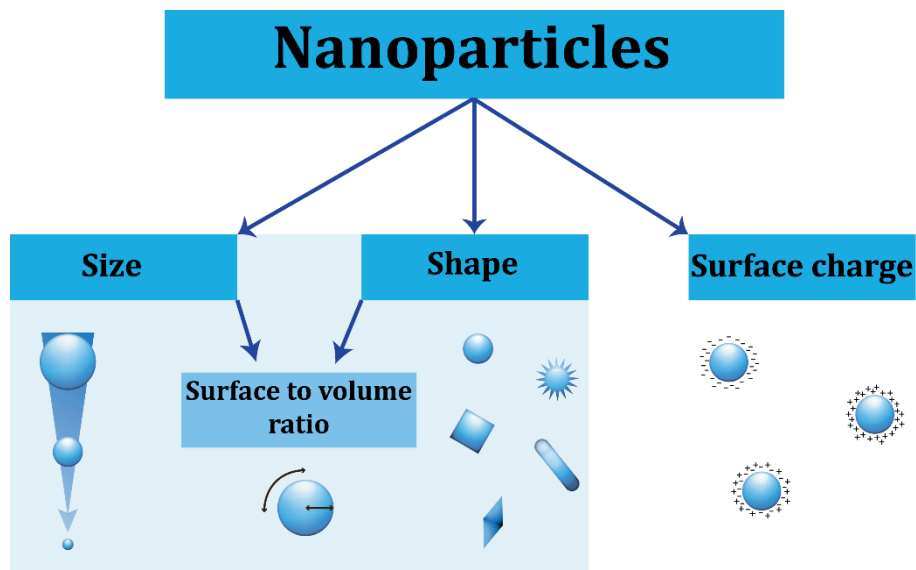


Figure 1. Most important aspects of nanoparticles. Different aspects of nanoparticles are important for their uptake in and toxicity to cells and organisms. Besides size and shape, which are the focus points of this thesis, surface charge (negative, positive or neutral) influences the uptake of particles.

Uptake of nanoparticles

Once organisms are surrounded by particles, the impact is based on the effective exposure: the fraction of the nanoparticles that is accessible for the organism. More importantly: the effective exposure determines whether the particles are taken up. With the large surface to volume ratio, membranes can attach to the relative large surface area, wrap around the particle and transport it inside the cell^{16,17}. In general, the surface charge also influences the uptake of the particles (Figure 1). This charge is based on the material properties, as well as the layer (corona) formed by organic materials¹⁸. Different charges have been found to behave differently: positively charged particles are in general found to be taken up much faster than negative or neutral charged particles. The reason for this is supposedly the slightly negative charge of the cell membrane, causing uptake by electrostatic attractions¹⁹. The surface charge also results in the adhesion of proteins to the particle. Particles with surface ligands (e.g., peptides, antibodies, etc.) are able to target specific organs²⁰. The amount of proteins that absorb onto the surface can for instance be reduced by decorating the particle with

a coating²¹. This layer improves stability and therewith prolongs the *in vivo* circulation time and subsequently the duration of the effective exposure²¹.

Besides size, the surface to volume ratio is also influenced by shape (Figure 1)²². The surface to volume ratio (which is related to the aspect ratio) has large influences on the membrane wrapping^{22,23}. Flat, disc-like shapes adhere to the outside of the membrane, forming aggregated rather than internalized particles²⁴. For other shapes, rotation during endocytosis is important in order to find the most optimal position for cell entry^{22,25,26}. With increasing aspect ratio (i.e. with increasing particle length), cellular uptake becomes more difficult^{26,27}. This also explains why the flat particles remain on the outside of the cell membrane. Therefore, on average, small and elongated particles are easily taken up by cells, whereas big, long and flat particles are a much bigger challenge for cells to internalize²⁸. Even within the cell, the shape of the particle influences its position²⁹.

Due to the difference in cellular uptake of nanoparticles and larger mixed materials of metallic compositions (from now on called bulk), different exposure routes are possible. The bulk form (for metals) tends to dissolve in free ions, which can only pass certain ion channels and or ion pumps³⁰. However, nanoparticles can, as previously discussed, either pass through membranes or enter the cell via membrane wrapping. In nanoparticle grouping efforts, a distinction is made between metallic particles that are either stable (inert) or non-stable (dissolving ions)³¹. At this point, non-stable nanoparticles start to act like a Trojan horse being an uptake route for colloid metals (see Figure 2): while dissolving, their shed ions reach places that they would have never reached when present in their ion form^{30,32}. Another type of Trojan horse principle can also occur: not the shedding of ions, but other molecules that adhere on the surface of the particle accompany the particle inside the cell (Figure 2)³³. This mechanism of co-exposure is beneficial for medicines delivered to cancer cells^{34,35}, but can result in unpredicted exposures of organisms in the environment.

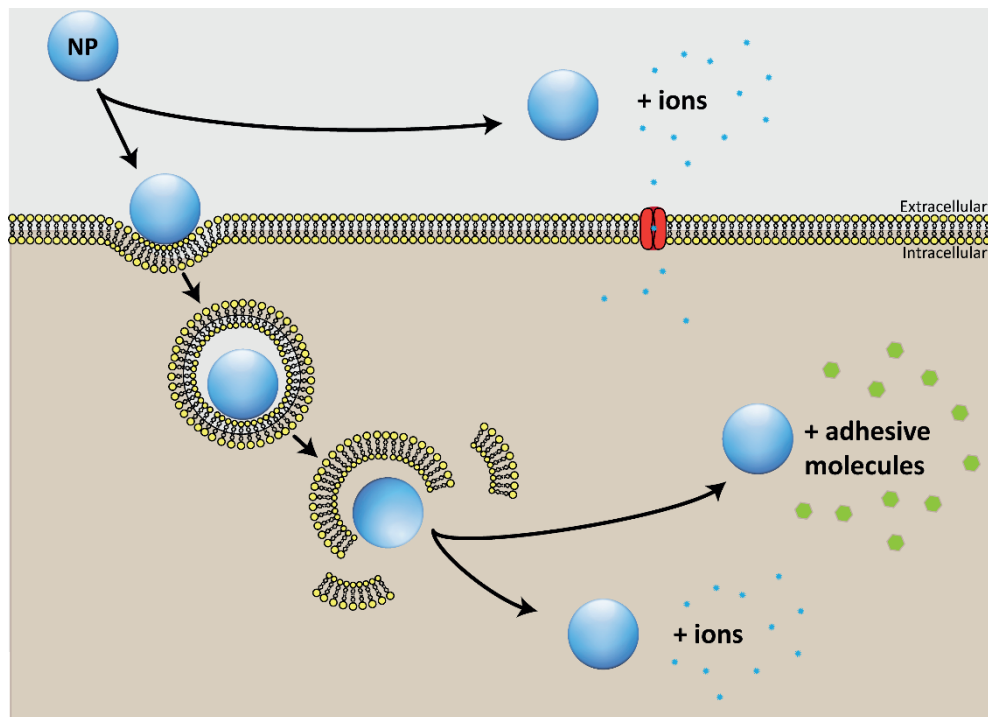


Figure 2. Trojan horse principles. Metallic nanoparticles can shed of their ions in their surrounding media, from where they can enter the cell via channels. However, the particle itself can also work as a Trojan horse: either it can shed of ions once it is inside the cell, resulting in much higher concentrations of ions, or the particle carries adhesive molecules inside the cell, where they are released.

Besides effects of the material, the particle itself can induce effects as well. Once the particles are inside the cell, interactions with the biological processes can occur. If the particles are small enough, they can enter the nucleus and bind to the DNA, causing DNA damage³⁶. Moreover, their presence in the nucleus may also interfere with the DNA replication³⁷. Particles that are not entering the nucleus, might bind to proteins and disrupt their function by protein unfolding, fibrillation, thiol cross-linking and enzymatic activity loss³⁷⁻³⁹. For instance, thiol groups in enzymes like NADH dehydrogenase are popular binding places, causing disruption of the respiratory chain and subsequently generate reactive oxygen species (ROS)³⁶. This in turn can induce oxidative stress, cell damage and eventually cell death⁴⁰⁻⁴². Both *in vitro* and *in vivo* studies have shown that particle toxicity might be related to ROS formation⁴³⁻⁴⁵. Since particles induce toxicity via other pathways than the ions of the core material, distinct adverse outcomes can be found for the particles and the ions³⁸.

The effects of nanoparticles on organisms

Cellular uptake gives an indication of the possible effects induced by nanoparticles, but the picture is incomplete. With regard to upscaling of *in vitro* results to effects on whole organisms, the key issue is that particles do not induce effects at only one location. Epithelial tissues like skin and intestine generally protect organisms from hazardous materials. However, nanoparticles are small enough to penetrate into cells⁴⁶. Once they are inside the cells of the barrier tissue, they may start to distribute throughout the body^{47,48}. Because of this biodistribution, particles can accumulate in secondary organs^{12,49}: accumulation in the body. Besides the biodistribution, the time that the particle stays within the organism also influences nanoparticle toxicity: the residence time. This duration is most importantly influenced by size: particles smaller than 6nm can quickly be excreted by the kidneys, whereas particles with a size larger than 200nm accumulate in spleen and liver, after which they are processed by mononuclear phagocyte system (MPS) cells¹⁹. This knowledge emphasizes the importance of understanding the factors that determine whether particles cross membrane barriers and subsequent distribute throughout the body. Therefore, if we want to know where the particle ends up irrespective of the material, *in vitro* studies can provide only half of the story.

Just as for particle uptake, shape is also an important factor for uptake, biodistribution and toxicity. Particle shape has been found to influence both the circulation time of the particles, as well as their distribution. Wires, discs and lamella, compared to spherical nanoparticles, were found to have a longer circulation time in the body, whereas cylindrical shapes display the longest circulation time⁵⁰. With regard to the distribution, rod shaped particles distribute much further inside the tissue, whereas spheres and disk-like particles stay on the edge of the tissue⁵¹. Furthermore, the length of the rod is important for biodistribution: short rods are trapped in the liver, bigger rods are trapped in the spleen⁵². This knowledge is gathered in cancer research, where the study is performed by injecting rodents: biodistribution via the blood and / or lymphatic system is guaranteed. Studies in which environmentally relevant exposure routes are used still focus mainly on the effect of size. However, examples like given by Dai et al., (2015) provide nice evidence that also in environmentally relevant exposures, rod shaped nanoparticles display much higher uptake rates than plates and spheres.

Different types of organisms result in different types of exposure routes and biodistribution. In the animal kingdom, there is a division made in two distinct types of organisms: invertebrates and vertebrates (representatives can be found in Figure 3, top left + bottom right and top right + bottom left respectively). In general, invertebrates are smaller than vertebrates. This results in a larger surface to volume ratio and subsequent more relative exposure than animals with a smaller surface to volume ratio. Additional organs like gills may increase the amount of surface even further. However, not only do their sizes differ. Especially insects and arthropods exhibit different external properties compared to vertebrate species. Where vertebrate species obtain their name from their spine (consisting of vertebra), invertebrates usually have an exoskeleton that supports their body. This exoskeleton is for instance composed of chitin, and is much harder to penetrate by chemicals than the soft surface burdens of vertebrates. Therefore, hard-body invertebrates are usually exposed via specific structures like pleopods or via the digestive tract⁵⁴.

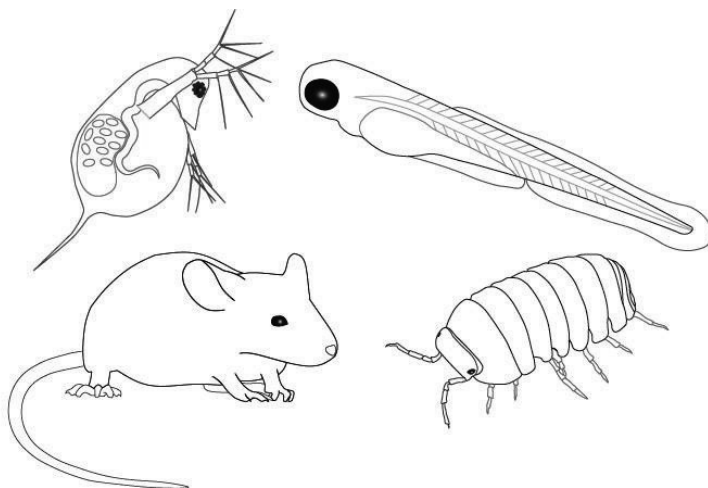


Figure 3. Model species. In (eco)toxicology, model species are used to test chemicals. In this picture, an overview of two vertebrate species (Zebrafish larvae: *Danio rerio*; Mouse: *Mus musculus*) and two invertebrate species (Waterflea: *Daphnia magna*; Woodlice: *Porcellio scaber*). The top represents aquatic organisms, whereas the bottom row represents terrestrial organisms. Note: animals are not on scale.

Not only does the uptake route differ between vertebrates and invertebrates, but also their accumulation pattern. Structural and functional differences in organs for instance modify the biodistribution pattern. For instance, most invertebrates have a hepatopancreas where (bulk) metals accumulate⁵⁴. In vertebrates however, this

structure continued to develop in two individual organs: the liver and the pancreas⁵⁵. Indeed, a large number of particles have been found to accumulate in the liver and are being excreted in the bile^{32,56-60}. Other specific excretion routes that can occur are for instance via the kidneys for vertebrates⁶¹⁻⁶³ and via the maxilla gland for invertebrate species⁵⁴.

As we have seen up to now, most of our knowledge on nanoparticle (eco)toxicity on vertebrate species is based on *in vitro* studies or *in vivo* injection studies. However, these studies do not provide information about the effective exposure in the environment, and do not answer the key question: are particles able to penetrate and enter the organism (uptake) at realistic environmental exposure conditions? As mentioned above, knowledge obtained on particle uptake in invertebrate species might not be applicable to vertebrate species due to their morphological differences. It is therefore important to assess the ability of particles to penetrate the borders of vertebrate species (epidermis, gut lining, etc.) under environmentally relevant conditions. By doing so, more relevant information about potential hazard for both ecological vertebrate species and for humans can be obtained.

After particles have crossed the exterior borders of the organism, particles will distribute throughout the organism. Although *in vivo* injection studies provide information on where particles distribute to once they have entered the blood stream, it is not warranted that every internalized particle travels through the blood stream. For instance, distribution via the lymphatic system is also a possibility. Additionally, most *in vivo* injection studies deal with induced tumor tissue, which influences the accumulation of the particles and the focus area of the researchers. It furthermore is known that size and shape influence the *in vitro* uptake of the particles, but it is largely unknown how these characteristics influence the particle distribution inside the healthy organism. Knowing where particles accumulate (biodistribution) may provide an indication of long-term effects.

Besides the usually stable nanoparticles used for imaging, nanoparticles can be made from various materials. Within the aim of the 3Rs, to Reduce, Replace or Refine animal testing, understanding the effect of particle shape on toxicity irrespective of the core material may provide valuable knowledge for modeling purposes. If there is a shape related effect irrespective of the core material, then the (eco)toxicological effects of an unknown/untested shape of a known material can be modeled rather than tested using animal tests.

The zebrafish as an example

A suited vertebrate model organism to screen for uptake and effect of nanoparticles is the zebrafish (*Danio rerio*; Figure 3, top right). This sub-tropical fish is due to its size (2-3 cm) easy to maintain. With 100 eggs or more in a clutch of one female, this model organism is ideal for high-throughput screening. The life-stages of the zebrafish embryos are well documented and therefore uniform to use for each researcher⁶⁴. During the first 24 hours of development (see Figure 4), when the majority of the organs are formed, the embryos are transparent. This makes the embryos ideal for monitoring developmental processes. After the first day, pigmentation starts and the embryos lose their transparency. However, transparent fish lines, called *Caspers*, do not develop this pigmentation and are therefore ideal for imaging for instance uptake of particles at later life stages.

Although zebrafish are cold-blooded, they are well suited as a vertebrate model. With the full genome known, it has been found that at least 71% of the human proteins have a zebrafish orthologue⁶⁵. This indicates that numerous genes are well conserved among the vertebrate group⁶⁶. With a fully known genome and a generation time of 3 months, the zebrafish is an ideal model organism for mutant and transgenic fish lines. Moreover, transgenic fish lines with fluorescent-labeled proteins or cell types are enabling targeted screenings⁶⁷. For instance, with the first innate immune system cell present after 24 hours post fertilization, immune system responses can be easily monitored using fluorescent microscopy.

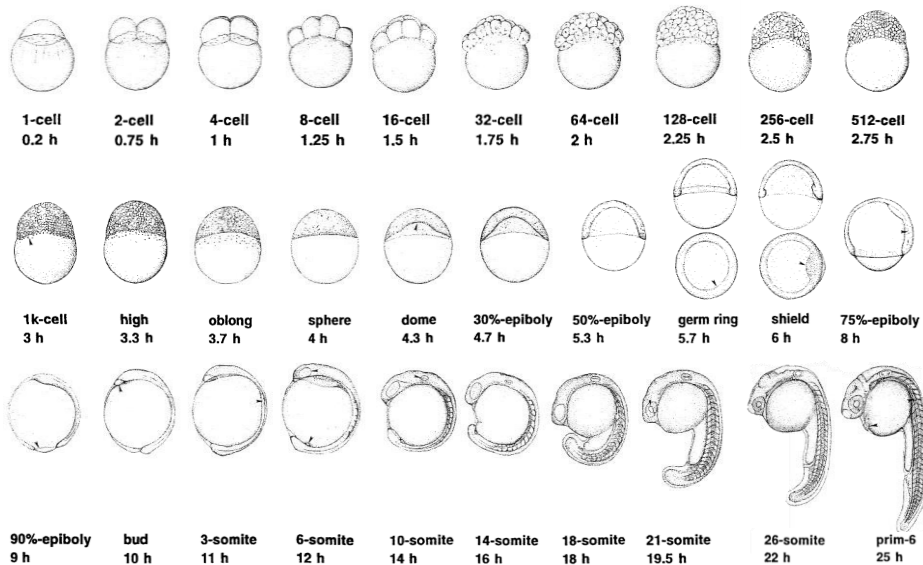


Figure 4. Embryonic development. In this picture, the developmental stages of a zebrafish embryo during the first 25 hours post fertilization (hpf) are depicted. Reprinted from Kimmel et al., 1995.

Zebrafish, both larvae and adults, have been used in (bio)medical and toxicological research for a while. Early medical researcher Dr. George Streisinger started using the zebrafish as a model in the 1970's⁶⁸. With the establishment of the zebrafish as a (medical) model organism, the zebrafish became also a representative for the aquatic vertebrates in toxicological assessments^{69,70}. Standardized tests were developed to be used for systematic testing of chemicals under the European REACH initiative^{71,72}. With a variety of endpoints ranging from lethality to malformations to behavioral effects^{73,74}, the zebrafish presents itself as a diverse model for toxicity testing. Due to the high rate of conservancy in the genome of vertebrate species, adverse outcome pathways for emerging contaminants in the environment can be extrapolated from zebrafish to different species of ecological relevance⁷⁵.

Outline of this Thesis

The work described in this thesis focusses on the uptake and biodistribution of nanoparticles in zebrafish larvae (up to 5 days post fertilization). For this, we covered different characteristics of the nanoparticles and studied the corresponding influence

on the uptake in and also their effect on the zebrafish larvae. The aim of this thesis is to understand the main drivers behind uptake and the subsequent biodistribution of nanoparticles, and how the effects they induce translates to ecotoxicological effects.

Chapter 2 focusses on the influence of the size of particles on the uptake and subsequent biodistribution in zebrafish larvae. In addition, we studied the importance of the exposure route on the uptake of particles. Using fluorescent polystyrene nanoparticles, we investigated where the particles were located inside the organisms after waterborne exposure.

Continuing on uptake, we shifted in **Chapter 3** our focus from size to shape. Using the exposure route that resulted in the highest uptake in Chapter 2, we continued our work with differently shaped particles. Since shaped polystyrene particles are not commercially available, we used gold nanoparticles that we imaged using two photon multi-focal laser microscopy and we imaged the subsequent immune response with stereo fluorescence microscopy.

In **Chapter 4**, we took a closer look at the impact of differently shaped particles on zebrafish fitness. By testing different shapes of silver nanoparticles for toxicity effects, we determined the effect of particle shape. In addition, by combining our data with existing data, we made an effort to model the particle effect irrelative to the core material.

Until now, we have focused on the uptake and induced effects of mono-material nanoparticles. However, as described earlier in this introduction, nanotechnology is advancing and building multi-material nanoparticles. For this reason, we investigated in **Chapter 5** what the interaction effects between TiO₂ nanoparticles and differently dissolving nanoparticles are on the mixture toxicity.

In **Chapter 6** the main findings of this thesis are summarized and discussed in context of environmental safety and future perspectives for nanotechnology.

References

- (1) Cup, T. H. E.; The, D.; Of, D.; Temper, V.; His, O. N. E. O. F. The Lycurgus Cup - A roman nanotechnology. *Cold Bull.* **2007**.
- (2) Drexler, K. E. *Engines of Creation: The Coming Era of Nanotechnology*; Anchor Press/Doubleday, 1986.

- (3) EU. Commission regulation No 1043/2011. *Off. J. Eur. Union* **2011**, 54, 1–40.
- (4) British Standards Institution. Terminology for nanomaterials. *Publicly Available Specif.* **2007**, No. 136, 16.
- (5) Science for Environment Policy. *Assessing the environmental safety of manufactured nanomaterials Science for Environment Policy Assessing the environmental safety of manufactured nanomaterials About Science for Environment Policy Keep up-to-date The contents and views included in Scienc;* 2017.
- (6) Boysen, E. Nanotechnology in Solar Cells <http://www.understandingnano.com/solarcells.html> (accessed Feb 1, 2018).
- (7) Garner, K. L.; Keller, A. a. Emerging patterns for engineered nanomaterials in the environment: a review of fate and toxicity studies. *J. Nanoparticle Res.* **2014**, 16 (8), 2503.
- (8) O'Brien, N.; Cummins, E. Recent Developments in Nanotechnology and Risk Assessment Strategies for Addressing Public and Environmental Health Concerns. *Hum. Ecol. Risk Assess. An Int. J.* **2008**, 14 (3), 568–592.
- (9) Gajewicz, A.; Rasulev, B.; Dinadayalane, T. C.; Urbaszek, P.; Puzyn, T.; Leszczynska, D.; Leszczynski, J. Advancing risk assessment of engineered nanomaterials: Application of computational approaches. *Adv. Drug Deliv. Rev.* **2012**, 64 (15), 1663–1693.
- (10) Westerhoff, P.; Song, G.; Hristovski, K.; Kiser, M. a. Occurrence and removal of titanium at full scale wastewater treatment plants: implications for TiO₂ nanomaterials. *J. Environ. Monit.* **2011**, 13 (5), 1195–1203.
- (11) Hennebert, P.; Avellan, A.; Yan, J.; Aguerre-Chariol, O. Experimental evidence of colloids and nanoparticles presence from 25 waste leachates. *Waste Manag.* **2013**, 33 (9), 1870–1881.
- (12) Bacchetta, R.; Moschini, E.; Santo, N.; Fascio, U.; Del Giacco, L.; Freddi, S.; Camatini, M.; Mantecca, P. Evidence and uptake routes for Zinc oxide nanoparticles through the gastrointestinal barrier in *Xenopus laevis*. *Nanotoxicology* **2014**, 8 (7), 728–744.
- (13) Gattoo, M. A.; Naseem, S.; Arfat, M. Y.; Dar, A. M.; Qasim, K.; Zubair, S. Physicochemical properties of nanomaterials: implication in associated toxic manifestations. *Biomed Res. Int.* **2014**, 2014, 498420.
- (14) Klaine, S. J.; Alvarez, P. J. J.; Batley, G. E.; Fernandes, T. F.; Handy, R. D.; Lyon, D. Y.; Mahendra, S.; McLaughlin, M. J.; Lead, J. R. Nanomaterials in the environment: behaviour, fate, bioavailability, and effects. *Environ. Toxicol. Chem.* **2008**, 27 (9), 1825.
- (15) Nichols, G.; Byard, S.; Bloxham, M. J.; Botterill, J.; Dawson, N. J.; Dennis, A.; Diart, V.; North, N. C.; Sherwood, J. D. A review of the terms agglomerate and aggregate with a recommendation for nomenclature used in powder and particle characterization. *J. Pharm. Sci.* **2002**, 91 (10), 2103–2109.

- 1
- (16) Zhu, M.; Nie, G.; Meng, H.; Xia, T.; Nel, A.; Zhao, Y. Physicochemical Properties Determine Nanomaterial Cellular Uptake, Transport, and Fate. *Acc. Chem. Res.* **2013**, *46* (3), 622–631.
- (17) Zhang, S.; Gao, H.; Bao, G. Physical principles of nanoparticle cellular endocytosis. *ACS Nano* **2015**, *9* (9), 8655–8671.
- (18) Cupi, D.; Hartmann, N. B.; Baun, A. The influence of natural organic matter and aging on suspension stability in guideline toxicity testing of silver, zinc oxide, and titanium dioxide nanoparticles with *Daphnia magna*. *Environ. Toxicol. Chem.* **2015**, *34* (3), 497–506.
- (19) Albanese, A.; Tang, P. S.; Chan, W. C. W. The effect of nanoparticle size, shape, and surface chemistry on biological systems. *Annu. Rev. Biomed. Eng.* **2012**, *14* (1), 1–16.
- (20) Pasqualini, R.; Ruoslahti, E. Organ targeting in vivo using phage display peptide libraries. *Nature* **1996**, *380*, 364–366.
- (21) Truong, L.; Tilton, S. C.; Zaikova, T.; Richman, E.; Waters, K. M.; Hutchison, J. E.; Tanguay, R. L. Surface functionalities of gold nanoparticles impact embryonic gene expression responses. *Nanotoxicology* **2013**, *7* (2), 192–201.
- (22) Dasgupta, S.; Auth, T.; Gompper, G. Shape and orientation matter for the cellular uptake of nonspherical particles. *Nano Lett.* **2014**, *14*, 687–693.
- (23) Kinnear, C.; Rodriguez-Lorenzo, L.; Clift, M. J. D.; Goris, B.; Bals, S.; Rothen, B.; Fink, A. S. Decoupling the shape parameter to assess gold nanorod uptake by mammalian cells. *Nanoscale* **2016**, *8*, 16416–16426.
- (24) Swiston, A. J.; Gilbert, J. B.; Irvine, D. J.; Cohen, R. E.; Rubner, M. F. Freely suspended cellular “backpacks” lead to cell aggregate self-assembly. *Biomacromolecules* **2010**, *11* (7), 1826–1832.
- (25) Li, Y.; Yue, T.; Yang, K.; Zhang, X. Molecular modeling of the relationship between nanoparticle shape anisotropy and endocytosis kinetics. *Biomaterials* **2012**, *33* (19), 4965–4973.
- (26) Chithrani, B. D.; Ghazani, A. a; Chan, W. C. W. Determining the size and shape dependence of gold nanoparticle uptake into mammalian cells. *Nano Lett.* **2006**, *6* (4), 662–668.
- (27) Carnovale, C.; Bryant, G.; Shukla, R.; Bansal, V. Size, shape and surface chemistry of nano-gold dictate its cellular interactions, uptake and toxicity. *Prog. Mater. Sci.* **2016**, *83*, 152–190.
- (28) Nazareus, M.; Zhang, Q.; Soliman, M. G.; del Pino, P.; Pelaz, B.; Carregal-Romero, S.; Rejman, J.; Rothen-Rutishauser, B.; Clift, M. J. D.; Zellner, R.; et al. In vitro interaction of colloidal nanoparticles with mammalian cells: What have we learned thus far? *Beilstein J. Nanotechnol.* **2014**, *5*, 1477–1490.
- (29) Hinde, E.; Thammasiraphop, K.; Duong, H. T. T.; Yeow, J.; Karagoz, B.; Boyer, C.;

- Gooding, J. J.; Gaus, K. Pair correlation microscopy reveals the role of nanoparticle shape in intracellular transport and site of drug release. *Nat. Nanotechnol.* **2016**, *12* (1), 81–89.
- (30) Limbach, L. K.; Wick, P.; Manser, P.; Grass, R. N.; Bruinink, A.; Stark, W. J. Exposure of Engineered Nanoparticles to Human Lung Epithelial Cells: Influence of Chemical Composition and Catalytic Activity on Oxidative Stress. *Environ. Sci. Technol.* **2007**, *41* (11), 4158–4163.
- (31) Arts, J. H. E.; Irfan, M. A.; Keene, A. M.; Kreiling, R.; Lyon, D.; Maier, M.; Michel, K.; Neubauer, N.; Petry, T.; Sauer, U. G.; et al. Case studies putting the decision-making framework for the grouping and testing of nanomaterials (DF4nanoGrouping) into practice. *Regul. Toxicol. Pharmacol.* **2016**, *76* (2), 234–261.
- (32) Park, E.-J.; Yi, J.; Kim, Y.; Choi, K.; Park, K. Silver nanoparticles induce cytotoxicity by a Trojan-horse type mechanism. *Toxicol. In Vitro* **2010**, *24* (3), 872–878.
- (33) Zhu, M.; Li, Y.; Shi, J.; Feng, W.; Nie, G.; Zhao, Y. Exosomes as extrapulmonary signaling conveyors for nanoparticle-induced systemic immune activation. *Small* **2012**, *8* (3), 404–412.
- (34) Choi, M.-R.; Stanton-Maxey, K. J.; Stanley, J. K.; Levin, C. S.; Bardhan, R.; Akin, D.; Badve, S.; Sturgis, J.; Robinson, J. P.; Bashir, R.; et al. A cellular Trojan Horse for delivery of therapeutic nanoparticles into tumors. *Nano Lett.* **2007**, *7* (12), 3759–3765.
- (35) Service, R. F. Nanoparticle Trojan Horses Gallop From the Lab Into the Clinic. *Science* (80-.). **2010**, *330* (6002), 314–315.
- (36) Asharani, P. V.; Low Kah Mun, G.; Hande, M. P.; Valiyaveetil, S. Cytotoxicity and genotoxicity of silver nanoparticles in human cells. *ACS Nano* **2009**, *3* (2), 279–290.
- (37) Yu, S.; Yin, Y.; Liu, J. Silver nanoparticles in the environment. *Environ. Sci. Process. Impacts* **2013**, *15* (1), 78–92.
- (38) Chang, Y.-N.; Zhang, M.; Xia, L.; Zhang, J.; Xing, G. The Toxic Effects and Mechanisms of CuO and ZnO Nanoparticles. *Materials (Basel)*. **2012**, *5* (12), 2850–2871.
- (39) Farkas, J.; Christian, P.; Urrea, J. A. G.; Roos, N.; Hassellöv, M.; Tollefsen, K. E.; Thomas, K. V. Effects of silver and gold nanoparticles on rainbow trout (*Oncorhynchus mykiss*) hepatocytes. *Aquat. Toxicol.* **2010**, *96* (1), 44–52.
- (40) Holt, K. B.; Bard, A. J. Interaction of silver(I) ions with the respiratory chain of *Escherichia coli*: an electrochemical and scanning electrochemical microscopy study of the antimicrobial mechanism of micromolar Ag⁺. *Biochemistry* **2005**, *44* (39), 13214–13223.
- (41) Liu, J.; Sonshine, D. a; Shervani, S.; Hurt, R. H. Controlled release of biologically active silver from nanosilver surfaces. *ACS Nano* **2010**, *4* (11), 6903–6913.
- (42) Chen, M.; Yin, J.; Liang, Y.; Yuan, S.; Wang, F.; Song, M.; Wang, H. Oxidative stress and immunotoxicity induced by graphene oxide in zebrafish. *Aquat. Toxicol.* **2016**, *174*, 54–60.

- (43) Zhang, L.; He, Y.; Goswami, N.; Xie, J.; Zhang, B.; Tao, X. Uptake and effect of highly fluorescent silver nanoclusters on *Scenedesmus obliquus*. *Chemosphere* **2016**, *153*, 322–331.
- (44) Farkas, J.; Christian, P.; Gallego-Urrea, J. A.; Roos, N.; Hassellöv, M.; Tollefsen, K. E.; Thomas, K. V. Uptake and effects of manufactured silver nanoparticles in rainbow trout (*Oncorhynchus mykiss*) gill cells. *Aquat. Toxicol.* **2011**, *101* (1), 117–125.
- (45) Nath Roy, D.; Goswami, R.; Pal, A. Nanomaterial and toxicity: what can proteomics tell us about the nanotoxicology? *Xenobiotica* **2017**, *47* (7), 632–643.
- (46) Zhai, Y.; Hunting, E. R.; Wouters, M.; Peijnenburg, W. J. G. M.; Vijver, M. G. Silver Nanoparticles, Ions, and Shape Governing Soil Microbial Functional Diversity: Nano Shapes Micro. *Front. Microbiol.* **2016**, *7* (1123).
- (47) Fenaroli, F.; Westmoreland, D.; Benjaminsen, J.; Kolstad, T.; Skjeldal, F. M.; Meijer, A. H.; van der Vaart, M.; Ulanova, L.; Roos, N.; Nyström, B.; et al. Nanoparticles as drug delivery system against tuberculosis in zebrafish embryos: direct visualization and treatment. *ACS Nano* **2014**, *8* (7), 7014–7026.
- (48) Speshock, J. L.; Elrod, N.; Sadoski, D. K.; Maurer, E.; K Braydich-Stolle, L.; Brady, J.; Hussain, S. Differential organ toxicity in the adult zebra fish following exposure to acute sub-lethal doses of 10 nm silver nanoparticles. *Front. Nanosci. Nanotechnol.* **2016**, *2* (3), 114–120.
- (49) Yang, H.; Du, L.; Tian, X.; Fan, Z.; Sun, C.; Liu, Y.; Keelan, J. a; Nie, G. Effects of nanoparticle size and gestational age on maternal biodistribution and toxicity of gold nanoparticles in pregnant mice. *Toxicol. Lett.* **2014**, *230* (1), 10–18.
- (50) Hu, X.; Hu, J.; Tian, J.; Ge, Z.; Zhang, G.; Luo, K.; Liu, S. Polyprodrug amphiphiles: Hierarchical assemblies for shape-regulated cellular internalization, trafficking, and drug delivery. *J. Am. Chem. Soc.* **2013**, *135*, 17617–17629.
- (51) Black, K. C. L.; Wang, Y.; Luehmann, H. P.; Cai, X.; Xing, W.; Pang, B.; Zhao, Y.; Cutler, C. S.; Wang, L. V.; Liu, Y.; et al. Radioactive ¹⁹⁸Au-doped nanostructures with different shapes for in vivo analyses of their biodistribution, tumor uptake, and intratumoral distribution. *ACS Nano* **2014**, *8* (5), 4385–4394.
- (52) Huang, X.; Li, L.; Liu, T.; Hao, N.; Liu, H.; Chen, D.; Tang, F. The shape effect of mesoporous silica nanoparticles on biodistribution, clearance, and biocompatibility in vivo. In *ACS Nano*; 2011; Vol. 5, pp 5390–5399.
- (53) Dai, L.; Banta, G. T.; Selck, H.; Forbes, V. E. Influence of copper oxide nanoparticle form and shape on toxicity and bioaccumulation in the deposit feeder, *Capitella teleta*. *Mar. Environ. Res.* **2015**, *111*, 99–106.
- (54) Vijver, M. G.; Vink, J. P. M.; Jager, T.; van Straalen, N. M.; Wolterbeek, H. T.; van Gestel, C. A. M. Kinetics of Zn and Cd accumulation in the isopod *Porcellio scaber* exposed to contaminated soil and/or food. *Soil Biol. Biochem.* **2006**, *38* (7), 1554–1563.
- (55) Cox, A. G.; Goessling, W. The lure of zebrafish in liver research: Regulation of

hepatic growth in development and regeneration. *Curr. Opin. Genet. Dev.* **2015**, *32*, 153–161.

(56) Boyle, D.; Al-Bairuty, G. A.; Ramsden, C. S.; Sloman, K. A.; Henry, T. B.; Handy, R. D. Subtle alterations in swimming speed distributions of rainbow trout exposed to titanium dioxide nanoparticles are associated with gill rather than brain injury. *Aquat. Toxicol.* **2013**, *126*, 116–127.

(57) Connolly, M.; Fernández, M.; Conde, E.; Torrent, F.; Navas, J. M.; Fernández-Cruz, M. L. Tissue distribution of zinc and subtle oxidative stress effects after dietary administration of ZnO nanoparticles to rainbow trout. *Sci. Total Environ.* **2016**, *551–552*, 334–343.

(58) Jang, M.; Kim, W.; Lee, S.; Henry, T. B.; Park, J. Uptake, tissue distribution, and depuration of total silver in common carp (*Cyprinus carpio*) after aqueous exposure to silver nanoparticles. *Environ. Sci. Technol.* **2014**, *48* (19), 11568–11574.

(59) Kashiwada, S. Distribution of nanoparticles in the see-through medaka (*Oryzias latipes*). *Environ. Health Perspect.* **2006**, *114* (11), 1697–1702.

(60) Zhao, J.; Wang, Z.; Liu, X.; Xie, X.; Zhang, K.; Xing, B. Distribution of CuO nanoparticles in juvenile carp (*Cyprinus carpio*) and their potential toxicity. *J. Hazard. Mater.* **2011**, *197*, 304–310.

(61) Hainfeld, J. F.; Slatkin, D. N.; Focella, T. M.; Smilowitz, H. M. Gold nanoparticles: A new X-ray contrast agent. *Br. J. Radiol.* **2006**, *79* (March), 248–253.

(62) Balogh, L.; Nigavekar, S. S.; Nair, B. M.; Lesniak, W.; Zhang, C.; Sung, L. Y.; Kariapper, M. S. T.; El-Jawahri, A.; Llanes, M.; Bolton, B.; et al. Significant effect of size on the in vivo biodistribution of gold composite nanodevices in mouse tumor models. *Nanomedicine Nanotechnology, Biol. Med.* **2007**, *3*, 281–296.

(63) Elbially, N. S.; Fathy, M. M.; Khalil, W. M. Doxorubicin loaded magnetic gold nanoparticles for in vivo targeted drug delivery. *Int. J. Pharm.* **2015**, *490* (1–2), 190–199.

(64) Kimmel, C. B.; Ballard, W. W.; Kimmel, S. R.; Ullmann, B.; Schilling, T. F. Stages of embryonic development of the zebrafish. *Dev. Dyn.* **1995**, *203* (3), 253–310.

(65) Howe, K.; Clark, M. D.; Torroja, C. F.; Tarrant, J.; Berthelot, C.; Muffato, M.; Collins, J. E.; Humphray, S.; McLaren, K.; Matthews, L.; et al. The zebrafish reference genome sequence and its relationship to the human genome. *Nature* **2013**, *496* (7446), 498–503.

(66) Macrae, C. A.; Peterson, R. T. Zebrafish as tools for drug discovery. *Nat. Publ. Gr.* **2015**, *14* (10), 721–731.

(67) Lin, S.; Lin, S.; Zhao, Y.; Nel, A. E. Zebrafish: An in vivo model for nano EHS studies. *Small* **2013**, *9* (9–10), 1608–1618.

(68) ZFIN. Dr. George Streisinger lab <http://zfin.org/action/profile/view/ZDB-LAB-980209-8> (accessed Dec 13, 2017).

- (69) Scholz, S.; Fischer, S.; Gündel, U.; Küster, E.; Luckenbach, T.; Voelker, D. The zebrafish embryo model in environmental risk assessment—applications beyond acute toxicity testing. *Environ. Sci. Pollut. Res.* **2008**, *15* (5), 394–404.
- (70) Stegeman, J. J.; Goldstone, J. V.; Hahn, M. E. *Perspectives on zebrafish as a model in environmental toxicology*; Elsevier, 2010; Vol. 29.
- (71) Lammer, E.; Carr, G. J.; Wendler, K.; Rawlings, J. M.; Belanger, S. E.; Braunbeck, T. Is the fish embryo toxicity test (FET) with the zebrafish (*Danio rerio*) a potential alternative for the fish acute toxicity test? *Comp. Biochem. Physiol. - C Toxicol. Pharmacol.* **2009**, *149* (2), 196–209.
- (72) The Organisation for Economic Co-operation and Development (OECD). *Test No. 236: Fish Embryo Acute Toxicity (FET) Test*; Paris, France, 2013.
- (73) Legradi, J.; el Abdellaoui, N.; van Pomeran, M.; Legler, J. Comparability of behavioural assays using zebrafish larvae to assess neurotoxicity. *Environ. Sci. Pollut. Res.* **2015**, *22* (21), 16277–16289.
- (74) The Organisation for Economic Co-operation and Development (OECD). Overview testing guidelines <http://www.oecd-ilibrary.org/search?option1=titleAbstract&option2=&value2=&option3=&value3=&option4=&value4=&option5=&value5=&option6=imprint&value6=http%3A%2F%2Focd.metastore.ingenta.com%2Fcontent%2Fimprint%2Foecd&option23=&value23=&option7=&value7=&opt> (accessed Feb 1, 2018).
- (75) Veneman, W. J.; Spaink, H. P.; Brun, N. R.; Bosker, T.; Vijver, M. G. Pathway analysis of systemic transcriptome responses to injected polystyrene particles in zebrafish larvae. *Aquat. Toxicol.* **2017**, *190* (June), 112–120.
- (76) Handy, R. D.; Henry, T. B.; Scown, T. M.; Johnston, B. D.; Tyler, C. R. Manufactured nanoparticles: their uptake and effects on fish—a mechanistic analysis. *Ecotoxicology* **2008**, *17* (5), 396–409.
- (77) Skjolding, L. M.; Ašmonaitė, G.; Jølck, R. I.; Andresen, T. L.; Selck, H.; Baun, A.; Sturve, J. An assessment of the importance of exposure routes to the uptake and internal localisation of fluorescent nanoparticles in zebrafish (*Danio rerio*), using light sheet microscopy. *Nanotoxicology* **2017**, *11* (3), 351–359.
- (78) van Pomeran, M.; Brun, N. R.; Peijnenburg, W. J. G. M.; Vijver, M. G. Exploring uptake and biodistribution of polystyrene (nano) particles in zebrafish embryos at different developmental stages. *Aquat. Toxicol.* **2017**, *190* (June), 40–45.
- (79) Truong, N. P.; Whittaker, M. R.; Mak, C. W.; Davis, T. P. The importance of nanoparticle shape in cancer drug delivery. *Expert Opin. Drug Deliv.* **2015**, *12* (1), 1–14.
- (80) Qiu, Y.; Liu, Y.; Wang, L.; Xu, L.; Bai, R.; Ji, Y.; Wu, X.; Zhao, Y.; Li, Y.; Chen, C. Surface chemistry and aspect ratio mediated cellular uptake of Au nanorods. *Biomaterials* **2010**, *31* (30), 7606–7619.
- (81) Chu, Z.; Zhang, S.; Zhang, B.; Zhang, C.; Fang, C.-Y.; Rehor, I.; Cigler, P.; Chang, H.-

- C.; Lin, G.; Liu, R.; et al. Unambiguous observation of shape effects on cellular fate of nanoparticles. *Sci. Rep.* **2014**, *4*, 4495.
- (82) Khlebtsov, N.; Dykman, L. Biodistribution and toxicity of engineered gold nanoparticles: a review of in vitro and in vivo studies. *Chem. Soc. Rev.* **2011**, *40* (3), 1647–1671.
- (83) Takeuchi, I.; Nobata, S.; Oiri, N.; Tomoda, K.; Makino, K. Biodistribution and excretion of colloidal gold nanoparticles after intravenous injection: Effects of particle size. *Biomed. Mater. Eng.* **2017**, *28* (3), 315–323.
- (84) Simpson, C. A.; Huffman, B. J.; Gerdon, A. E.; Cliffel, D. E. Unexpected toxicity of monolayer protected gold clusters eliminated by PEG-thiol place exchange reactions. *Chem. Res. Toxicol.* **2010**, *23* (10), 1608–1616.
- (85) Bogdanov, A. a; Gupta, S.; Koshkina, N.; Corr, S. J.; Zhang, S.; Curley, S. a; Han, G. Gold Nanoparticles Stabilized with MPEG-Grafted Poly(l -lysine): in Vitro and in Vivo Evaluation of a Potential Theranostic Agent. *Bioconjug. Chem.* **2015**, *26* (1), 39–50.
- (86) Browning, L. M.; Lee, K. J.; Huang, T.; Nallathamby, P. D.; Lowman, J. E.; Nancy Xu, X.-H. Random walk of single gold nanoparticles in zebrafish embryos leading to stochastic toxic effects on embryonic developments. *Nanoscale* **2009**, *1* (1), 138.
- (87) Arts, J. H.; Hadi, M.; Irfan, M. A.; Keene, A. M.; Kreiling, R.; Lyon, D.; Maier, M.; Michel, K.; Petry, T.; Sauer, U. G. A decision-making framework for the grouping and testing of nanomaterials (DF4nanoGrouping). *Regul. Toxicol. Pharm.* **2015**, *71* (2), S1–S27.
- (88) Mesquita, B.; Lopes, I.; Silva, S.; Bessa, M. J.; Starykevich, M.; Carneiro, J.; Galvão, T. L. P.; Ferreira, M. G. S.; Tedim, J.; Teixeira, J. P.; et al. Gold nanorods induce early embryonic developmental delay and lethality in zebrafish (*Danio rerio*). *J. Toxicol. Environ. Heal. - Part A Curr. Issues* **2017**, *80* (13–15), 672–687.
- (89) Bruinink, A.; Wang, J.; Wick, P. Effect of particle agglomeration in nanotoxicology. *Arch. Toxicol.* **2015**, *89* (5), 659–675.
- (90) Kumar, R.; Roy, I.; Ohulchanskyy, T. Y.; Vathy, L. a; Bergey, E. J.; Sajjad, M.; Prasad, P. N. In vivo biodistribution and clearance studies using multimodal organically modified silica nanoparticles. *ACS Nano* **2010**, *4* (2), 699–708.
- (91) Brun, N. R.; Koch, B. E. V.; Varela, M.; Peijnenburg, W. J. G. M.; Spaink, H. P.; Vijver, M. G. Nanoparticles induce dermal and intestinal innate immune system responses in zebrafish embryos. *Environ. Sci. Nano* **2018**, *5* (4), 904–916.
- (92) OECD. *Validation report (phase 1) for the zebrafish embryo toxicity test, part I*; 2011.
- (93) van Pomeran, M.; Peijnenburg, W.; Brun, N.; Vijver, M. A novel experimental and modelling strategy for nanoparticle toxicity testing enabling the use of small quantities. *Int. J. Environ. Res. Public Health* **2017**, *14* (11), 1348.
- (94) Pan, Y.; Leifert, A.; Graf, M.; Schiefer, F.; Thoröe-Boveleth, S.; Broda, J.; Halloran,

- M. C.; Hollert, H.; Laaf, D.; Simon, U.; et al. High-sensitivity real-time analysis of nanoparticle toxicity in green fluorescent protein-expressing zebrafish. *Small* **2013**, *9* (6), 863–869.
- (95) Schindelin, J.; Arganda-Carreras, I.; Frise, E.; Kaynig, V.; Longair, M.; Pietzsch, T.; Preibisch, S.; Rueden, C.; Saalfeld, S.; Schmid, B.; et al. Fiji: an open-source platform for biological-image analysis. *Nat. Methods* **2012**, *9* (7), 676–682.
- (96) Balasubramanian, V.; Srinivasan, R.; Miskimins, R.; Sykes, A. G. A simple azacrown ether containing an anthraquinone fluorophore for the selective detection of Mg(II) in living cells. *Tetrahedron* **2016**, *72* (1), 205–209.
- (97) van den Broek, B.; Ashcroft, B.; Oosterkamp, T. H.; van Noort, J. Parallel nanometric 3D tracking of intracellular gold nanorods using multifocal two-photon microscopy. *Nano Lett.* **2013**, *13* (3), 980–986.
- (98) Hua, J.; Vijver, M. G.; Ahmad, F.; Richardson, M. K.; Peijnenburg, W. J. G. M. Toxicity of different-sized copper nano- and submicron particles and their shed copper ions to zebrafish embryos. *Environ. Toxicol. Chem.* **2014**, *33* (8), 1774–1782.
- (99) Huwyler, J.; Kettiger, H.; Schipanski, A.; Wick, P. Engineered nanomaterial uptake and tissue distribution: from cell to organism. *Int. J. Nanomedicine* **2013**, *8*, 3255.
- (100) Kim, K. T.; Zaikova, T.; Hutchison, J. E.; Tanguay, R. L. Gold nanoparticles disrupt zebrafish eye development and pigmentation. *Toxicol. Sci.* **2013**, *133* (2), 275–288.
- (101) Sun, L.; Li, Y.; Liu, X.; Jin, M.; Zhang, L.; Du, Z.; Guo, C.; Huang, P.; Sun, Z. Cytotoxicity and mitochondrial damage caused by silica nanoparticles. *Toxicol. Vitro.* **2011**, *25* (8), 1619–1629.
- (102) Danilova, N.; Steiner, L. A. B cells develop in the zebrafish pancreas. *Proc. Natl. Acad. Sci.* **2002**, *99* (21), 13711–13716.
- (103) Mattsson, K.; Ekvall, M. T.; Hansson, L.-A.; Linse, S.; Malmendal, A.; Cedervall, T. Altered behavior, physiology, and metabolism in fish exposed to polystyrene nanoparticles. *Environ. Sci. Technol.* **2015**, *49* (1), 553–561.
- (104) Chen, Y.; Xu, Z.; Zhu, D.; Tao, X.; Gao, Y.; Zhu, H.; Mao, Z.; Ling, J. Gold nanoparticles coated with polysarcosine brushes to enhance their colloidal stability and circulation time in vivo. *J. Colloid Interface Sci.* **2016**, *483*, 201–210.
- (105) Asharani, P. V.; Lianwu, Y.; Gong, Z.; Valiyaveetil, S. Comparison of the toxicity of silver, gold and platinum nanoparticles in developing zebrafish embryos. *Nanotoxicology* **2011**, *5* (1), 43–54.



Fluorescence overlay image of a ZF embryo exposed to 25nm red fluorescent polystyrene NPs

Chapter 2

Exploring uptake and biodistribution of polystyrene (nano)particles in zebrafish embryos at different developmental stages

M. van Pomerén^{1,*}, N.R. Brun¹, W.J.G.M. Peijnenburg^{1,2}, M.G. Vijver¹.

¹ *Institute of Environmental Sciences (CML), Leiden University, 2300 RA, Leiden, The Netherlands.*

² *National Institute of Public Health and the Environment, Center for the Safety of Substances and Products, 3720 BA, Bilthoven, The Netherlands.*

Published in *Aquatic Toxicology* 2017, DOI: 10.1016/j.aquatox.2017.06.017

Abstract

2 In ecotoxicology, it is continuously questioned whether (nano)particle exposure results in particle uptake and subsequent biodistribution or if particles adsorb to the epithelial layer only. To contribute to answering this question, we investigated different uptake routes in zebrafish embryos and how they affect particle uptake into organs and within whole organisms. This is addressed by exposing three different life stages of the zebrafish embryo in order to cover the following exposure routes: via chorion and dermal exposure; dermal exposure; oral and dermal exposure. How different nanoparticle sizes affect uptake routes was assessed by using polystyrene particles of 25, 50, 250 and 700 nm.

In our experimental study, we showed that particle uptake in biota is restricted to oral exposure, whereas the dermal route resulted in adsorption to the epidermis and gills only. Ingestion followed by biodistribution was observed for the tested particles of 25 and 50 nm. The particles spread through the body and eventually accumulated in specific organs and tissues such as the eyes. Particles larger than 50 nm were predominantly adsorbed onto the intestinal tract and outer epidermis of zebrafish embryos. Embryos exposed to particles via both epidermis and intestine showed highest uptake and eventually accumulated particles in the eye, whereas uptake of particles via the chorion and epidermis resulted in marginal uptake. Organ uptake and internal distribution should be monitored more closely to provide more in depth information of the toxicity of particles.

1. Introduction

Nano- and microparticles of varying sizes are increasingly detected in aquatic ecosystems¹. Once in the environment, biota are exposed to particles and may subsequently be adversely affected, although field studies about these effects are scarce and complicated to perform². To assess the origin of the effects from small particles, a better understanding of uptake routes and internalization is required.

Particles can enter organisms via various ways: via the epidermis and/or gills (dermal exposure), via the gastrointestinal tract (oral exposure) or via inhalation. This latter exposure route is only applicable for organisms with lungs, whereas the first two apply to all multicellular organisms. To our knowledge, it is still unknown whether in *in vivo* exposures particles cross one of these barriers and which barrier they cross most effectively. Forced uptake routes via injection directly in the blood system³ or in muscles⁴ as used e.g. in cancer-research, can lead to metallic particle distribution through the whole body. This knowledge about biodistribution emphasizes the importance of understanding the factors that determine whether or not (metallic and polystyrene) particles cross the cell membrane barrier of the epithelial layer.

Studies linking waterborne exposure of whole organisms to target organs and biodistribution report that particles in the GI tract are common⁵. Particles are not only taken up from the surrounding medium, but can also accumulate from the food. Based on their experimental data, Kalman et al. (2015)⁶ even stated that in freshwater exposures, uptake of metallic nanoparticles (MNPs) via ingestion of exposed food can have major effects on higher organisms and induces more severe effects than via waterborne exposure. This was also argued by Jackson et al. (2012)⁷ when the amphipod *Leptocheirus plumulosus* fed on Cd/Se quantum dot exposed algae showed more severe lethal effects of Cd/Se quantum dots as compared to waterborne exposure. Both Cedervall et al. (2012)⁸ and Mattsson et al. (2015)⁹ exposed fish to polystyrene nanoparticles (PS NPs) by feeding them *Daphnia magna*, which in turn were fed NP contaminated algae. These studies showed that polystyrene NPs administered via the food altered brain texture and water content indicating biodistribution towards the brain. Also for TiO₂ NPs and carbon nanotubes it was found that accumulation occurred within multiple consumer species¹⁰.

The route of particle uptake and subsequent target organ are hitherto uncertain, and especially the impact of exposure route on uptake is to be further substantiated. In this study, we investigated if polystyrene (nano)particles adsorb to

2

the intestine or epidermis, or if the particles are taken up and internalized. Thereby we explore if this is related to different sizes of PSPs. We defined internalization as absorption, thus cellular uptake of particles. Uptake is defined as particles being found within the organs and/or tissue of the organism. The word 'biodistribution' is used to describe the process of particles trafficking through cells and organisms. Ingestion is not considered uptake inside the body, only presence in the GI tract.

We investigated the major uptake routes that determine uptake into organs and biodistribution within whole organisms. In this experiment we use the development of zebrafish embryos to obtain 3 different uptake routes: uptake via chorion and epidermis; uptake via epidermis; and uptake via epidermis and intestine due to ingestion of the particles, to answer the following research questions:

(1) Is the exposure route important for (nano)particle uptake in zebrafish embryos and is this influenced by size? And (2) does the uptake route dictates the target organ?

For the first research question, we hypothesize that oral uptake plays an important role, since uptake over an internal mucosal membrane occurs faster than over an intact dermal epithelial membrane. On the other hand, the chance of particle penetration is proportional to the surface area of the epidermis. Based on previous observations^{5,11,12} we hypothesize that uptake of particles increases with decreasing particles size.

The second research question is based on previously detected target organs of particles in fish. Particles that enter the blood stream via the intestine pass the hepatic portal vein and are often detected in the liver^{5,13-15}, Therefore we hypothesize that particles taken up via oral exposure target the liver, whereas particles taken up via dermal exposure might target other organs.

2. Materials and Methods

2.1 Preparation of particle suspensions

Fluorescent polystyrene particles (PSPs) of 25 and 50 nm in H₂O were purchased from ThermoFisher Scientific (Catalog number R25 and R50 resp.; Waltham, USA) and particles of 250 and 700 nm in H₂O were purchased from CorpuScular Inc. (Catalog number 103127-05 and 103129-05 resp.; Cold spring, USA), both with a density of 1.05 g/cm³. Exposure solutions were prepared by adding the purchased stock solutions

to egg water (60 µg/ml Instant Ocean Sea Salt, Sera GmbH, Heinsberg, Germany). Immediately before exposure, the solutions were freshly prepared and sonicated for 10 min using an ultrasonic water bath (USC200T, VWR, Amsterdam, The Netherlands).

2.2 Physicochemical characterization

Transmission electron microscopy (TEM; JEOL 1010, JEOL Ltd., Tokyo, Japan) was used to characterize the size and morphology of the PSPs after 1 hour of incubation in egg water. Due to the chemical properties of polystyrene, the contrast of especially the 25 nm PSP TEM images was limited. Dynamic light scattering (DLS) assessments were performed on a Zetasizer Nano-ZS instrument (Malvern Instruments Ltd, Malvern, UK) to detect the size distribution and zeta-potential of PSP suspensions in egg water at 0 h and 24 h.

2.3 Experimental setup

2.3.1 Zebrafish husbandry

Zebrafish were handled as described by animal welfare regulations and maintained according to standard protocols (<http://ZFIN.org>). Adult zebrafish were maintained at 25 ± 0.5 °C in a 14 h light : 10 h dark cycle. Fertilized zebrafish eggs were obtained from an AB/TL wild-type zebrafish.

2.3.2 Exposure of zebrafish embryo life stages to PSPs

In order to test the importance of different uptake routes, three different exposure starting points were tested. Developing zebrafish embryos undergo different stages: at first the embryo is protected by the chorion, followed by the second stage in which the mouth of the hatched embryo is closed until the third stage in which the morphogenesis is completed and oral uptake and excretion are fully functioning. This provides the opportunity to test the three uptake routes as mentioned in the introduction. This can also be seen in Table 1. Zebrafish embryos were exposed in 24-well plates and an exposure regime of 48 hours was maintained within each group (n=10). Particle suspensions and egg water were renewed every 24 hours. Particle concentrations were selected based on pilot tests (data not shown) and are given in Table 1. The concentration selected showed clear visibility of the particles without observations of

negative effects in the embryos. Temperature was maintained at 28 ± 0.8 °C during the experiments.

Table 1. Overview of the different exposure regimes indicating the age of the embryos expressed in hours post fertilization (hpf), the targeted uptake routes and nominal concentrations used. 'Dechorionated' indicates that the embryos were manually dechorionated before exposure.

Regime	Developmental stage (hpf)	Uptake route	Nominal concentration (mg/L)	
			25/50 nm	250/700 nm
1	0 - 48	Chorion and dermal uptake	25	5
2	24 - 72 (dechorionated)	Dermal uptake	50	5
3	72 - 120	Oral and dermal uptake	50	5

2.3.3 Microscopy

Prior to the experiments, pilot studies were executed with a 2 photon confocal laser microscope and a stereo fluorescent microscope (Supplementary material, SM) in order to determine the most suited method for visualizing adsorbed, ingested or biodistributed particles. Since the visualization of the 2 photon confocal laser microscopy was limited to a few cell layers hampering NP tracking, the experiment was conducted with a stereo fluorescent microscope capturing the whole embryo.

Zebrafish embryos were examined and imaged daily during the exposure to check fitness (malformations and mortality) using a fluorescence stereo microscope (M205 FA, Leica). During the final examination, embryos were rinsed three times with egg water and kept under anesthesia (0,02% Tricaine, Sigma) in egg water. Fitness was not affected during this inspection. Embryos exposed until 48 hours post fertilization (hpf) were manually dechorionated prior to examination (Henn and Braunbeck, 2011).

2.3.4 Eye size measurement

From exposure regime 3, a minimum of 4 zebrafish embryos were imaged per exposure group using the fluorescence stereo microscope. Eye width and length were measured using the image processing package Fiji¹⁶.

2.4 Statistical analysis

Significance ($p < 0,05$) for effects on eye-size among the different treatments was tested using a one way ANOVA using the SPSS 23 software package. Results are given as mean \pm standard deviation (SD).

3. Results

3.1 Physico-chemical characterization of polystyrene particles

TEM images showing the size of the PSPs after 1 h of incubation in egg water are given in Figure 1. All PSPs were spherical, and only small clusters of less than 4 particles were detected in the samples.

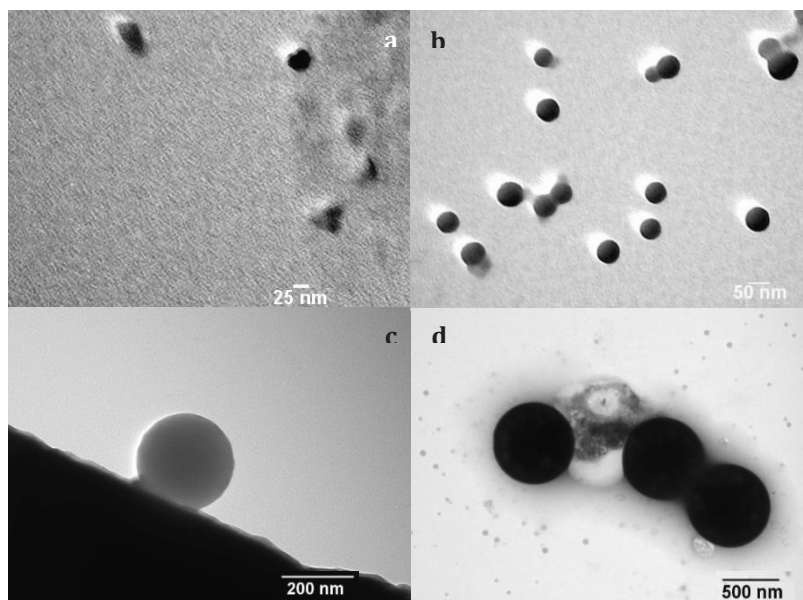


Figure 1. TEM image of a) 25 nm, b) 50 nm, c) 250 and d) 700 nm PSPs.

According to the TEM pictures, actual and nominal sizes of the particles at T0 deviated less than 2-5%. The 25 nm particles had an actual average size of ca. 27 nm. The average size of the 50 nm NPs was measured to be 50 nm. The 250 and 700 nm particles had a diameter of 217 and 727 nm respectively. From the DLS measurements (Table 2) it can be concluded that the 25 and 700 nm particles behaved slightly different in the exposure medium of the zebrafish embryos as compared to the behavior of the

50 and 250 nm particles. The 25 nm NPs tended to form agglomerates over time. Suspensions of the 50 and 250 nm particles appeared stable, whereas the suspensions of the 700 nm PSPs were found to agglomerate directly after preparation. The clusters of PSPs formed declined in size over time. It is also apparent that the 25 and 50 nm NPs were present in clusters of a few particles within the samples at both T0 and T24, whereas the DLS measurements of the 250 and 700 nm PSPs indicated that only single particles were present after 24 hour. It should be noted that due to the fluorescent properties of the particles, the DLS measurements might be less accurate than for non-fluorescent particles. The zeta potential measurements indicated that the 25 and 50 nm particles were negatively charged and maintained the zeta potential over time. In contrast, 250 nm particles became less negatively charged over time, and the 700 nm particles became more negatively charged. These zeta potentials indicate that the 25 and 50 nm particles will form agglomerates within 24 h, whereas the 250 and 700 nm particles will remain a stable particle at 24 h which is also shown in the DLS results.

Table 2. Overview of the zeta potential and size distribution after 0 and 24 h of exposure. In case of size distribution, the two dominant peaks in size are given with the first peak representing the highest number of counts.

Particle	Zeta potential (mV ± SD)		Size distribution by DLS (nm± SD)			
	0 h	24 h	0 h		24 h	
			Peak one	Peak two	Peak one	Peak two
25 nm	-5.1 ± 2.0	-6.1 ± 1.1	38.1 ± 7.1	134.8 ± 53.9	125 ± 5.4	32.0 ± 1.0
50 nm	-15.8 ± 5.2	-19.5 ± 1.5	70.6 ± 18.1	3408.3 ± 2952.0	67.0 ± 1.7	5338.3 ± 118.4
250 nm	-20 ± 1.4	-9.7 ± 2.9	298.4 ± 24.7	-	277.7 ± 13.6	-
700 nm	-17.4 ± 8.9	-31.9 ± 2.2	943.6 ± 108.2	-	735 ± 57.6	-

3.2 Uptake and biodistribution of PSPs

Uptake and biodistribution of the differently sized PSPs were monitored after 48 h of exposure starting at three different time points (based upon hpf), of which representative pictures are shown in Figure 2. Per group, all embryos (n=10) showed the same degree of uptake. The embryos exposed directly after fertilization (regime 1) had no particles taken up. In fact, all NPs were adsorbed to the chorion. The embryos exposed after 24 hpf (regime 2) displayed particle adsorption to the epidermis and no uptake of PSPs was observed (Figure 2). As can be seen from Figure 2, uptake of PSPs was observed only when the exposure started at 72 hpf (third exposure regime, at which oral and dermal exposure is possible). The smallest particles of 25 and 50 nm

were taken up by the embryo between 72 and 120 hpf, as shown by their accumulation in the eye (Figure 3). The 250 and 700 nm PSPs were found only in the digestive tract and absorbed to the gills of the exposed zebrafish embryos and were not found in the eye.

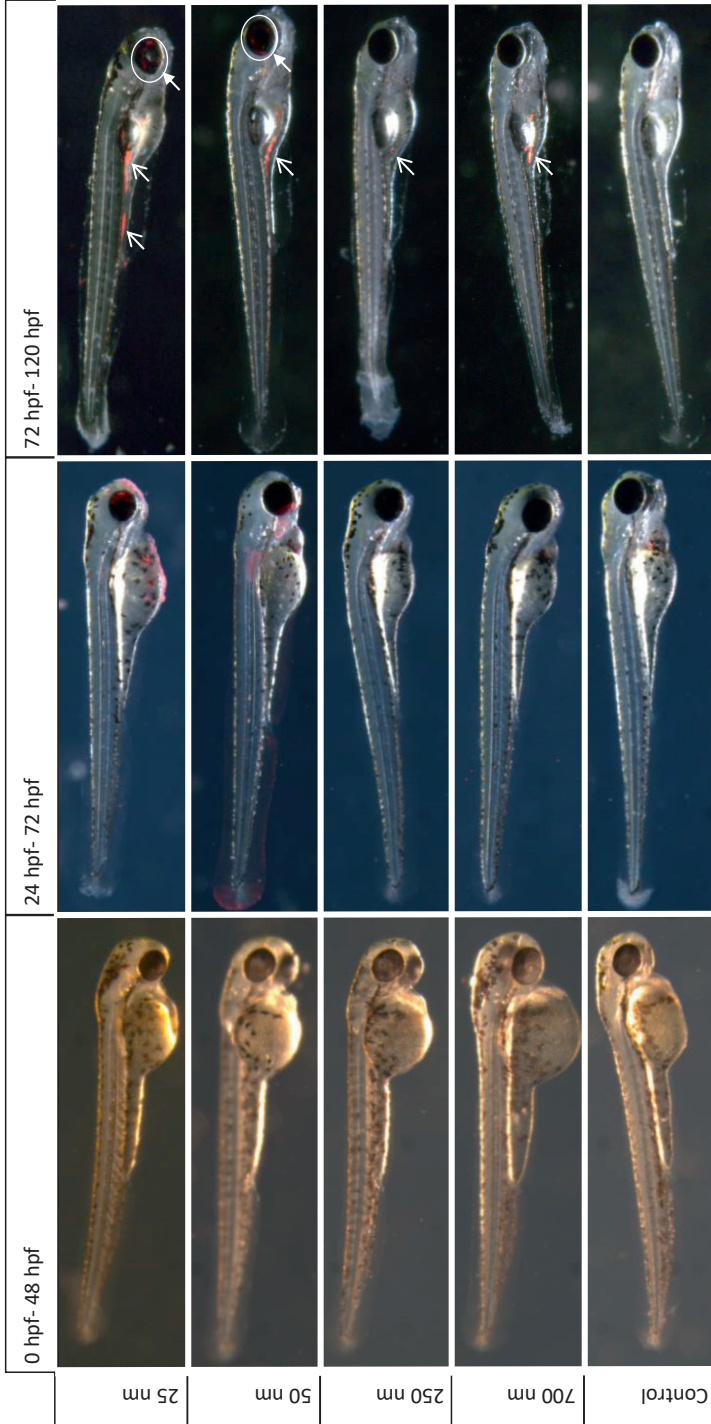


Figure 2. Images of fluorescent PSPs in zebrafish embryos. For each of the four PSPs of different size, a representative picture of each group after the exposure regime is given. Open arrows show PSPs in the digestive tract, closed arrows indicate PSPs in the eye of the zebrafish.

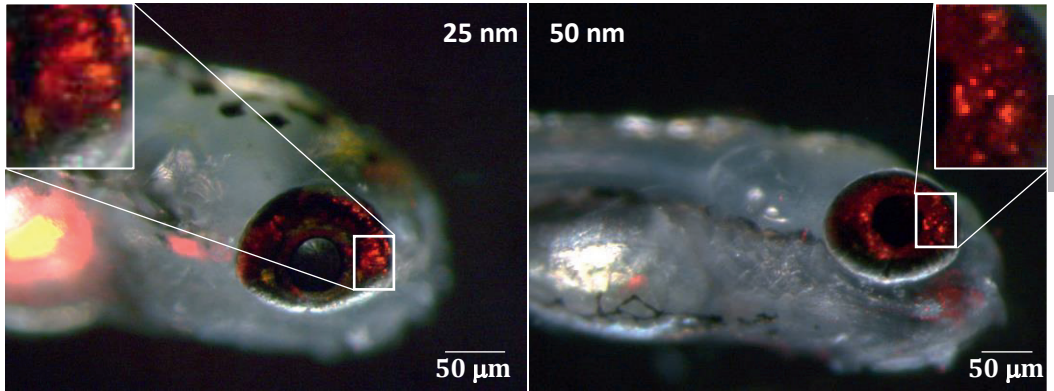


Figure 3. Images of fluorescent PSPs in the eye of zebrafish embryos after exposure to 25 nm and 50 nm PSPs exposed from 72 till 120 hpf. The inset is providing further details using 10 times magnification.

3.3 Eye size measurement

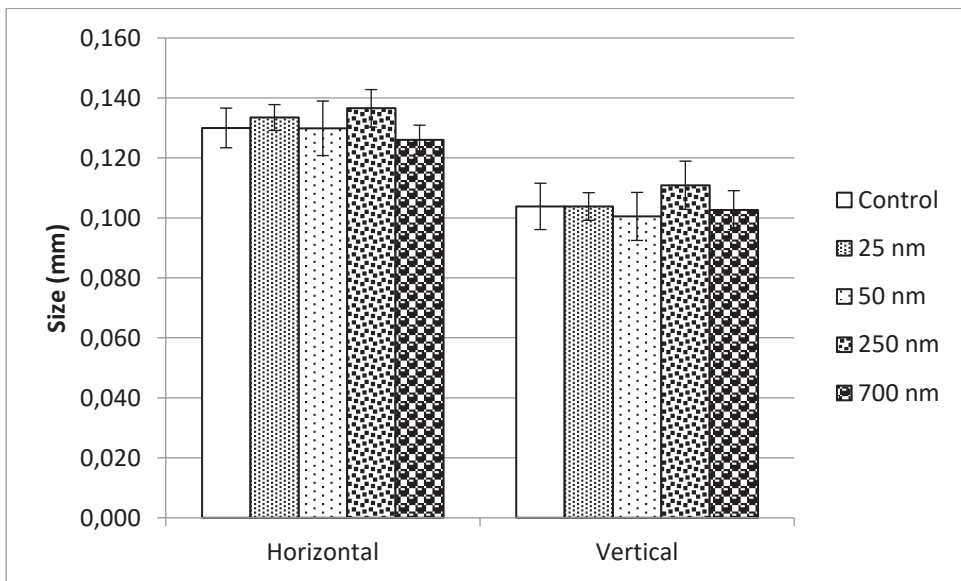


Figure 4. Eye size measurement of embryos exposed to different sized PSPs from 72 till 120 hpf ($n=4$). Vertical and horizontal refer to the measurement direction.

The eye size of embryos in which PSPs were present in the eye was compared with the eye size of embryos in which PSPs were absent in the eyes. No significant difference in eye size was found between any of the treatments and the control (see Figure 4). Thus, the PSPs present in the eye did not affect ocular development.

4. Discussion

2 In this contribution, the first question we aimed to answer is whether the exposure route is important for the uptake of particles. Differentiation between uptake routes in nanotoxicology is a yet unexplored avenue of research and only a few studies distinguish oral uptake from other uptake routes. Since exposure via food (here defined as oral exposure) also resulted in metallic particles in the gills¹³, the difference between oral exposure and full body exposure becomes undistinguishable. Irrespective of the exposure route, only particles adsorbed in the intestine were further biodistributed^{5,13-15}, suggesting that the epithelial layer is an important route for particle uptake and biodistribution. Our results underline the importance of the oral exposure route and its impacts on internalization of particles. When embryos were exposed solely via the dermal route, PSPs adsorbed on the epidermis and gills. However, no PSPs were detected inside the embryos, indicating that oral exposure is the most important route for PSP uptake in zebrafish. Subsequently this means that embryonic stages after 72 hpf are most suited for studying internalization and uptake of particles from waterborne exposures. The results indicate that especially for higher organisms, oral exposure is the major route of uptake and source for subsequent internal distribution of particles.

Besides the exposure route, other factors are found to be important for particle uptake. Most commonly, size is reported to influence uptake, with a restricted particle size of maximal 50 nm^{12,17}. This is confirmed by the results of our experimental study as only the tested particles equal to or smaller than 50 nm were taken up into the embryos and particles equal or larger than 250 nm were not found to be taken up in the eye of embryos. The larger particles (≥ 250 nm) were not able to penetrate body tissue in any of the exposure scenarios. Even more, large particles cannot cross the epidermis-barrier or intestine lining and are also often too large to be consumed by the organisms¹⁸⁻²⁰. Here we show that particles of up to 700 nm can be ingested by zebrafish embryos.

Not only size, but also other factors can influence uptake of particles, such as the surface characteristics of the particle^{21,22}. In our experiments, the negative surface charge of the PSPs might have prevented uptake via the relatively large pore channels (500 to 700 nm²³) of the chorion, since the chorion showed to be an effective barrier to all sizes of our PSPs. Also the chorion of the Japanese medaka (*Oryzias latipes*) is capable of protecting recently fertilized embryos from intruding polystyrene NPs smaller than 50 nm⁵. Also other studies found only size-dependent effects after hatching, with no effects prior to hatching²³. Surface charge of the PSPs might have resulted in large

adsorption to the chorion. It can be speculated that transport of particles over the chorion occurs only when the chorion has reached its adsorption maximum (maximum strength to bind particles). Another possibility is that large clusters of particles, which were adsorbed to the chorion, hampered passage through the pore channels. Yet, at a later stage of development, while still being protected by the chorion, particles were found internalized in the medaka⁵. Since medaka embryos have a longer developmental time whilst still being in the chorion (hatching around 216 hpf²⁴) than zebrafish embryos (hatching around 72 hpf), exposure over a longer time period might allow NPs to cross the more slowly thinning chorion and to enter the organism.

The second question we aimed to answer in this article is whether the uptake route influences the target organ. In our study we show an exposure route dependent effect on uptake. Our tested particles larger than 50 nm were not taken up, even though they were found to distribute through the intestine when the mouth opens. In contrary, accumulation of small PSPs (≤ 50 nm) in the eyes was observed. This was only observed after exposure of embryos via the dermal + oral route (while the mouth was open), whereas this accumulation was not observed when the mouth was still closed i.e. under conditions of dermal uptake only. Although particles might have been taken up via the maturing epidermis of the zebrafish, the exposure route is most likely via the gastrointestinal tract as direct dermal exposure induced no uptake of particles.

Particles tend to accumulate in specific organs after uptake^{25,26}. In general, most particles are found to accumulate in the liver of fish^{5,13-15}. This observation is according to expectation, since the liver is primarily used to clear the body from toxicants. Other organs are also targeted by particles, since particles were found to be distributed throughout the whole body – including the brain – once the particles have entered the blood stream or lymphatic system of vertebrates²⁷⁻²⁹. In our experiments, particle exposure via the intestine and epidermis led to accumulation in the eye of the zebrafish. It is not clear if transport occurred via the blood stream or via the lymphatic system, or that uptake occurred after epidermal exposure, since there were no particles detected in both systems. Over time, the free PSPs might be further distributed through the body at a later stage of development and accumulate in other organs such as the brain. This distribution of particles was found for other particles, and for instance Ag NPs were located in both the eye and the brain of zebrafish embryos³⁰. However, for metallic NPs that dissolve in aquatic and biological media it is hard to distinguish between the biodistribution of the NPs and the ions. Lee et al. (2012)³⁰ focused at the signal of the particles, but often total internal Ag concentrations are measured with no

2 distinction between ions and particles¹⁴. Not only particles shedding off ions, but also stable NPs were found to be distributed within an organism. For instance presence of polystyrene NPs altered the structure of the brain from adult rainbow trout and subsequently influenced their behavior⁹ indicating that NPs not only have short term effects, but also long term behavioral effects³¹.

An important part in understanding the significance of uptake and internalization of PSPs are the biodistribution and elimination possibilities³². Investigation of clearing mechanisms in zebrafish embryos is limited due to short assay time span of 120 h. However, in adult zebrafish most particles are excreted from the body via the liver, spleen and gall bladder^{5,27,33,34}. Excretion from cells and subsequently from tissues occurs at a much slower rate than uptake, which can occur within half an hour (particles found intracellular³⁵). For carbon quantum dots, the fastest excretion time (in which all of the particles were cleared from the body) of internalized particles was 56 hours²⁸. Thus it can be expected that once accumulated, PSP may be excreted again. However, if this is actually the case and in what time span remains to be investigated.

5. Conclusions

The exposure route influences the uptake and target organ of particles in zebrafish embryos. The three different uptake routes we tested (chorion and epidermis; epidermis; epidermis and intestine via ingestion) provided insight in the contribution of uptake routes to actual uptake. Our data suggest that the predominant uptake route of PSPs was the oral route, while dermal uptake only marginally contributed to uptake and subsequent biodistribution. Therefore, the time window between 72 and 120 hpf is of importance in zebrafish embryo exposure. The main physicochemical factor accounting for uptake, internalization and further distribution was particle size. Particles with a diameter of 25 and 50 nm were the largest particles found to be taken up in the eye. Accumulation in the eye might either originate from outer epidermal exposure or from uptake through the intestinal epidermis and subsequent internal biodistribution. Organ uptake and internal distribution should be monitored more closely to provide more in depth information of the toxicity of particles. As a future perspective, we suggest that measurements of the biodistribution and depuration of NPs may become a useful sub-lethal endpoint. Simultaneous examination of

biodistribution and depuration endpoints will provide insight in the bioaccumulation capacity of particles by biota.

Acknowledgements

The authors would like to thank Dr. Wouter J. Veneman and Roel Heutink for their assistance during the experiments. The staff of the ZF facility of the Cell Observatory is thanked for providing the experimental work environment. Marinda van Pomerén, Nadja R. Brun and Martina G. Vijver were funded by NWO-VIDI 864.13.010 granted to Martina G. Vijver. The research described in this work was supported by the European Union Seventh Framework Programme under EC-GA No. 604602 'FUTURENANONEEDS'.

Supplemental material

Supplemental material can be found on:

<http://www.sciencedirect.com/science/article/pii/S0166445X17301716>

References

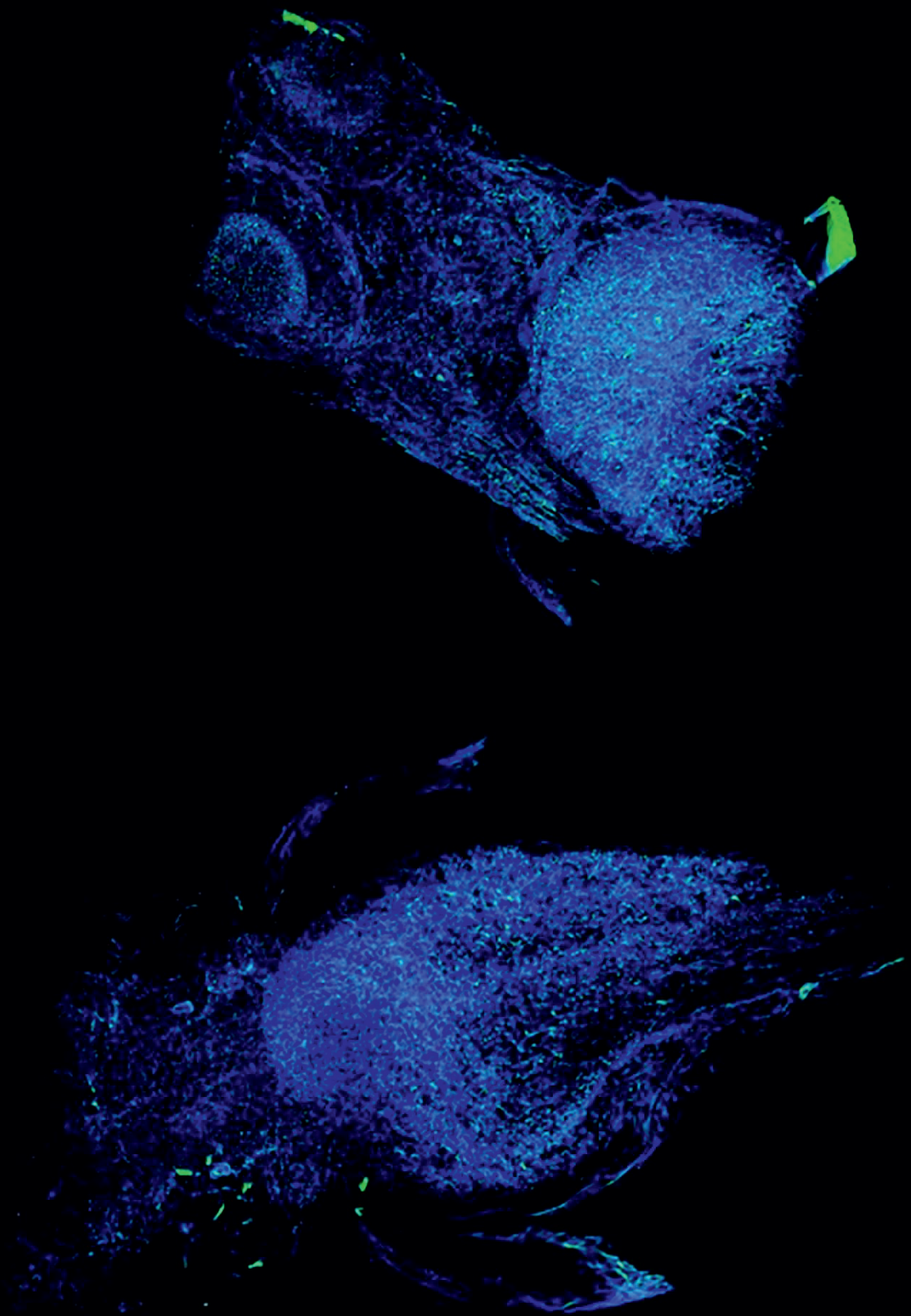
- (1) Gottschalk, F.; Sun, T.; Nowack, B. Environmental concentrations of engineered nanomaterials: Review of modeling and analytical studies. *Environ. Pollut.* **2013**, *181*, 287–300.
- (2) Schaumann, G. E.; Philippe, A.; Bundschuh, M.; Metreveli, G.; Klitzke, S.; Rakcheev, D.; Grün, A.; Kumahor, S. K.; Kühn, M.; Baumann, T.; et al. Understanding the fate and biological effects of Ag- and TiO₂-nanoparticles in the environment: The quest for advanced analytics and interdisciplinary concepts. *Sci. Total Environ.* **2015**, *535*, 3–19.
- (3) Fenaroli, F.; Westmoreland, D.; Benjaminsen, J.; Kolstad, T.; Skjeldal, F. M.; Meijer, A. H.; van der Vaart, M.; Ulanova, L.; Roos, N.; Nyström, B.; et al. Nanoparticles as drug delivery system against tuberculosis in zebrafish embryos: direct visualization and treatment. *ACS Nano* **2014**, *8* (7), 7014–7026.
- (4) Speshock, J. L.; Elrod, N.; Sadoski, D. K.; Maurer, E.; K Braydich-Stolle, L.; Brady, J.; Hussain, S. Differential organ toxicity in the adult zebra fish following exposure to acute sub-lethal doses of 10 nm silver nanoparticles. *Front. Nanosci. Nanotechnol.* **2016**, *2* (3), 114–120.
- (5) Kashiwada, S. Distribution of nanoparticles in the see-through medaka (*Oryzias latipes*). *Environ. Health Perspect.* **2006**, *114* (11), 1697–1702.
- (6) Kalman, J.; Paul, K. B.; Khan, F. R.; Stone, V.; Fernandes, T. F. Characterisation of bioaccumulation dynamics of three differently coated silver nanoparticles and aqueous silver in a simple freshwater food chain. *Environ. Chem.* **2015**, *12* (6), 662.

- (7) Jackson, B. P.; Bugge, D.; Ranville, J. F.; Chen, C. Y. Bioavailability, toxicity, and bioaccumulation of quantum dot nanoparticles to the amphipod *Leptocheirus plumulosus*. *Environ. Sci. Technol.* **2012**, *46* (10), 5550–5556.
- (8) Cedervall, T.; Hansson, L.-A.; Lard, M.; Frohm, B.; Linse, S. Food chain transport of nanoparticles affects behaviour and fat metabolism in fish. *PLoS One* **2012**, *7* (2), e32254.
- (9) Mattsson, K.; Ekvall, M. T.; Hansson, L.-A.; Linse, S.; Malmendal, A.; Cedervall, T. Altered behavior, physiology, and metabolism in fish exposed to polystyrene nanoparticles. *Environ. Sci. Technol.* **2015**, *49* (1), 553–561.
- (10) Yeo, M. K.; Nam, D. H. Influence of different types of nanomaterials on their bioaccumulation in a paddy microcosm: A comparison of TiO₂ nanoparticles and nanotubes. *Environ. Pollut.* **2013**, *178*, 166–172.
- (11) Rosenkranz, P.; Chaudhry, Q. A comparison of nanoparticle and fine particle uptake by *Daphnia magna*. *Environ. Toxicol. Chem.* **2009**, *28* (10), 2142–2149.
- (12) Manabe, M.; Tatarazako, N.; Kinoshita, M. Uptake, excretion and toxicity of nano-sized latex particles on medaka (*Oryzias latipes*) embryos and larvae. *Aquat. Toxicol.* **2011**, *105* (3–4), 576–581.
- (13) Connolly, M.; Fernández, M.; Conde, E.; Torrent, F.; Navas, J. M.; Fernández-Cruz, M. L. Tissue distribution of zinc and subtle oxidative stress effects after dietary administration of ZnO nanoparticles to rainbow trout. *Sci. Total Environ.* **2016**, 551–552, 334–343.
- (14) Jang, M.; Kim, W.; Lee, S.; Henry, T. B.; Park, J. Uptake, tissue distribution, and depuration of total silver in common carp (*Cyprinus carpio*) after aqueous exposure to silver nanoparticles. *Environ. Sci. Technol.* **2014**, *48* (19), 11568–11574.
- (15) Pan, Y.; Leifert, A.; Graf, M.; Schiefer, F.; Thoröe-Boveleth, S.; Broda, J.; Halloran, M. C.; Hollert, H.; Laaf, D.; Simon, U.; et al. High-sensitivity real-time analysis of nanoparticle toxicity in green fluorescent protein-expressing zebrafish. *Small* **2013**, *9* (6), 863–869.
- (16) Schindelin, J.; Arganda-Carreras, I.; Frise, E.; Kaynig, V.; Longair, M.; Pietzsch, T.; Preibisch, S.; Rueden, C.; Saalfeld, S.; Schmid, B.; et al. Fiji: an open-source platform for biological-image analysis. *Nat. Methods* **2012**, *9* (7), 676–682.
- (17) Bisesi, J. H.; Merten, J.; Liu, K.; Parks, A. N.; Afrooz, A. R. M. N.; Glenn, J. B.; Klaine, S. J.; Kane, A. S.; Saleh, N. Bin; Ferguson, P. L.; et al. Tracking and quantification of single-walled carbon nanotubes in fish using near infrared fluorescence. *Environ. Sci. Technol.* **2014**, *48* (3), 1973–1983.
- (18) Fent, K.; Weisbrod, C. J.; Wirth-Heller, A.; Pielers, U. Assessment of uptake and toxicity of fluorescent silica nanoparticles in zebrafish (*Danio rerio*) early life stages. *Aquat. Toxicol.* **2010**, *100* (2), 218–228.
- (19) Ronneberger, D. Uptake of latex beads as size-model for food of planktonic rotifers. *Hydrobiologia* **1998**, *387/387*, 445–449.

- (20) Van Hoecke, K.; De Schamphelaere, K. A. C.; Ali, Z.; Zhang, F.; Elsaesser, A.; Rivera-Gil, P.; Parak, W. J.; Smagghe, G.; Howard, C. V.; Janssen, C. R. Ecotoxicity and uptake of polymer coated gold nanoparticles. *Nanotoxicology* **2013**, *7* (1), 37–47.
- (21) Albanese, A.; Tang, P. S.; Chan, W. C. W. The effect of nanoparticle size, shape, and surface chemistry on biological systems. *Annu. Rev. Biomed. Eng.* **2012**, *14* (1), 1–16.
- (22) Fröhlich, E. The role of surface charge in cellular uptake and cytotoxicity of medical nanoparticles. *Int. J. Nanomedicine* **2012**, *7*, 5577.
- (23) Lee, K. J.; Nallathamby, P. D.; Browning, L. M.; Osgood, C. J.; Xu, X.-H. N. In vivo imaging of transport and biocompatibility of single silver nanoparticles in early development of zebrafish embryos. *ACS Nano* **2007**, *1* (2), 133–143.
- (24) Iwamatsu, T. Stages of normal development in the medaka *Oryzias latipes*. *Mech. Dev.* **2004**, *121* (7–8), 605–618.
- (25) Handy, R. D.; Henry, T. B.; Scown, T. M.; Johnston, B. D.; Tyler, C. R. Manufactured nanoparticles: their uptake and effects on fish--a mechanistic analysis. *Ecotoxicology* **2008**, *17* (5), 396–409.
- (26) Zhu, M.; Li, Y.; Shi, J.; Feng, W.; Nie, G.; Zhao, Y. Exosomes as extrapulmonary signaling conveyors for nanoparticle-induced systemic immune activation. *Small* **2012**, *8* (3), 404–412.
- (27) Jung, Y.-J.; Kim, K.-T.; Kim, J. Y.; Yang, S.-Y.; Lee, B.-G.; Kim, S. D. Bioconcentration and distribution of silver nanoparticles in Japanese medaka (*Oryzias latipes*). *J. Hazard. Mater.* **2014**, *267*, 206–213.
- (28) Kang, Y.-F.; Li, Y.-H.; Fang, Y.-W.; Xu, Y.; Wei, X.-M.; Yin, X.-B. Carbon quantum dots for zebrafish fluorescence imaging. *Sci. Rep.* **2015**, *5*, 11835.
- (29) Reisch, A.; Klymchenko, A. S. Fluorescent polymer nanoparticles based on dyes: seeking brighter tools for bioimaging. *Small* **2016**, *12* (15), 1968–1992.
- (30) Lee, K. J.; Browning, L. M.; Nallathamby, P. D.; Desai, T.; Cherukuri, P. K.; Xu, X.-H. N. In vivo quantitative study of sized-dependent transport and toxicity of single silver nanoparticles using zebrafish embryos. *Chem. Res. Toxicol.* **2012**, *25* (5), 1029–1046.
- (31) Wang, Q.; Zhou, Y.; Song, B.; Zhong, Y.; Wu, S.; Cui, R.; Cong, H.; Su, Y.; Zhang, H.; He, Y. Linking Subcellular Disturbance to Physiological Behavior and Toxicity Induced by Quantum Dots in *Caenorhabditis elegans*. *Small* **2016**, 3143–3154.
- (32) Vijver, M. G.; van Gestel, C. A. M.; van Straalen, N. M.; Lanno, R. P.; Peijnenburg, W. J. G. M. Biological significance of metals partitioned to subcellular fractions within earthworms (*Aporrectodea caliginosa*). *Environ. Toxicol. Chem.* **2006**, *25* (3), 807.
- (33) Boyle, D.; Al-Bairuty, G. A.; Ramsden, C. S.; Sloman, K. A.; Henry, T. B.; Handy, R. D. Subtle alterations in swimming speed distributions of rainbow trout exposed to titanium dioxide nanoparticles are associated with gill rather than brain injury. *Aquat. Toxicol.* **2013**, *126*, 116–127.

(34) Zhao, J.; Wang, Z.; Liu, X.; Xie, X.; Zhang, K.; Xing, B. Distribution of CuO nanoparticles in juvenile carp (*Cyprinus carpio*) and their potential toxicity. *J. Hazard. Mater.* **2011**, *197*, 304–310.

(35) Fang, C. Y.; Vaijayanthimala, V.; Cheng, C. A.; Yeh, S. H.; Chang, C. F.; Li, C. L.; Chang, H. C. The exocytosis of fluorescent nanodiamond and its use as a long-term cell tracker. *Small* **2011**, *7* (23), 3363–3370.



X-ray tomography image of a control ZF embryo (top) and a ZF embryo exposed to gold NPs (bottom)

Chapter 3

The biodistribution and immuno-responses of differently shaped non-modified gold particles in zebrafish embryos

3

M. van Pomerena*, W.J.G.M. Peijnenburg^{a,b}, R.C. Vlieg^c, S.J.T. van Noort^c, M.G. Vijver^a.

^a *Institute of Environmental Sciences (CML), Leiden University, Leiden, The Netherlands;*

^b *Center for the Safety of Substances and Products, National Institute of Public Health and the Environment, Bilthoven, The Netherlands;*

^c *Leiden Institute of Physics (LION), Leiden University, Leiden, The Netherlands*

Published in *Nanotoxicology* 2018, DOI: 10.1080/17435390.2018.1564079

Abstract

3

Important questions raised in (nano)ecotoxicology are whether biodistribution of nanoparticles is affected by particle shape and to what extent local adverse responses are subsequently initiated. For nanomedicine, these same questions become important when the labeled nanoparticles lose the labeling. In this study, we investigated the biodistribution patterns of gold nanoparticles (Au NPs) as well as immune-related local and systemic sub-lethal markers of exposure and behavioral assessment. Hatched zebrafish embryos were exposed to four differently shaped non-coated Au NPs with comparable sizes: nanospheres, nanorods, nano-urchins, and nano-bipyramids.

Shape-dependent trafficking of the particles resulted in a different distribution of the particles over the target organs. The differences across the distribution patterns indicate that the particles behave slightly different, although they eventually reach the same target organs – yet in different ratios. Mainly local induction of the immune system was observed, whereas systemic immune responses were not clearly visible. Macrophages were found to take Au NPs from the body fluid, be transferred into the veins and transported to digestive organs for clearance. No significant behavioral toxicological responses in zebrafish embryos were observed after exposure.

The trafficking of the particles in the macrophages indicates that the particles are removed via the mononuclear phagocytic system. The different ratios in which the particles are distributed over the target organs, indicate that the shape influences their behavior and eventually possibly the toxicity of the particles. The observed shape-dependent biodistribution patterns might be beneficial for shape-specific targeting in nanomedicine and stress the importance of incorporating shape-features in nanosafety assessment.

1. Introduction

A central paradigm of toxicology is that toxic effects induced by a xenobiotic are due to a cascade of processes including Adsorption at sites of uptake, Distribution to target organs where the toxicant potentially induces a response, and ultimate storage in either the target organ or in any other organ, followed by Metabolization and Excretion (ADME)¹. To make the chain of events even more complicated, it is to be acknowledged that different chemicals commonly follow different pathways, although they might end up in the same storage organ or tissue². The myriad of processes may lead to various adverse effects, which makes it important to understand the mechanistic pathways and the main parameters affecting toxicity. While *in vitro* assays provide only limited information about the ADME of compounds, *in vivo* studies such as with zebrafish embryos provide more in depth insights³ because cells in living organisms communicate and are specialized to perform specific essential functions. Using either *in vitro* or *in vivo* methods, it is key to understand the factors influencing (parts of) the ADME of xenobiotic compounds.

In the case of nanoparticles (NPs), uptake across epithelial membranes is dictated (among other factors) by size, shape and surface charge⁴. Just as for size⁴, both the shape of particles as well as the accessory surface area influence how particles behave in exposure media⁵. Particle aggregation and dissolution for those particles that can dissolve (which is not the case for gold nanoparticles (Au NPs)) are in general the most important fate-determining processes. While size has been shown to influence uptake and biodistribution in zebrafish embryos^{6,7}, the impact of different nano-shapes on biodistribution is less investigated. Particle shape can be an important factor for cellular uptake, circulation time within the organism, and subsequently the biodistribution of nanoparticles⁵. In general, small, elongated nanoparticles are more easily taken up by cells than large and flat individual, non-aggregated particles⁸. This same tendency was found for the endpoint of biodistribution, as nanorods distributed throughout tumor tissues, whereas gold spheres and discs were located only at the surface of the tumor⁹. In addition, nanorods showed the fastest uptake and clearance over spherical and star shaped nanoparticles¹⁰. Moreover, the aspect ratio of rods was found to determine uptake and internal distribution: short rods were taken up faster and were trapped in the liver, while longer rods with a smaller aspect ratio showed lower uptake efficiency and were trapped in the spleen of mice¹¹⁻¹³. Additionally, sharp gold nanostars can pierce the membranes of endosomes and escape to the cytoplasm regardless of their surface chemistry, size or composition^{12,14}.

3

As a noble metal with low toxicity, gold has been an ideal material in nanomedicine for diagnostic and therapeutic purposes such as imaging agents and drug-delivery systems^{12,15,16}. Specifically coating/labeling the gold nanoparticles enables researchers to guide the particles to the desired target⁹. What happens to the gold nanoparticle when the coating or labeling is released is hardly studied, although some studies found that the coating can change¹⁷ and even separate from the particles¹⁸ under *in vivo* conditions. Gold is found to be biocompatible^{16,19}, and its nanoform is categorized as an active and insoluble material which promotes cellular effects and/or mobility in organisms²⁰. Therefore, it can be used as a platform for delivery in nanomedicine and for *in vivo* imaging experiments without major adverse effects. Due to their distinctive plasmonic resonances²¹, high Rayleigh scattering¹⁹, and resistance against photo-bleaching and photo-blinking²¹, are gold particles very suitable for a variety of imaging techniques. Additionally, gold particles can be synthesized relatively easily, with control of their size and shape²¹. The fact that gold nanoparticles are synthesized in different shapes, combined with their inert properties makes gold the perfect material for testing the effect of shape on particle toxicity.

In this study, we aimed to determine the biodistribution and subsequent adverse responses to differently shaped, non-modified gold particles in zebrafish embryos. We used the word trafficking for active movement across the body of the organism, and the word biodistribution for where the Au NPs are located in the ZF embryo at a given time (static measurement 48 hours after exposure). The underlying research questions were:

- (1) Do differently shaped Au NPs induce different biodistribution patterns and hence do they accumulate in different target organs?

To answer this research question, the biodistribution of Au NPs was measured after 2 days of NP exposure. Our assumption is that once particles are accumulated in organs, due to agglomeration they are no longer available for biodistribution since biodistribution is limited to particles and agglomerates smaller than 250 nm²². By imaging after 2 day of exposure the Au NPs can be visualized in the target organs as sufficient uptake of Au NPs is expected to have taken place after this exposure duration without experiencing any morphological malformation^{15,21}.

- (2) What type of trafficking can we identify for Au NPs?

In general, nanoparticle clearance can occur via the hepatobiliary pathway or via the kidneys²³. For the first pathway, uptake by macrophages is essential, whereas

clearance via the urine occurs without intervention of macrophages. By tracking the movement of particles directly after internalization (simulated by microinjection), the initial clearance mechanism of the organism can be visualized.

- (3) Is the difference in biodistribution patterns also reflected in different response patterns?

As shown by previous research²⁴, immune responses, both local and systemic, are valuable endpoints for monitoring biodistribution. We therefore investigated the extent of recognition of the particles by neutrophils and macrophages.

- (4) Is the exposure to Au NPs also translated into effects on the behavior of hatched zebrafish embryos?

In ecotoxicology, assessment of the behavioral response of hatched zebrafish embryos after exposure is a commonly used sub-lethal and sensitive apical endpoint²⁵. By investigating sensitive sub-lethal endpoints, early signs of toxicity can be detected.

2. Material and methods

2.1 Preparation of particle suspensions

Gold nanospheres and nano-urchins with nominal sizes of 60 nm were purchased from Sigma Aldrich (Zwijndrecht, The Netherlands). The particles were suspended in 0.1 mM phosphate buffered saline. Gold nanorods with a nominal size of 40 x 60 nm, stabilized with polyvinylpyrrolidone and suspended in water, were purchased from Nanopartz Inc. (Loveland, USA). Gold nano-bipyramids with a nominal size of 45 x 140 nm were purchased from Nanoseedz, Ltd. (Hong Kong, China). The bipyramids were stabilized with polyethylene glycol in water and rinsed before use with demineralized water. Exposure suspensions were prepared by adding the purchased stock suspensions to egg water (60 µg/ml Instant Ocean Sea Salt, Sera GmbH, Heinsberg, Germany). All dilutions were freshly prepared and sonicated for 10 minutes in an ultrasonic water bath (USC200T, 45kHz, VWR, Amsterdam, The Netherlands), after which the embryos were immediately exposed. For each shape, we selected the diameter (for the urchin from one spike to the opposite spike) as the dimension to be similar in size, namely a range of 45-60nm.

2.2 Physicochemical characterization

The size and morphology of the suspended AuNPs at test concentrations were characterized using transmission electron microscopy (TEM; JEOL 1010, JEOL Ltd., Tokyo, Japan) after 1 hour of incubation in egg water. Dynamic light scattering assessments were performed on a Zetasizer Nano-ZS instrument (Malvern Instruments Ltd, Malvern, UK) to detect the size distribution and zeta-potential of Au NP suspensions in egg water at 0 h, 1 h and 24 h, treating them as if they were spherical particles.

2.3 Experimental setup

2.3.1 Zebrafish husbandry

Zebrafish were handled as described by animal welfare regulations and maintained according to standard protocols (<http://ZFIN.org>). Adult zebrafish were maintained at 25 ± 5 °C in a 14 h: 10 h light-dark cycle. Fertilized zebrafish eggs were obtained from Casper zebrafish (*Danio rerio*), MPEG1.4:mCherry/MPX:GFP zebrafish and KDRL:GFP zebrafish, dependent on the analysis.

2.3.2 Waterborne exposure of zebrafish embryos to Au NPs

The OECD guideline 157 for the standard ZebraFish Embryo Test-protocol²⁶ was modified as described in Van Pomeran et al. (2017b). We used the exposure window from 3 days post fertilization (dpf) till 5 dpf, since this exposure window was found to be associated with the highest amount of uptake⁷. Embryos were exposed to nominal concentrations of 5 mg/L. At this concentration, we expect to obtain sufficient signal for imaging while not observing any morphological malformations^{15,21,28}. As a result, the concentration applied is expected to be too low to observe any sub-lethal effects as well.

2.3.3 Confocal microscopy

During the exposure period, Casper zebrafish embryos were examined daily to check fitness (malformations and mortality) using a dissecting microscope. During the final examination, embryos were rinsed three times with egg water, kept under anesthesia (0.02% Tricaine, Sigma) in egg water and embedded with low melting agarose (CAS 39346-81-1, Sigma Aldrich, Zwijndrecht). Fitness was not affected during this inspection. Final examination was performed using the reflection of Au NPs according

to the method described by Kim et al. (2015)²⁹, using a confocal microscope (Zeiss LSM5 Exciter).

2.3.4 Stereo fluorescence microscopy

Biodistribution and subsequent identification of target organs can be visualized by examination of the immune responses that are locally induced by the particles⁹¹. Similar to the analysis described above and applying the same exposure period, transgenic MPEG1.4:mCherry/MPX:GFP zebrafish embryos were examined daily. During the final examination, embryos were rinsed three times with egg water, kept under anesthesia (0.02% Tricaine, Sigma) in egg water and imaged in an agarose (CAS 9012-36-6, Sigma Aldrich, Zwijndrecht) covered Petri dish. Final examination was performed using the fluorescent signal of the fluorescent-labeled neutrophils (GFP) and the macrophages (mCherry) with a fluorescence stereo microscope (MZ 205 FA, Leica). Doing so, each image contains three channels: bright field, fluorescent green (GFPgreen/neutrophils), and fluorescent red (DRSred/macrophages). Using ImageJ software³⁰, images were assessed for fluorescence intensity and a corrected total cell fluorescence (CTCF) value was calculated³¹.

2.3.5 Two photon multi-focal laser microscopy

In order to investigate the clearance mechanism of the organism, the time dynamics of nanoparticles was tracked in order to follow the clearance. The time dynamics of particle trafficking was visualized with a two photon multi-focal laser microscope³². Using this method, single particles can be followed *in vivo* (supplementary materials (SM)). For this, the particle with the most optimal optical properties was chosen, as this method is only suited for particles with a plasma resonance close to 830 nm. For that reason, we use this method as a proof of principle for nanoparticle trafficking in macrophages. For our selection of particles, the nano-bipyramids showed to be best suited since their plasma resonance was 850 nm. A high, non-environmental relevant concentration (19 mg/L) was selected to guarantee good visibility. To assure high concentrations of particles present in the organism, 3 day old transgenic KDRL:GFP zebrafish embryos were injected in the duct of Cuvier with 2nL nano-bipyramid gold NPs using a Femtojet injector (Eppendorf), half an hour prior to scanning. During the scanning, embryos were kept under anesthesia (0.02% Tricaine) in egg water while

they were embedded in 0.4% low melting agarose. The success of the injections was assessed by looking at the absence of leakage to the yolk and the displacement of blood cells by injection-fluid.

2.3.6 Behavioral analysis

Since gold rarely induces lethal effects at the tested concentration, behavioral analysis was chosen as a more sensitive toxicity endpoint, as commonly used in neurotoxicity²⁵. Before behavioral analysis, all living embryos (120 hpf) were evaluated in terms of normal development, morphological defects and vitality using a stereo dissecting microscope. The behavioral analysis was performed by subjecting the embryos to the light-dark challenge test as modified according to Hua et al. (2014). Low locomotor activity of zebrafish embryos occurred under light exposure (basal phase). A sharp spike of fast swimming activity was induced by a sudden transition to dark, lasting less than 2 s (challenge phase³³). A total of 22 min of recording was used: 10 minutes acclimatization, 4 minutes basal phase, 4 minutes challenge phase and 4 minutes recovery phase. The total distance moved and the velocity of each zebrafish embryo was tracked using the ZebraBox (Viewpoint, Lyon, France) and analyzed using EthoVision software (Noldus Information Technology, Wageningen, The Netherlands).

2.3.7 Statistical analysis

Data of the behavioral test and the immune responses (represented as CTCF) were presented as mean \pm standard error of the mean (SEM). The homogeneity of variance was checked using the SPSS 23 software package. The significance level for all calculations was set at $p < 0.05$. Significant differences between the different exposures within each phase were tested using an one-way analyses of variance (ANOVA) with Tukey's multiple comparison post-test.

3. Results

3.1 Physicochemical characterization

Using TEM images (Figure 1), size and shape of the particles were verified. According to the pictures, no large size deviations nor impurities were observed. This was in agreement with the information received from the producers.

Hydrodynamic size measurements obtained by means of DLS showed little variation over time (Table 1). This was with the exception of the nano-Au bipyramids as these particles did not follow this general pattern and formed aggregates/agglomerates immediately after preparation of the test suspension, which became even larger over time. This observation is probably related to the observation of the zeta potential being close to zero, which is indicative of lack of repulsive forces.

Table 1. Zeta potential and size distribution as measured by DLS of the different gold nanoparticles over time.

	Zeta potential (mV \pm SD)			Size distribution (nm \pm SD)		
	0h	1h	24h	0h	1h	24h
Nanosphere	-24 \pm 2	-28 \pm 4	-18 \pm 5	74 \pm 0	76 \pm 2	79 \pm 0
Nanorod	-27 \pm 1	-28 \pm 0	-11 \pm 1	71 \pm 0	73 \pm 0	79 \pm 3
Nano-urchin	-8 \pm 1	-9 \pm 0	-30 \pm 1	88 \pm 6	98 \pm 6	72 \pm 1
Nano-bipyramid	9 \pm 1	3 \pm 1	-4 \pm 1	501 \pm 45	1158 \pm 151	5014 \pm 2138

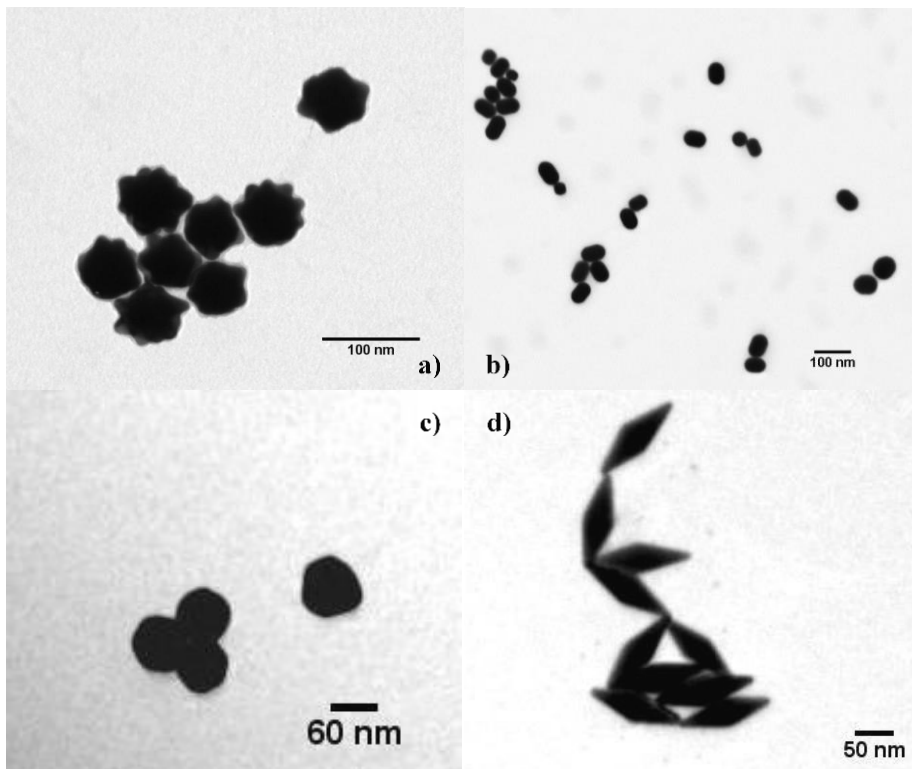


Figure 1. TEM images of the four tested nanogold particles: a) nano-urchins b) nanorods c) nanospheres and d) nano-bipyramids.

3.2 Biodistribution of Au NPs

Using a confocal laser-scanning microscope, clusters of nanoparticles could be visualized in exposed zebrafish embryos. Independent of the shape, every type of particle was observed to be present in the intestinal tract (examples of confocal images of particles in the intestinal tract can be found in the supplementary materials). Nanorods were found to efficiently distribute to other digestive organs of the embryo as well, such as the liver/gallbladder (Figure S1, SM). For most of the particle shapes, clusters were also found in most probably a blood vessel near the eye (Figure 2).

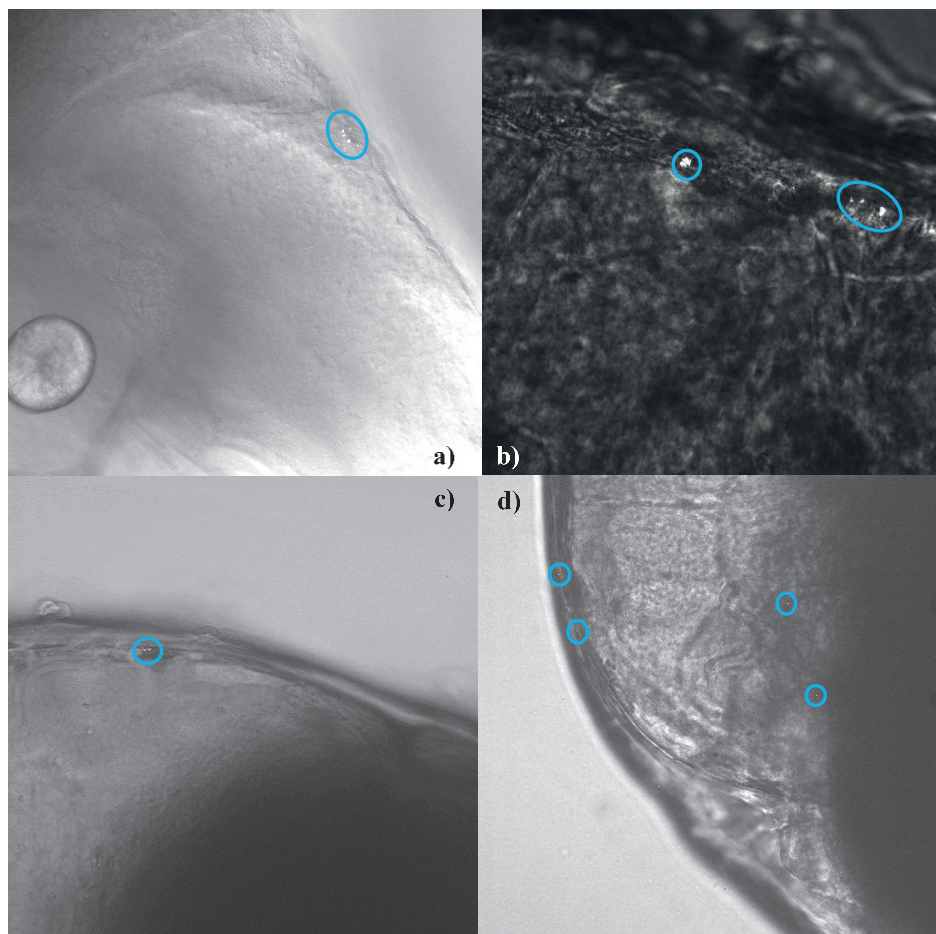


Figure 2. Confocal images showing particle clusters in blood vessels near the eye of the zebrafish embryo (5 dpf) for different nanogold particles: a) nanorods b) nano-urchins c) nanospheres and d) nano-bipyramids.

3.3 Trafficking of Au NPs

For the optical most optimal nanoparticles, the nano-bipyramids, the time dynamics of biodistribution were examined. After intravenous injection, the particles were found to be distributed throughout the tail of the embryo (Figure 3). As can be observed from Figure 3 or even more clearly from the movie (Movie S1, SM), free particles and clusters distributed through the bloodstream. Particles are thereafter phagocytosed by macrophages. A macrophage loaded with particles can be observed in the tissue (confirmed by the fluorescent signal), which moved over the tissue to the vein (Figure 3 and Movie S1, SM). From there, it will go to the liver or spleen to be cleared from the organism³⁴.

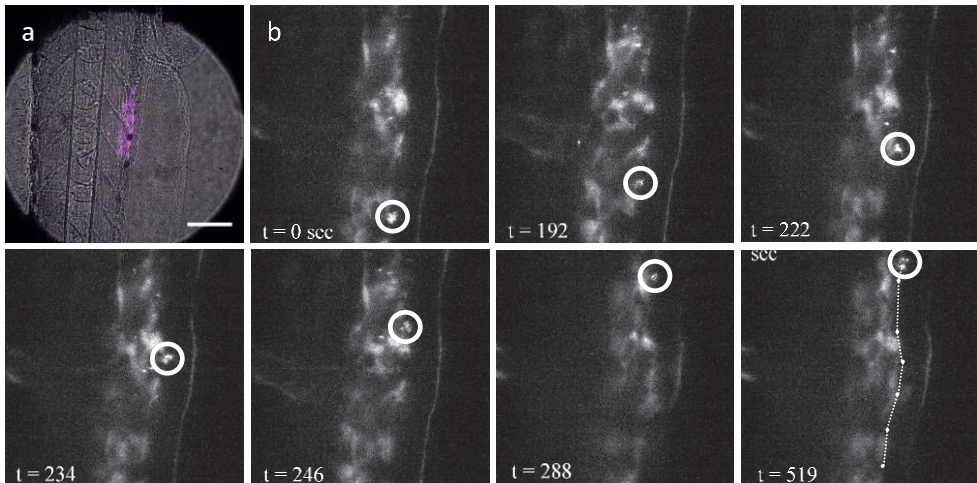


Figure 3. Macrophage filled with gold bipyramids moves along the artery wall after which it is released into the bloodstream. a) Transmission image with emission overlay (magenta) of the imaged region (scale bar 2 μ m). b) Macrophage (white circle) moves along the artery wall, at $t = 519$ seconds the macrophage releases from the artery wall into the bloodstream.

3.4 Immuno-responses

Upon inspection of the response of the immune system of the whole organism and of responses in specific regions (Figure 4 and Figure S2, SM), different response patterns were observed. In case of the neutrophils (Figure 4; a, c, e), the nano-urchins, nanorods and nano-bipyramids did not induce any visible effect on the immune system at the whole organismal scale (Figure 4a) and in the tail (Figure 4c). However, embryos exposed to spherically shaped gold particles induced a reduced amount of neutrophils at the whole organism scale and in the tail region. Examination of the intestine (Figure

4e) learned that more neutrophils were present in embryos that were exposed to rods compared to the control), whereas the embryos exposed to nanospheres again reduced the amount of neutrophils.

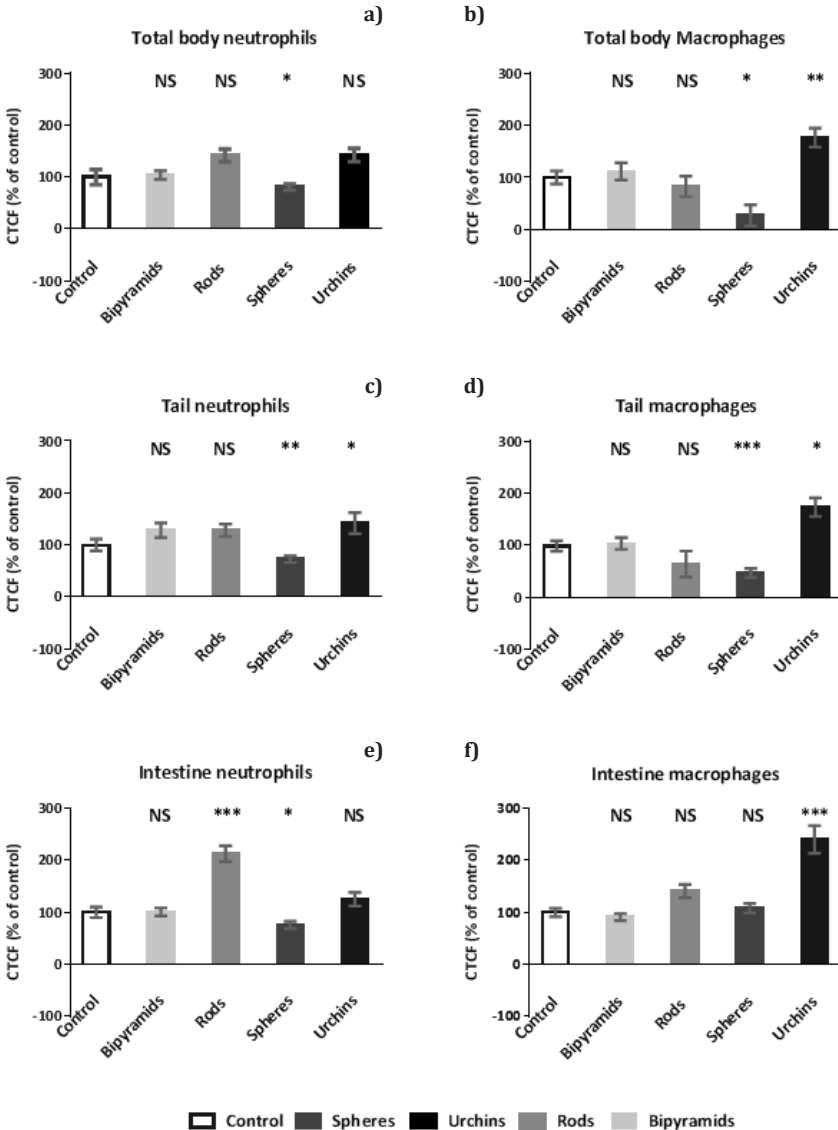


Figure 4. Abundance (relative to control) of neutrophils (a, c and e) and macrophages (b, d and f) in 5 dpf zebrafish embryos after exposure to differently shaped nanogold particles. The abundance in three different sections is provided: Whole organism (a and b), tail section (c and d) and intestine region (e and f). Asterisks indicate statistically significant differences to controls (* $p < 0.05$, ** $p < 0.01$, and *** $p < 0.001$). Data are provided as mean and standard error of the mean ($n=20$).

For the macrophages (Figure 4; b, d, f) at each examination level (whole body (b), tail (d) and intestine (f)) the embryos exposed to urchin shaped nanogold were observed to have a higher level of macrophages. For the embryos that were exposed to spherical nanogold particles, the overall abundance of macrophages was decreased for both the whole body and the tail region, whereas the intestine region had macrophages abundances that were comparable to the control.

Table 2. Percentage of fish that showed high numbers of immune cells in the specified organs ($n=19\pm 1$). Note that one single fish might be scored for multiple organs.

	Gall bladder	Pancreas	Liver
Nanospheres	41 %	35 %	71 %
Nanorods	32 %	74 %	37 %
Nano-urchins	20 %	80 %	5 %
Nano-bipyramids	16 %	79 %	57 %

The differently shaped particles showed different distribution patterns into the main digestive organs: gall bladder, pancreas and liver (Table 2). Embryos that had a high expression of either neutrophils or macrophages in the intestinal region, generally showed high abundance of immune cells in the gallbladder (Figure 5), pancreas and / or liver (Figure 6; different combinations have been observed). The majority of the particles were transported to the pancreas, except for the nanospheres. Nanospheres were predominantly found within the liver. Nanospheres and nano-urchins were thereafter mostly found in the gall bladder, whereas nanorods and nano-bipyramids distributed mostly to the liver.

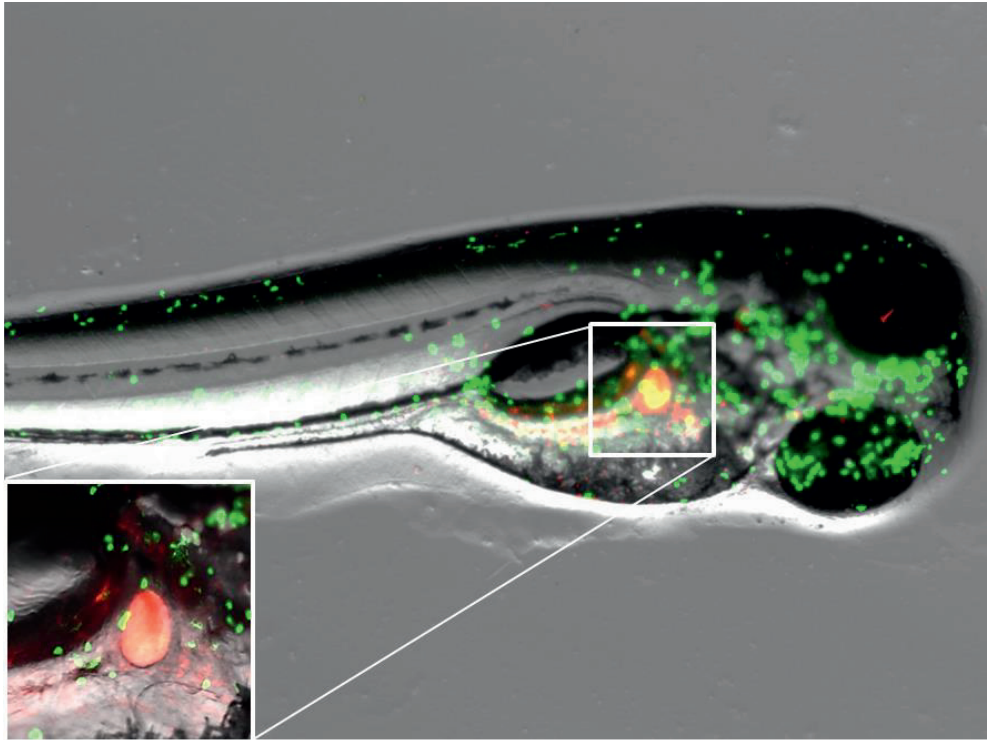


Figure 5. Images of fluorescent neutrophils (green) and macrophages (red) in zebrafish embryos after exposure to gold nano-urchins. The inset is providing further details using 2 times magnification.

The observed distribution patterns (Table 2) were consistent with the observed abundance of immune cells (expressed as CTCF value) in the embryos (Figure 4): the nanorods and nano-urchins showed a high increase of the CTCF value in the intestine region and both shapes showed high abundance of immune cells in the pancreas. In some cases, the immune cells accumulated more at the top of the pancreas, at the islets of Langerhans, rather than accumulating in the whole pancreas (Figure 6).

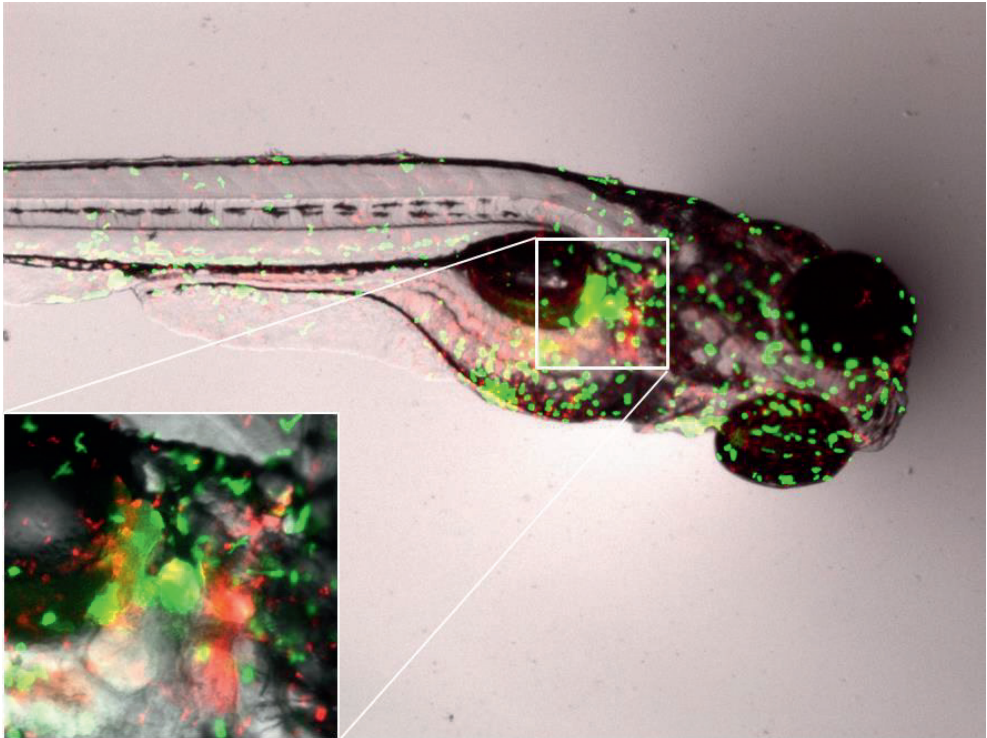


Figure 6. Images of fluorescent neutrophils (green) and macrophages (red) in zebrafish embryos after exposure to gold nano-bipyramids. The inset is providing further details using 6 times magnification.

For the nano-bipyramids, no obvious relation between the total amount of immune cells and the presence of immune cells in specific organs was observed. Exposure to nanospheres induced a reduction in the total amount of immune cells in the body as well as a strong reduction in fluorescent signal in the tail. However, no difference compared to the control was observed in fluorescent signal in the intestine region. This suggests that there was an overall reduction in the amount of immune cells and that the majority of the immune cells were translocated from the tail to the digestive organs and intestine.

3.5 Behavioral response

In order to investigate induced toxic effects related to the shape dependent biodistribution, a behavioral test was performed. The results of the behavior test showed that in the base phase a slight difference was observable with regard to the total distance that the hatched embryo moved (Figure 7). For embryos exposed to urchin

shaped particles, the total distance moved was increased in the base phase whereas the other exposed groups did not show large differences, not even for the nano-bipyramids that also were predominantly found in the pancreas. In addition, accumulation of spherical particles in a high-energy demanding organ as the liver did not reduce the activity of the embryos. In the challenge phase, when stress was induced, embryos exposed to nano-bipyramids showed a reduced movement distance (Figure 7) and subsequent velocity (data not shown). On the other hand, the embryos exposed to nanorods traveled a longer distance per time interval and in total (Figure 7). In the recovery phase, the same tendency for the embryos exposed to nano-urchins as in the base phase was observed, although the effect is not that profound.

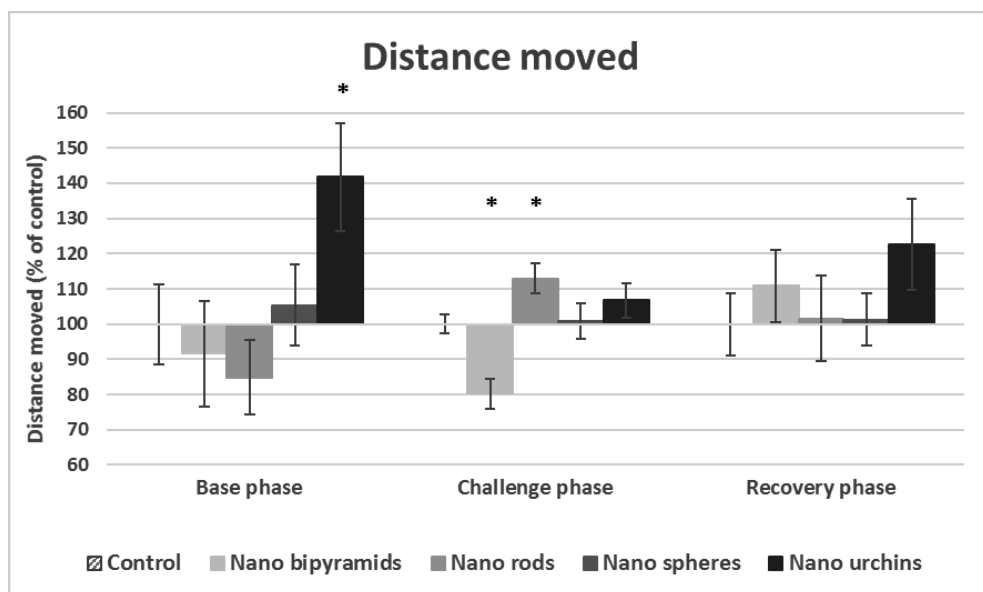


Figure 7. Total distance moved of 5dpf embryos exposed to different nanogold particles. Results are provided per stage of the behavior test (mean and standard error of the mean). Asterisks indicate significant differences to controls (* $p < 0.05$, ** $p < 0.01$, and *** $p < 0.001$).

4. Discussion

The first question we aimed to answer is whether differently shaped Au NPs are differently distributed within zebrafish embryos and whether the NPs reach different target organs. All shapes were found to accumulate on the intestinal mucosa. Yet adsorption to the intestinal mucosa is still not to be considered as either uptake or biodistribution. Evidence of the particles actually crossing the intestinal mucosa is

provided by their presence in other digestive organs (such as the liver and gall bladder) as proven by confocal imaging. It should be noted that all differently shaped gold particles were found to be present in a blood vessel near the eye of the embryo. This is in line with our previous study⁷, using fluorescent polystyrene (PS) particles with comparable size as the Au NPs tested in this study. Exposure to smaller (1.3 nm) Au NPs resulted in disruption of the growth and pigmentation of the eye of the embryos³⁵. Due to high auto-fluorescence levels in the eye in our study, it was not feasible to examine the accumulation of gold in the eye. However, the presence and the mobility of the gold NPs in the blood veins, as shown by both our confocal imaging techniques, indicates a possibility of distribution throughout the organism and thus translocation to the eye.

Typically, xenobiotic particles that are taken up in the blood system are distributed throughout the organism and inflict harm to their host. To reduce or prevent harm, organisms evolved mechanisms to remove these particles from their body. For our second research question, we aimed to identify the clearance mechanism of the particles. As we saw in the time dynamic recording of the nano-bipyramids (Movie S1, SM), particles are taken up by macrophages and thereafter trafficking via the mononuclear phagocytic system (MPS). In general, spherical shaped particles show the fastest clearance rate compared to rod shaped particles¹², thereby favoring the hepatobiliary pathway over clearance via the kidneys^{23,28}. Moreover, the clearance rate is further reduced when the particles are disk- or lamella-shaped¹², become more elongated³⁶, or develop sharp structures¹⁴. Once particles are taken up in macrophages, clearance via the MPS continues via the spleen, liver and eventually via bile trough the gallbladder into the digestive tract and feces³⁴. In 5 dpf zebrafish embryos, the function of the spleen – which is not yet developed – is taken over by the pancreas³⁷. Indeed, the pancreas, liver, gall bladder and digestive tract were found to contain nanoparticles. Just as for PS NPs²⁴, gold particles induced intestinal inflammation. Even more, induced activity of the innate immune system in the digestive organs was observed, which confirms the presence of the particles in these organs. For more in-depth information on the immune response, it might be interesting for future studies to include the macrophage polarization and how this polarization influences the clearance of (differently shaped) particles.

By using the immune response of the embryos, we aimed to answer our third research question: is the biodistribution reflected in different response patterns. Actually, a shape dependent pattern can be observed. Specifically focusing on the gall bladder, liver and pancreas, the distribution of the particles over these organs depends

3

on particle shape. The differences across the distribution patterns indicate that the particles behave slightly different, although they eventually reach the same target organs – yet in different ratios. In *in vitro* studies, the shape of the particle was shown to influence the rate of uptake and the circulation time, and subsequently the target organ¹². Spherically shaped particles are most efficiently taken up compared to their rod and elliptical counterparts¹², whereas particles with sharp edges are capable of escaping the endosome and therewith prolonging their retention time¹⁴. Having a higher circulation time results in a larger probability to reach other target organs rather than the most prominent clearing organ – the liver¹². As a matter of fact, the shape that was found to accumulate the most in the liver was the nanosphere.

The fourth question we aimed to answer is whether the biodistribution is reflected in the organismal behavior responses. The observed differences in the behavior test were only marginally significant and not always repeatable. As stated earlier by Browning et al. (2009), random internal distribution of individual gold nanoparticles into vital organs of the zebrafish can result in effects on the individual level while this is not a concentration dependent effect. After long-term exposure to PS NPs, particles were found to distribute into the brain where they modified brain tissue and subsequently changed behavior³⁸. For that reason, exposure for a longer period might result in the presence of gold NPs in the brain of zebrafish, resulting in abnormal behavior patterns. Additionally, gold particles affecting the eye in early development induced behavioral effects³⁵. With our exposure concentration, we were not able to observe any strong effects on the behavior, indicating that for this exposure period the concentration is too low to induce any behavioral effects. However, the nano-bipyramids reduced the total distance moved in the challenge phase, indicating that the embryos lack the energy to produce the full energy burst as seen in the control group. At the same time, no visible in- or decreases in immune levels were observed. This combination of observations suggests that the total energy budget of the organism is decreased, where the organisms allocates most of their energy to the immune response leaving less energy for locomotive responses. Reduction in locomotive responses is detrimental for the survival of an individual and it might even indicate a possible reduced fecundity due to a lack in energy. So, although we did not find strong effects of any of the gold nanoparticles on the behavior in zebrafish embryos after short exposure time, such effects might occur at higher concentrations, after long-term exposure or after exposure from the fertilization onwards.

Although some minor effects were observed, the different distribution patterns per particle shape did not induce significant sub-lethal effects. Since most studies report no cytotoxicity³⁹ nor toxicity⁴⁰ of gold particles, the absence of significant effects is not surprising. Often within drug delivery systems in which gold nanoparticles are used, surface modifications of the nanoparticles or protein labels are used to assist delivering the particle to the target organ. Over time, it might be likely that those surface modifications become unstable, and fractions of bare particles appear. The absence of sub-lethal effects due to bare and differently shaped gold nanoparticles strengthens the justification for utilizing gold nanomaterials as tracing agents in biodistribution studies and nanomedicine. We echo the suggestion made by Truong et al. (2015), who stated on the basis of studying the biodistribution behavior more closely, that it will become possible to design particles that reach the desired target organ by choosing the appropriate particle shape. In this contribution, we showed that the biodistribution for all differently shaped gold NPs occurs rapidly via the circulatory system. However, harm remains limited, since the particles are distributed via the MPS towards the clearance organs where they are stored before elimination.

Conclusions

Internalized Au NPs were found to traffic throughout the blood system and reach via this medium most probably the whole organism. We observed presence of the particles in and trafficking via macrophages, indicating that the majority of the particles is removed via the MPS. Clearance via the MPS will result in biodistribution of particles in the digestive organs. In our study, exposure to differently shaped gold particles induced shape dependent biodistribution patterns. For each differently shaped particle, we found a different ratio in which they were distributed over the three assessed target organs: liver, gall bladder and pancreas. Although the particles were distributed differently over the examined digestive organs, in none of the cases major sub-lethal effects were observed. The biodistribution patterns indicated that long-term exposure might induce sub-lethal effects being shape-dependent. Finally, for nanosafety assessment, it is eminent that shape-features should be taken into account as a possible toxicity modifying factor as it affects the biodistribution patterns.

Acknowledgements

The authors would like to thank Roel Heutink (CML, Leiden University), Patrick van Hage (Student, Leiden University) and Gerda Lamers (IBL, Leiden University) for their assistance during the experiments, and Nadja Brun (WHOI, USA) for scientific discussions. The staff of the ZF facility of the Cell Observatory is thanked for providing the experimental working environment. Marinda van Pomeran and Martina G. Vijver were funded by NWO-VIDI 864.13.010 granted to Martina G. Vijver. The research described in this work was supported by the European Union's Horizon 2020 research and innovation programme under grant agreement number 760840 'GRACIOUS'.

Supplemental material

Supplemental material can be found on:

<http://dx.doi.org/10.1080/17435390.2018.1564079>

References

- (1) Handy, R. D.; Henry, T. B.; Scown, T. M.; Johnston, B. D.; Tyler, C. R. Manufactured nanoparticles: their uptake and effects on fish--a mechanistic analysis. *Ecotoxicology* **2008**, *17* (5), 396–409.
- (2) Vijver, M. G.; Vink, J. P. M.; Jager, T.; van Straalen, N. M.; Wolterbeek, H. T.; van Gestel, C. A. M. Kinetics of Zn and Cd accumulation in the isopod *Porcellio scaber* exposed to contaminated soil and/or food. *Soil Biol. Biochem.* **2006**, *38* (7), 1554–1563.
- (3) Macrae, C. A.; Peterson, R. T. Zebrafish as tools for drug discovery. *Nat. Publ. Gr.* **2015**, *14* (10), 721–731.
- (4) Carnovale, C.; Bryant, G.; Shukla, R.; Bansal, V. Size, shape and surface chemistry of nano-gold dictate its cellular interactions, uptake and toxicity. *Prog. Mater. Sci.* **2016**, *83*, 152–190.
- (5) Gatoo, M. A.; Naseem, S.; Arfat, M. Y.; Dar, A. M.; Qasim, K.; Zubair, S. Physicochemical properties of nanomaterials: implication in associated toxic manifestations. *Biomed Res. Int.* **2014**, *2014*, 498420.
- (6) Skjolding, L. M.; Ašmonaitė, G.; Jølcck, R. I.; Andresen, T. L.; Selck, H.; Baun, A.; Sturve, J. An assessment of the importance of exposure routes to the uptake and internal localisation of fluorescent nanoparticles in zebrafish (*Danio rerio*), using light sheet microscopy. *Nanotoxicology* **2017**, *11* (3), 351–359.
- (7) van Pomeran, M.; Brun, N. R.; Peijnenburg, W. J. G. M.; Vijver, M. G. Exploring uptake and biodistribution of polystyrene (nano) particles in zebrafish embryos at different developmental stages. *Aquat. Toxicol.* **2017**, *190* (June), 40–45.
- (8) Nazarenu, M.; Zhang, Q.; Soliman, M. G.; del Pino, P.; Pelaz, B.; Carregal-Romero,

- S.; Rejman, J.; Rothen-Rutishauser, B.; Clift, M. J. D.; Zellner, R.; et al. In vitro interaction of colloidal nanoparticles with mammalian cells: What have we learned thus far? *Beilstein J. Nanotechnol.* **2014**, *5*, 1477–1490.
- (9) Black, K. C. L.; Wang, Y.; Luehmann, H. P.; Cai, X.; Xing, W.; Pang, B.; Zhao, Y.; Cutler, C. S.; Wang, L. V.; Liu, Y.; et al. Radioactive ¹⁹⁸Au-doped nanostructures with different shapes for in vivo analyses of their biodistribution, tumor uptake, and intratumoral distribution. *ACS Nano* **2014**, *8* (5), 4385–4394.
- (10) Sangabathuni, S.; Murthy, R. V.; Chaudhary, P. M.; Subramani, B.; Toraskar, S.; Kikkeri, R. Mapping the glyco-gold nanoparticles of different shapes toxicity, biodistribution and sequestration in adult zebrafish. *Sci. Rep.* **2017**, *7* (1), 1–7.
- (11) Huang, X.; Li, L.; Liu, T.; Hao, N.; Liu, H.; Chen, D.; Tang, F. The shape effect of mesoporous silica nanoparticles on biodistribution, clearance, and biocompatibility in vivo. In *ACS Nano*; 2011; Vol. 5, pp 5390–5399.
- (12) Truong, N. P.; Whittaker, M. R.; Mak, C. W.; Davis, T. P. The importance of nanoparticle shape in cancer drug delivery. *Expert Opin. Drug Deliv.* **2015**, *12* (1), 1–14.
- (13) Qiu, Y.; Liu, Y.; Wang, L.; Xu, L.; Bai, R.; Ji, Y.; Wu, X.; Zhao, Y.; Li, Y.; Chen, C. Surface chemistry and aspect ratio mediated cellular uptake of Au nanorods. *Biomaterials* **2010**, *31* (30), 7606–7619.
- (14) Chu, Z.; Zhang, S.; Zhang, B.; Zhang, C.; Fang, C.-Y.; Rehor, I.; Cigler, P.; Chang, H.-C.; Lin, G.; Liu, R.; et al. Unambiguous observation of shape effects on cellular fate of nanoparticles. *Sci. Rep.* **2014**, *4*, 4495.
- (15) Khlebtsov, N.; Dykman, L. Biodistribution and toxicity of engineered gold nanoparticles: a review of in vitro and in vivo studies. *Chem. Soc. Rev.* **2011**, *40* (3), 1647–1671.
- (16) Takeuchi, I.; Nobata, S.; Oiri, N.; Tomoda, K.; Makino, K. Biodistribution and excretion of colloidal gold nanoparticles after intravenous injection: Effects of particle size. *Biomed. Mater. Eng.* **2017**, *28* (3), 315–323.
- (17) Simpson, C. A.; Huffman, B. J.; Gerdon, A. E.; Cliffel, D. E. Unexpected toxicity of monolayer protected gold clusters eliminated by PEG-thiol place exchange reactions. *Chem. Res. Toxicol.* **2010**, *23* (10), 1608–1616.
- (18) Bogdanov, A. a; Gupta, S.; Koshkina, N.; Corr, S. J.; Zhang, S.; Curley, S. a; Han, G. Gold Nanoparticles Stabilized with MPEG-Grafted Poly(l -lysine): in Vitro and in Vivo Evaluation of a Potential Theranostic Agent. *Bioconjug. Chem.* **2015**, *26* (1), 39–50.
- (19) Browning, L. M.; Lee, K. J.; Huang, T.; Nallathamby, P. D.; Lowman, J. E.; Nancy Xu, X.-H. Random walk of single gold nanoparticles in zebrafish embryos leading to stochastic toxic effects on embryonic developments. *Nanoscale* **2009**, *1* (1), 138.
- (20) Arts, J. H.; Hadi, M.; Irfan, M. A.; Keene, A. M.; Kreiling, R.; Lyon, D.; Maier, M.; Michel, K.; Petry, T.; Sauer, U. G. A decision-making framework for the grouping and testing of nanomaterials (DF4nanoGrouping). *Regul. Toxicol. Pharm.* **2015**,

- 71 (2), S1–S27.
- (21) Mesquita, B.; Lopes, I.; Silva, S.; Bessa, M. J.; Starykevich, M.; Carneiro, J.; Galvão, T. L. P.; Ferreira, M. G. S.; Tedim, J.; Teixeira, J. P.; et al. Gold nanorods induce early embryonic developmental delay and lethality in zebrafish (*Danio rerio*). *J. Toxicol. Environ. Heal. - Part A Curr. Issues* **2017**, *80* (13–15), 672–687.
- (22) Bruinink, A.; Wang, J.; Wick, P. Effect of particle agglomeration in nanotoxicology. *Arch. Toxicol.* **2015**, *89* (5), 659–675.
- (23) Kumar, R.; Roy, I.; Ohulchanskyy, T. Y.; Vathy, L. a; Bergey, E. J.; Sajjad, M.; Prasad, P. N. In vivo biodistribution and clearance studies using multimodal organically modified silica nanoparticles. *ACS Nano* **2010**, *4* (2), 699–708.
- (24) Brun, N. R.; Koch, B. E. V.; Varela, M.; Peijnenburg, W. J. G. M.; Spaink, H. P.; Vijver, M. G. Nanoparticles induce dermal and intestinal innate immune system responses in zebrafish embryos. *Environ. Sci. Nano* **2018**, *5* (4), 904–916.
- (25) Legradi, J.; el Abdellaoui, N.; van Pomeran, M.; Legler, J. Comparability of behavioural assays using zebrafish larvae to assess neurotoxicity. *Environ. Sci. Pollut. Res.* **2015**, *22* (21), 16277–16289.
- (26) OECD. *Validation report (phase 1) for the zebrafish embryo toxicity test, part I*; 2011.
- (27) van Pomeran, M.; Peijnenburg, W.; Brun, N.; Vijver, M. A novel experimental and modelling strategy for nanoparticle toxicity testing enabling the use of small quantities. *Int. J. Environ. Res. Public Health* **2017**, *14* (11), 1348.
- (28) Pan, Y.; Leifert, A.; Graf, M.; Schiefer, F.; Thoröe-Boveleth, S.; Broda, J.; Halloran, M. C.; Hollert, H.; Laaf, D.; Simon, U.; et al. High-sensitivity real-time analysis of nanoparticle toxicity in green fluorescent protein-expressing zebrafish. *Small* **2013**, *9* (6), 863–869.
- (29) Kim, C. S.; Li, X.; Jiang, Y.; Yan, B.; Tonga, G. Y.; Ray, M.; Solfiell, D. J.; Rotello, V. M. Cellular imaging of endosome entrapped small gold nanoparticles. *MethodsX* **2015**, *2*, 306–315.
- (30) Schindelin, J.; Arganda-Carreras, I.; Frise, E.; Kaynig, V.; Longair, M.; Pietzsch, T.; Preibisch, S.; Rueden, C.; Saalfeld, S.; Schmid, B.; et al. Fiji: an open-source platform for biological-image analysis. *Nat. Methods* **2012**, *9* (7), 676–682.
- (31) Balasubramanian, V.; Srinivasan, R.; Miskimins, R.; Sykes, A. G. A simple azacrown ether containing an anthraquinone fluorophore for the selective detection of Mg(II) in living cells. *Tetrahedron* **2016**, *72* (1), 205–209.
- (32) van den Broek, B.; Ashcroft, B.; Oosterkamp, T. H.; van Noort, J. Parallel nanometric 3D tracking of intracellular gold nanorods using multifocal two-photon microscopy. *Nano Lett.* **2013**, *13* (3), 980–986.
- (33) Hua, J.; Vijver, M. G.; Ahmad, F.; Richardson, M. K.; Peijnenburg, W. J. G. M. Toxicity of different-sized copper nano- and submicron particles and their shed copper ions to zebrafish embryos. *Environ. Toxicol. Chem.* **2014**, *33* (8), 1774–

1782.

- (34) Huwyler, J.; Kettiger, H.; Schipanski, A.; Wick, P. Engineered nanomaterial uptake and tissue distribution: from cell to organism. *Int. J. Nanomedicine* **2013**, *8*, 3255.
- (35) Kim, K. T.; Zaikova, T.; Hutchison, J. E.; Tanguay, R. L. Gold nanoparticles disrupt zebrafish eye development and pigmentation. *Toxicol. Sci.* **2013**, *133* (2), 275–288.
- (36) Sun, L.; Li, Y.; Liu, X.; Jin, M.; Zhang, L.; Du, Z.; Guo, C.; Huang, P.; Sun, Z. Cytotoxicity and mitochondrial damage caused by silica nanoparticles. *Toxicol. Vitr.* **2011**, *25* (8), 1619–1629.
- (37) Danilova, N.; Steiner, L. A. B cells develop in the zebrafish pancreas. *Proc. Natl. Acad. Sci.* **2002**, *99* (21), 13711–13716.
- (38) Mattsson, K.; Ekvall, M. T.; Hansson, L.-A.; Linse, S.; Malmendal, A.; Cedervall, T. Altered behavior, physiology, and metabolism in fish exposed to polystyrene nanoparticles. *Environ. Sci. Technol.* **2015**, *49* (1), 553–561.
- (39) Chen, Y.; Xu, Z.; Zhu, D.; Tao, X.; Gao, Y.; Zhu, H.; Mao, Z.; Ling, J. Gold nanoparticles coated with polysarcosine brushes to enhance their colloidal stability and circulation time in vivo. *J. Colloid Interface Sci.* **2016**, *483*, 201–210.
- (40) Asharani, P. V.; Lianwu, Y.; Gong, Z.; Valiyaveetil, S. Comparison of the toxicity of silver, gold and platinum nanoparticles in developing zebrafish embryos. *Nanotoxicology* **2011**, *5* (1), 43–54.



Confocal image of a prepared control ZF embryo gall bladder

Chapter 4

A novel experimental and modelling strategy for nanoparticle toxicity testing enabling the use of small quantities

4

Marinda van Pomerén, Willie J.G.M. Peijnenburg, Nadja R. Brun, Martina G. Vijver.

- ¹ *Institute of Environmental Sciences (CML), Leiden University, P.O. Box 9518, 2300 RA Leiden, The Netherlands; willie.peijnenburg@rivm.nl (W.J.G.M.P.); n.r.brun@cml.leidenuniv.nl (N.R.B.); vijver@cml.leidenuniv.nl (M.G.V.)*
- ² *National Institute of Public Health and the Environment, P.O. Box 1, 3720 BA Bilthoven, The Netherlands*

Published in *International Journal of Environmental Research and Public Health* 2017, DOI: 10.3390/ijerph14111348

Abstract

4

Metallic nanoparticles (NPs) differ from other metal forms with respect to their large surface to volume ratio and subsequent inherent reactivity. Each new modification to a nanoparticle alters the surface to volume ratio, fate and subsequently the toxicity of the particle. Newly-engineered NPs are commonly available only in low quantities whereas, in general, rather large amounts are needed for fate characterizations and effect studies. This challenge is especially relevant for those NPs that have low inherent toxicity combined with low bioavailability. Therefore, within our study, we developed new testing strategies that enable working with low quantities of NPs. The experimental testing method was tailor-made for NPs, whereas we also developed translational models based on different dose-metrics allowing to determine dose-response predictions for NPs. Both the experimental method and the predictive models were verified on the basis of experimental effect data collected using zebrafish embryos exposed to metallic NPs in a range of different chemical compositions and shapes. It was found that the variance in the effect data in the dose-response predictions was best explained by the minimal diameter of the NPs, whereas the data confirmed that the predictive model is widely applicable to soluble metallic NPs. The experimental and model approach developed in our study support the development of (eco)toxicity assays tailored to nano-specific features.

1. Introduction

Nowadays, the field of nanotechnology is accelerating in fabricating specifically engineered nanoparticles (NPs) which meet consumer needs. Economists predict, for the period from 2015 to 2020, an annual medial turnover of up to \$3 trillion¹. Next to first-generation NPs consisting of mono-elemental single sized nanomaterials, nowadays, complex nano-sized compounds, such as composites or oddly-shaped nanoparticles, are synthesized. For all these emerging NPs, information on fate and toxicity is vital knowledge to warrant the design of NPs that are safe for humans and the environment.

There are, nevertheless, concerns regarding NP-specific modifications needed for proper toxicity testing of NPs^{2,3}. A first challenge with regard to NPs is that they often are synthesized in small quantities, especially in the design and testing phases of product development. Standard testing guidelines based on soluble chemicals, such as those prescribed by the OECD (Organization for Economic Co-operation and Development)⁴, typically prescribe a vast amount of compound to be used in at least five test concentrations having twenty replicates. In the case of zebrafish embryo testing, a minimum of 2 mL exposure medium per replicate is needed in common practice (guideline 236, 2013)⁴. The exposure medium should be refreshed daily during the testing, whilst the maximum test duration is six days. This sums up to 240 mL of exposure suspension for each concentration to be tested and implies that, for instance, for testing a concentration of 1000 mg/L only (as often done in toxicity testing⁵), 240 mg of compound is needed. For a full range of five concentrations up to 1000 mg/L, this adds up to 720 mg of compound. On top of this, quite some additional material is needed for fate characterization and assessment of the physicochemical properties of the NPs. After all, not only the chemical fate of the NP should be determined, but also the colloidal and particle fate and behavior. Size determination of the colloids in solution (via dynamic light scattering assessment) commonly requires 10 mg of the NPs, including samples for transmission electron microscopy pictures. The measurements of the total concentration demands for a minimum of 25 mg of the NPs, followed by the same amount of the NPs needed to measure the ion concentration in the samples. This adds up to additional amount of at least 60 mg for chemical assessments. Overall, the amount of NPs needed to generate the very basic data regarding the fate and effect profile, strongly exceeds the quantities of material typically available in the initial research and development (R and D) phases. Hence, novel strategies are needed to reduce these amounts as much as possible.

The second challenge is the fact that debate is still ongoing regarding the question: which dose metric to use in order to properly express toxicity of NPs? Given the differences in size and shape of NPs and subsequent impacts of these properties on particle toxicity, it is unlikely that the mass of NPs administered is a proper descriptor of the actual dose causing toxicity^{6,7}.

The third challenge is that only rarely acute effects due to exposure to NPs are shown. Therefore, the determination of responses requires either availability of modified experimental protocols enabling to screen more sensitive sub-lethal endpoints, or increased modeling efforts that allow prediction of sub-lethal effects of hitherto non-tested NPs. With modeling effort, data gaps can be filled via interpolating approaches using similarity analysis⁸ and eventually extrapolated between species via toxicity relationship assessments⁹.

In view of these challenges, the aim of our study was to develop novel testing strategies that allow for efficient fate and toxicity assessments that require only small amounts of testing materials whilst achieving the same sensitivity with regard to the assessment of the endpoints of toxicity as in the corresponding standardized OECD tests. Previously, attempts were already made to reduce the amount of material needed^{10,11}, and these attempts are further improved in this study. Our study aimed to: (a) develop new experimental testing strategies enabling to work with low quantities of NPs; (b) determine the best dose-metric to describe the toxicity of particles, and (c) develop translational models for dose-response predictions for NPs even for those NPs that are classified as inducing low toxicity.

Experiments were conducted using three differently shaped Ag NPs. Since Ag NPs were found to display relative high rates of ion release, they are a clear example of non-stable metallic NPs. Ag NPs are classified as being toxic with LC₅₀ values between 1 and 10 mg/L¹². Experiments were also conducted with TiO₂ NPs. These NPs are known to be chemically inert, thus allowing to test suspensions of stable metallic NPs as opposed to the tests performed with metallic NPs that dissolve during testing (non-stable NPs). TiO₂ is classified to be harmful to the ecosystem (LC₅₀ value between 10 and 100 mg/L¹²). By comparing the predictive power of the translational models for non-stable NPs with predictions made for stable metallic NPs, the applicability of the model to a wide range of NPs was tested. The results obtained for non-spherical NPs are discussed in view of the development of a regulatory framework to assess the safety of manufactured nanomaterials.

2. Materials and Methods

2.1. Preparation of Particle Suspensions

Spherical Ag NPs with nominal size of 20 nm (nominal surface to volume ratio 0.3) were purchased from SkySpring Nanomaterials, Inc. (Houston, TX, USA). A suspension of Ag nanoplates was obtained from Moscow State University (Moscow, Russia). Elongated Ag rods with a nominal size of 50 nm × 0.6 to 12 μm (nominal surface to volume ratio of 0.08) in suspension were purchased from Fraunhofer ISC (Würzburg, Germany). Spherical TiO₂ NPs with a nominal size of 20 nm (nominal surface to volume ratio 0.3) were obtained from Io-Li-Tec nanomaterials (Heilbronn, Germany). Bipyramidal TiO₂ NPs and TiO₂ nanoplates were obtained from the Centre of BioNano Interaction (University College Dublin, Ireland). The Ag nanospheres and nanoplates were coated with PVP (polyvinylpyrrolidone), and all other NPs were uncoated. Stock solutions were prepared by weighing dry powdered Ag or TiO₂ particles and adding them into egg water (consisting of 60 μg/mL Instant Ocean Sea Salt, Sera Marin, in Milli-Q water, pH 6.5–7.0). Ag⁺ solutions were obtained by adding silver nitrate (AgNO₃: CAS 7761-88-8, Sigma Aldrich, Zwijndrecht, The Netherlands) to egg water. All stock solutions were freshly prepared and sonicated for 10 min in an ultrasonic water bath (USC200T, VWR, Amsterdam, The Netherlands). Prepared stock suspensions or manufactured suspensions were diluted using egg water and embryos were exposed immediately after preparation.

2.2. Physicochemical Characterization

The size and morphology of the suspended Ag NPs and TiO₂ NPs were characterized using transmission electron microscopy (TEM; JEOL 1010, JEOL Ltd., Tokyo, Japan) after 1 h of incubation in egg water. Dynamic light scattering assessments were performed on a Zetasizer Nano-ZS instrument (Malvern Instruments Ltd., Malvern, UK). The assessments allowed detection of the size distribution and the zeta-potential of Ag and TiO₂ suspensions in egg water at 1 h and 24 h.

The concentrations of dissolved Ag ions and Ag NP_(total) in egg water were analyzed using flame atomic absorption spectroscopy (AAS; Perkin Elmer 1100B, Waltham, MA, USA). Freshly-prepared dispersions ($t = 0$ h) and dispersions equilibrated for 24 h were used for this purpose. HCl (CAS 7647-01-0, Sigma Aldrich, Zwijndrecht, The Netherlands) was added to avoid loss of Ag due to precipitation and sorption to the wall of the vials. To

determine concentrations of dissolved Ag ions in the particle suspensions, 7.5 mL of the supernatant was sampled after centrifugation of Ag NP suspensions at $5000\times g$ for 10 min to remove NPs and ultimately determine the soluble silver fraction in the solution¹³.

Titanium concentrations in the suspensions of nanoplates and nanobipyramids were analyzed following digestion with aqua regia (HCl: CAS 7647-01-0; HNO₃: CAS 7697-37-2, Sigma Aldrich, Zwijndrecht, The Netherlands) and are determined using ICP-OES (Vista-MPX, Varian Inc., Santa Clara, CA, USA). The centrifugation step to determine ion concentrations in suspension was not included for TiO₂ NPs because TiO₂ particles do not undergo dissolution in aquatic suspensions¹⁴. Ti concentrations were measured immediately after preparation of the suspensions (0 h) and 24 h after preparation.

2.3. Experimental Setup

The OECD guideline 236 was modified as described in detail below. The modified experimental design uses in total roughly 1% of the amount of chemical required by the standard zebrafish embryo test protocol⁴.

2.4. Zebrafish Husbandry

Zebrafish were handled as described by animal welfare regulations established in 2014 and they were maintained according to standard protocols (<http://ZFIN.org>). Adult zebrafish were maintained at 25 ± 5 °C in a 14 h light: 10 h dark cycle. Fertilized zebrafish eggs were obtained from an AB/TL wild-type zebrafish.

2.5. Toxicity Assay for Ag NPs

An acute exposure regime of 120 h was used, from 24 h post fertilization (hpf) to 144 hpf, thus including exposure during all major stages of embryonic development. The background mortality at 24 hpf was less than 10% (data not shown). The first adjustment to the OECD guideline is by following the protocol of Hua et al. (2014)¹⁵, starting the exposure at 24 hpf. Thereafter, instead of transferring one embryo per well of a 24-well plate, 10 zebrafish embryos were distributed into each well of a 24-well plate in 2 mL of freshly prepared egg water containing a negative control, various concentrations of AgNO₃ or various concentrations of Ag NP suspensions. One well was used per concentration. The nominal concentration range for the spherical NPs was 5

to 100 mg/L; the dilution factors for plates and elongated rods ranged from three to 30,000 times; the nominal concentration range for AgNO₃ was 48 to 480 µg/L. Throughout the exposure, embryos and suspensions were kept at a temperature of 28 ± 0.8 °C. The exposure media were replaced with a freshly prepared suspension of NPs every day according to the OECD guideline 236⁴, except for days 4 (96 hpf) and 5 (120 hpf). The renewal procedure was shown not to increase NP concentrations over time⁶. Before each renewal, and at the end of the experiment, embryos were evaluated for morphological defects and death. All experiments were performed in triplicate. To verify the validity of our results obtained with the modified experimental protocol enabling to work with small amounts, we compared Cu NP data acquired with the modified test protocol to results obtained using existing methods as described by Hua et al. (2014)¹⁵, see Supplementary material (SM, Figure S1).

2.6. Toxicity Assay for TiO₂ NP

TiO₂ NPs were tested at a nominal concentration range from 10 to 1000 mg/L, using the same exposure conditions as described above for Ag NPs. The experiments with TiO₂ NPs were performed under a commonly-used light-dark regime (14:10 h) and in addition using UV-light illumination using ultraviolet-a light (350 nm) with an intensity of approximately 1700 µW cm⁻³ for 14 h¹⁶. Temperature was maintained at 28 ± 0.8 °C during the experiments. All experiments were performed in triplicate.

2.7. Behavioral Analysis for TiO₂ NPs

Before behavioral analysis, all living embryos (144 hpf) were evaluated in terms of normal development, morphological defects, and vitality using a stereo dissecting microscope. The behavioral analysis was performed by subjecting the embryos to the light–dark challenge test as modified according to Hua et al. (2014)¹⁰. Zebrafish embryos have a low locomotor activity under light exposure (basal phase). Sudden transition to dark induces a sharp spike of fast swimming activity lasting less than 2 s (challenge phase¹⁰). A total of 22 min of recording was used (SI, Figure S3): 10 min acclimatization, 4 min basal phase, 4 min challenge phase, and 4 min recovery phase. The total distance moved of each zebrafish embryo was tracked using the Zebrabox (Viewpoint, Lyon, France) and analyzed using VideoTrack software (Version 12, Viewpoint, Lyon, France).

2.8. Modeling

2.8.1. Dose-Response Curves

Observational data of the fish embryos as obtained at 144 hpf were used to determine dose-response relationships—using mortality data and the sub-lethal malformation endpoints. For calculating lethal and sub-lethal effect concentrations, a sigmoidal dose-response model was used, available from the SPSS 23 software package (IBM, Armonk, NY, USA).

2.8.2. Contribution to Toxicity of Ag Particles and Ions

An AgNO₃ solution was used to quantify the toxicity of Ag ions to zebrafish embryos. This allowed us to determine the effect of the dissolved ion fraction in the solution (Ag NP_{ion}; as measured with AAS. The toxicity of the suspension (Ag NP_{total}) to zebrafish embryos was determined as being the sum of the response of the suspended particles (Ag NP_{particle}) and the response of the dissolved ions (Ag NP_{ion}). We applied the concept of response addition¹⁷ as already used by Hua et al. (2014)¹⁵ to compute the joint toxicity of metal ions shed from particles and nanoparticles. The response addition model is used because Ag ions and Ag NPs are assumed to elicit a response through different mechanisms. The model can be depicted as:

$$E_{\text{total}} = 1 - [(1 - E_{\text{ion}})(1 - E_{\text{particle}})] \quad (1)$$

where E_{total} , E_{ion} , and E_{particle} represent the mortality of zebrafish embryos caused by the exposure to Ag NP_{total}, Ag NP_{ion}, and Ag NP_{particle} (scaled from 0 to 1), respectively.

2.8.3. Dose Metric Descriptors for the Translational Models

Dose metrics to be used within the dose-response modelling were chosen to be: minimal diameter, surface area, effective diameter, and surface to volume ratio. In each case, actual size information (obtained via TEM images) of the metallic NPs was used. When agglomeration occurred, identifiable single NPs present as commonly present on the surface of the agglomerates were used for size measurements. Only pristine sizes as derived from the TEM images were used for modeling, as is common for i.e., nano-QSAR (Quantitative Structure–Activity Relationship¹²) and nano-QRA (quantitative read-across⁸). For each dose metric, the parameter values were calculated based upon the diameter (d), length (l), and width (w) of the particles. For each metallic NP,

multiple particles ($n = 15$ to 25) were measured and average values were used. The formulas used for calculating surface area and volume of differently shaped NPs can be found in the supplementary material, Table S1.

In order to use dose metrics in the translational models, we tested the following hypotheses: (i) NP toxicity increases with increasing total surface area; (ii) toxicity of the NP decreases upon increasing the smallest diameter as explained below (minimal diameter); (iii) toxicity decreases with increasing NP diameter calculated on the basis of the volume of the particles, independent of shape (effective diameter); and (iv) toxicity of NPs increases with increasing surface to volume ratio of the particles.

2.8.4. Toxicity Prediction

Experimentally-obtained response data were plotted against the four dose metrics used. At first, the dose metric was expressed based on the total surface area of the particle¹⁸, as based on the hypothesis that a higher total surface area represents more reactive surface area.

Secondly, for spherical and non-spherical particles, the dose metric was expressed as the minimal diameter in any dimension of the particle. It is hypothesized that the ability to penetrate into cells increases with decreasing minimal diameter^{19,20}.

Thirdly, the dose metric of spherical and non-spherical particles was determined by using the volume of the particle to calculate a fictional spherical diameter²¹. This effective diameter is reflected by the diameter of a spherical particle with the same volume. Here, too, it was assumed that NPs with small diameters have a higher ability to penetrate cells.

Fourthly, the dose metric was expressed as the surface to volume ratio of the NP. Both decreasing size and differences in particle shape modify the surface to volume ratio. Similar to total surface area, here an increasing ratio implies a larger reactive surface and, hence, increased toxicity¹³.

For each parameter, a linear regression model was developed for the Ag NPs used in this study. Similar to the Ag NP_{particle} data, secondary data^{10,15,22-24} collected for Ag NP_{particle}, Cu NP_{particle}, Ni NP_{particle}, and ZnO NP_{particle} were plotted as a function of the different dose metrics. The obtained linear dose metric relations for the non-stable metals Ag NP, Cu NP, Ni NP, and ZnO NP were used to calculate an overall linear regression coefficient \pm standard deviation. Each regression line as obtained for the individual metallic NPs was

4

given equal weight. In addition, a p -value was calculated indicating whether the initial slopes of the regression lines obtained for the Ag NPs, Cu NPs, Ni NPs and ZnO NPs differed significantly. Similarity of slope is assumed to reflect the appropriateness of a dose metric to predict toxicity across metallic NPs. Thereupon, the intercepts of the individual regression equations were calculated as these reflect the intrinsic reactivity of metallic NPs. Using the overall linear regression coefficients thus obtained, and based upon the limited availability of experimental data on TiO₂ toxicity, the intercept of the dose metric relation of TiO₂ NPs was calculated, after which LC₅₀-values of TiO₂ nanobipyramids and nanospheres were predicted.

2.8.5. Statistical Analysis

Significant differences between the newly-developed and already-existing testing protocols¹⁵ were tested using a two-tailed T-test. Data collected on the behavioral test were presented as mean \pm standard error of the mean (SEM). The homogeneity of variance was checked using the SPSS 23 software package (Version 23, IBM, Amsterdam, The Netherlands). The significance level for all calculations was set at $p < 0.05$. Significant differences between the different exposures within each phase were tested using a one-way analyses of variance (ANOVA) with Tukey's multiple comparison post-test. Dose-metric linear regression modeling was performed using Prism (Version 7, GraphPad, La Jolla, California, USA), followed by comparison of the aligning of the regressions developed for the different metallic NPs (comparable with an ANCOVA), using the same software. The limit of significance was set at $p < 0.01$ to account for the low numbers of experimental data that were typically available for generating the regression lines.

3. Results

3.1. Physico-Chemical Characterization of Ag NPs and TiO₂ NPs

3.1.1. Transmission Electron Microscopy and Dynamic Light Scattering

TEM images showing size, shape, and clustering of the NPs after 1 h of incubation in egg water are given in Figure 1.

Large aggregates/agglomerates were formed immediately after the NPs were suspended in egg water. The PVP coated nanospheres aggregated/agglomerated to the

largest extent. This general behavior was also evident from the size distribution patterns, with an average size of the Ag NP aggregates/agglomerates that was 43 times larger than the actual size of the individual NPs (Table S2, SM). PVP-coated Ag nanoplates responded differently and showed an aggregation/agglomeration size of only three times the actual individual NP size. Aggregates/agglomerates of TiO₂ NPs were even larger, with average aggregate/agglomerate sizes being 56 times the size of the individual NPs. The zeta-potential of all NPs ranged between -30 to +0.6 mV over the test period and none of the zeta-potentials of the NPs changed significantly over time. Ag nanoplates appeared to contain Ag nanorods as well (see Figure 1b) in a number ratio of 10:90. Both shapes were, therefore, included into the calculation of the average surface to volume ratio.

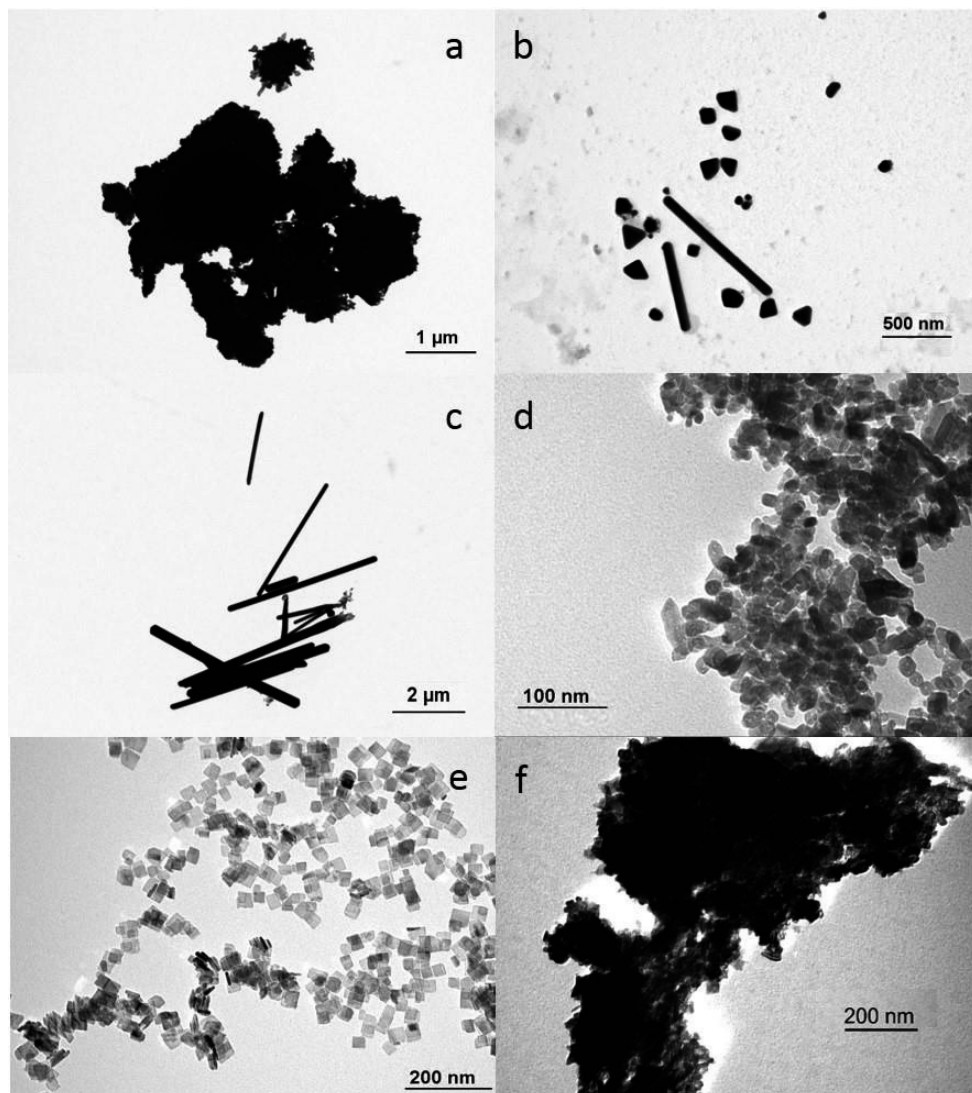


Figure 1. TEM images of (a) Ag nanospheres; (b) Ag nanoplates; (c) Ag elongated nanorods; (d) TiO₂ nanobipyramids; (e) TiO₂ nanoplates; and (f) TiO₂ nanospheres.

3.1.2. Metal Concentrations and Ion Release

As can be seen in Table 1, there was slight dissolution of Ag NPs after suspension. The amount of Ag ions released was related to the total concentrations measured (Table 1), and the shape of the Ag NPs was found to influence the extent of ion release. Nanoplates displayed the highest extent of dissolution, followed by nanospheres, whereas elongated nanorods released the lowest amount of Ag ions.

Table 1. Actual concentrations of Ag NPs and TiO₂ NPs in suspension at 0 and 24 h. For each dilution step, total concentration (NP_{total}), dissolved ion concentration (NP_{ion}) at 0 h, and total concentration (NP_{total}) at 24 h are displayed for each NP tested.

Particles	Dilution	NP_{total} concentration 0 h (mg/L)	NP_{ion} concentration 0 h (mg/L)	NP_{total} concentration 24 h (mg/L)
Ag nanospheres	1	17.20	0.83	2.28
PVP coated	2	11.40	0.17	2.04
	10	3.50	≤ 0.016	0.62
Ag nanoplates	30	14.00	1.50	9.35
PVP coated	100	0.06	≤ 0.016	0.02
	3000	≤ 0.016	≤ 0.016	0.09
Ag elongated nanorods	30	328.00	0.22	4.30
	100	1.21	0.028	0.10
	3000	0.41	0.028	0.19
TiO ₂ nanoplates	1	22.7	-	0.10
	10	2.17	-	0.09
	100	0.28	-	0.05
TiO ₂ nanobipyramids	1	20.7	-	0.08
	10	0.70	-	0.15
	100	0.18	-	0.08
TiO ₂ nanospheres	1	50.9	-	0.20
	10	-	-	-
	100	-	-	-

3.2. Toxicity Evaluation

Observations on mortality and developmental malformations of zebrafish embryos exposed to Ag NPs and TiO₂ NPs were recorded. In addition, for TiO₂ NPs exposures observations on behavioral movement (or swimming activity after light-dark challenge test) were also assessed and UV light was used to enlarge sub-lethal effects.

The results obtained using the modification of OECD test guideline 236, are given in Figure S1 of the SM. As can be deduced from this figure, implementation of this modification induced no statistically significant differences in toxicity between the original and the modified testing strategy ($p > 0.05$).

3.2.1. Lethal and Sub-Lethal Effects of Ag NPs and TiO₂ NPs

In Figure 2, the dose-response curves of Ag NPs and TiO₂ NPs after five days of exposure (six days post fertilization; dpf) are displayed (lethality and malformations). The dose was calculated using actual total concentrations of suspensions of NPs at time 0 (T 0). Ag ions (Figure 2a,b), as tested using the AgNO₃ solution, induced the highest toxicity with up to a factor of 50 higher toxicity in comparison to any of the Ag NPs suspensions tested. Ag nanospheres and elongated Ag nanorods displayed almost similar toxicity and spherically shaped Ag NPs were found to be the least toxic of all Ag NPs tested. Interestingly, when examining mortality (Figure 2a), Ag nanoplates were more toxic than elongated Ag nanorods. However, the nanospheres and elongated nanorods induced sub-lethal effects in up to 90% and 50% of the organisms, respectively, whereas the nanoplates and AgNO₃ induced lower amounts of sub-lethal effects with 29% and 20% malformations, respectively (Figure 2b).

All LC₅₀ and EC₅₀ values were calculated based on the actual average Ag NP_{total} and TiO₂ NP_{total} concentrations as measured at 0 h and after 24 h (Table S3, SM). In case of effects in between 20 and 50%, LC₅₀ and EC₅₀ values were predicted by extrapolation of the dose response curve. Since the effects observed for TiO₂ NP bipyramids and nanospheres (data not shown) remained below 20% at all concentrations tested (Figure 2), full dose-response curves could not be assessed.

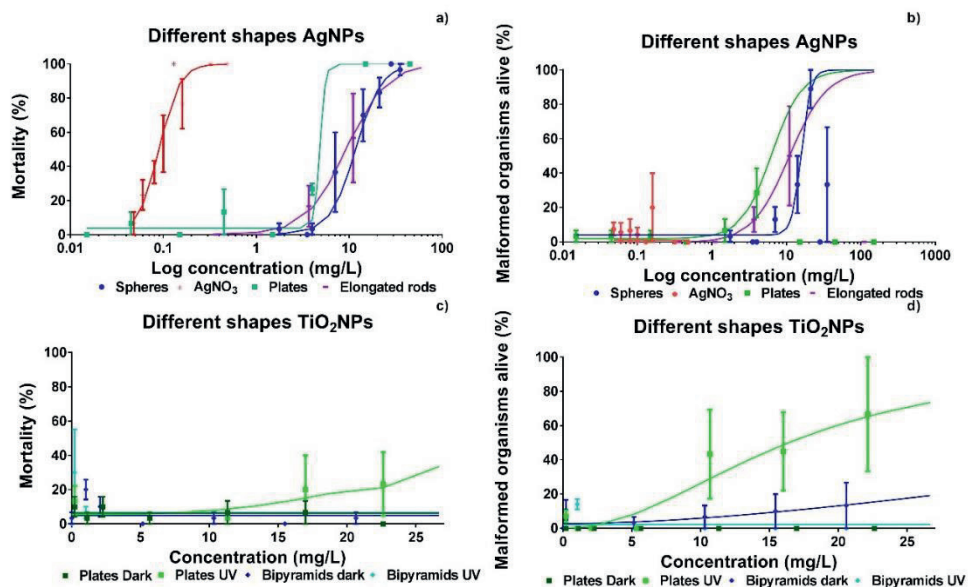


Figure 2. Dose-response curves for Ag NPs (a,b) and TiO₂ NP (c,d) based on mortality and on number of malformed organisms. The dose is expressed as the log-transformed actual total concentration at T₀. Response data relate to 6 dpf embryos after days of exposure and are presented as means of three independent replicates \pm standard error of the mean (SEM).

3.2.2. Behavioral Assessment of TiO₂ NPs

The results of the behavioral test using light-dark stress are displayed in Figure S2 (SM). In the behavioral test the total distance moved in mm is being used as a more sensitive sub-lethal endpoint compared to malformations. The results for embryos exposed to different concentrations of TiO₂ NPs revealed lack of significant impact ($p > 0.05$ for all comparisons) of any of the TiO₂ NPs tested.

3.2.3. Relative Contribution to Toxicity of the Ag NP Particles and Ag Ions

In Table 2 the relative contribution to toxicity of the ions versus the particles is shown at the experimental LC₅₀ levels of the suspensions tested. According to Table 2, most of the toxicity is induced by the particles, except for the Ag nanospheres. The EC₅₀ levels are in the same range as the LC₅₀ levels (Tables S4 and S5), which is related to the shape of the dose-effect curves. For AgNO₃, only lethality was found. Hence, no EC₅₀ value could be determined for Ag ions. Therefore, quantification of the relative contribution of Ag NPs for morphological responses is not possible.

Table 2. Relative contribution (%) of Ag NP_{ion} and Ag NP_{particle} to toxicity at the LC₅₀ (lethality) level. LC₅₀ concentrations are presented as median concentration (95% confidence interval) and n = 3.

Particles	Median Concentration (mg Ag/L)	Relative Contribution to Toxicity (%)	
		NP _{ion}	NP _{particle}
LC ₅₀			
Ag ions	0.09 (0.08–0.10)	100	0
Nanospheres	11.7 (9.9–13.6)	100	0
Nanoplates	4.9 (4.8–5.0)	9.2	90.8
Nanorods	9.2 (5.7–12.7)	3.8	96.2

3.3. Similarity Modeling to Estimate TiO₂ NP Toxicity

In order to predict the missing LC₅₀ values (i.e., the effect levels for which even at the highest dose tested, no adverse response was recorded) of TiO₂ nanospheres and nanobipyramids, similarity modeling was applied using the newly generated data and the collected secondary data. LC₅₀ values of Ag NPs, Cu NPs, Ni NPs, ZnO NPs, and, where relevant, LC₅₀ values calculated by SPSS (Version 23, IBM, Amsterdam, The Netherlands) for TiO₂ NPs were expressed as particle numbers and plotted against the different dose metrics (Figure 3). Thereupon, predicted LC₅₀ values for TiO₂ nanospheres and nanobipyramids were plotted (Figure 3, open squares, the actual values are given in Table S4, SM). Reliability of these predictions was related to the predictive strength of each model. The predictive strength of each dose metric was assessed based upon the adjusted R² values. The power of prediction decreased along the following dose-metrics: surface to volume ratio > minimal diameter > effective diameter > total surface area.

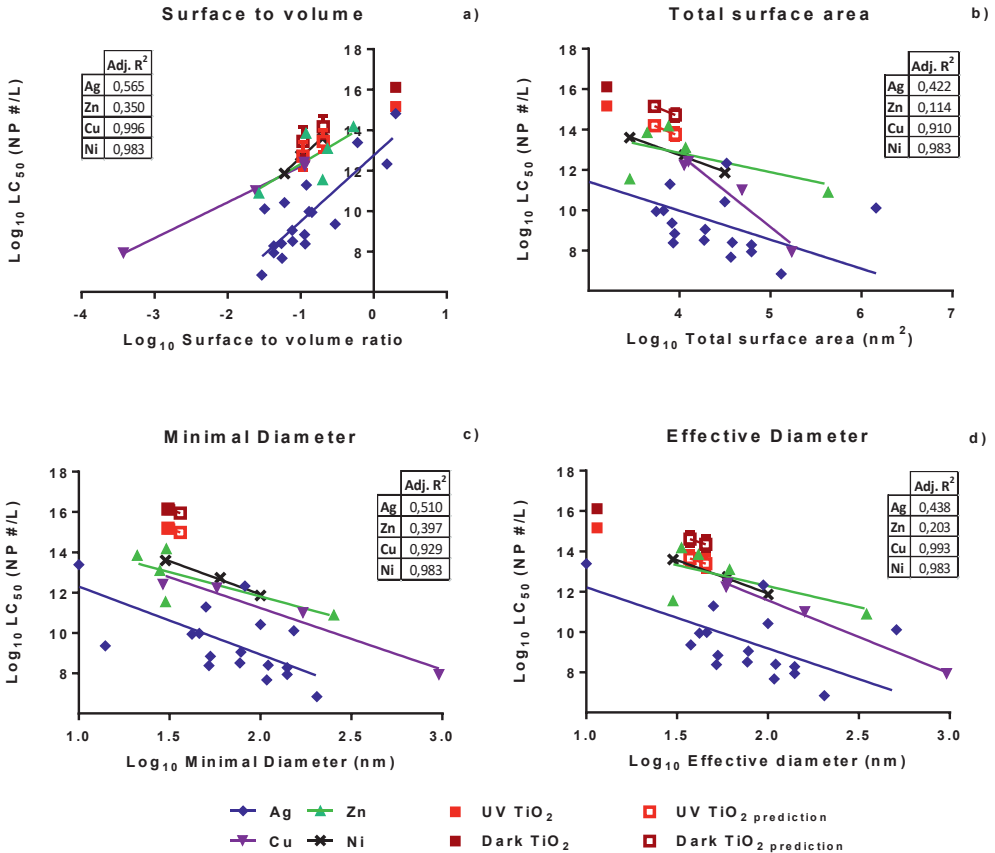


Figure 3. LC_{50} values of $NP_{particle}$ (based on actual particle number concentrations at T_0) expressed using the following dose metrics: (a) surface to volume ratio; (b) total surface area; (c) minimal diameter; and (d) effective diameter. For each line the adjusted R^2 is provided in the inserted table. Experimental LC_{50} values for TiO_2 (filled squares) were calculated using SPSS. Predicted TiO_2 values are shown by open squares with calculated standard error.

The average slopes and the corresponding p -values that are used to indicate the significance of the deviation of the slopes of Ag NPs, Cu NPs, Ni NPs, and ZnO NPs are given in Table 3. In comparison to the adjusted R^2 values, the aligning of the slopes and their variance in intercepts changed the order in which the strongest predictive power is ranked to: minimal diameter > effective diameter > surface to volume ratio > total surface area. The minimal diameter, as well as the effective diameter showed the lowest variance of the slope across the various types of particles tested and resulted in significant differences in the values of the intercept of the regression lines (Table 3). This indicates the highest level of parallelism of the regression lines when using any of these two dose metrics to express toxicity. This highest level of parallelism in combination with the highest values of the adjusted R^2 values depicted in Figure 3 was

found for the case of the minimal diameter, indicating that the minimal diameter is the best descriptor of particle toxicity of metallic NPs like Ag, Cu, Ni, and ZnO, albeit with a marginal difference with the effective diameter. The differences in intercepts reflect differences in the intrinsic toxicity of metallic nanoparticles of similar volume.

Table 3. Calculated average slope and corresponding standard deviation (SD) for effective diameter, surface to volume ratio, minimal diameter, and total surface area. For each parameter, the difference of the individual slopes of the metallic NPs is depicted by means of the *p*-value and the corresponding *F*-value in combination with the number of slopes (*n*), as well as the difference of the intercept (elevation) of the regression lines. For regression lines that are based on a maximum of five data points (see Figure 3), the significance level was set at $p < 0.01$.

Parameter	Average Slope	SD Slope	<i>n</i>	Slope		Intercept	
				<i>p</i> -Value	<i>F</i>	<i>p</i> -Value	<i>F</i>
Minimal diameter	-3.04	0.43	3	0.95	0.15	<0.0001	8.37
Effective diameter	-2.95	0.59	3	0.90	0.16	<0.0001	7.83
Surface to volume ratio	2.62	0.78	3	0.25	0.97	<0.0001	10.74
Total surface area	-1.91	1.17	3	0.49	0.73	0.0007	6.44

4. Discussion

There are at least two challenges to overcome when modifying conventional ecotoxicity assays to comply with nano-specific needs. The first challenge that we identified is the observation that, in the case of newly-synthesized nanoparticles, often only small amounts of materials are available for toxicity testing and fate assessment. The other challenge is that the dose metric to express toxicity is still under debate, which hinders the development of predictive models.

4.1. Novel Experimental Setup

Dealing with small amounts of NPs for testing implies that the required test volume is a limiting factor in testing full dose-response relationships. In recent publications, adjustments to the OECD guideline 236⁴ were proposed using a 96-well plate in order to limit the amounts of test chemicals to be used^{10,11}. Our experimental test setup described here could even reduce the total amount from 720 mL, as required within the OECD standard test, to 8 mL of exposure medium for each concentration by lowering

the total test volume, combined with the addition of a higher number of embryos in a single well, without losing accuracy. In our case, this reduced the total amount of compound needed for the whole experiment (in triplicate) from 1900 mg to 66 mg. Although the setup of Lin et al. (2011)¹¹ achieved a similar reduction, their method was not suited for nanoparticles. Nanoparticles typically tend to sediment, and frequent renewal of the medium is required in order to maintain the experimental concentration as renewal reduces the particle loss due to sedimentation. Unfortunately, medium renewal is not included in the modification proposed by Lin et al. (2011)¹¹. The quantitative deviations between the outcomes of the regular and the novel testing strategy were found to not differ significantly ($p > 0.05$; Figure S1, SM).

However, within the concentration range tested, response levels could not be determined for some of the nanoparticles (TiO₂ nanospheres and nanobipyramids). In order to allow for testing of NPs with a low intrinsic toxicity, we used three differently-shaped TiO₂ NPs, since TiO₂ NPs are classified as being moderately harmful with LC₅₀ values found to range between 10 and 100 mg/L¹²). The TiO₂ nanospheres (data not shown) and nanobipyramids showed no effects even at the highest concentration tested (Figure 2). Additional UV-irradiation of the TiO₂ NPs^{5,14} increased the effects induced by nanoplates of TiO₂, but this was not the case for the other two shapes. These two particles were not the only exception, since Faria et al. (2014)²⁵ also report extremely low toxicity of TiO₂ particles in 8 dpf larvae which were exposed under a series of illumination intensities. Thereupon, these results are in line with the findings of Bar-Ilan et al. (2009)²⁴ on acute toxicity, reporting 50% mortality after chronic exposure of zebrafish during 12 days to suspensions containing 0.1 mg/L nanospheres having a diameter of 21 nm. The observation of a lack of morphological effects at early life stages of TiO₂ NPs is supported by other authors^{26,27} who report particle-dependent effects at the gene level only. This may eventually lead to reproductive effects^{28,29}.

In line with all previous studies on this topic^{23,25-29}, our results showed that actual concentrations were significantly lower for all tested NPs compared to nominal concentrations. Especially for TiO₂ NPs, it is noteworthy to mention that the actual concentration was only 2–3% of the nominal concentration, hence, the amount of bioavailable NPs is much lower than the nominal concentration. This observation can be attributed to the agglomeration and sedimentation processes that occurred extremely rapidly during the experimental course (Table 1), as also reported by Bar-Ilan et al. (2009)²³. Sedimentation of TiO₂ NPs was reported to increase in suspensions of high ionic strength³⁰, which is the case in the exposure medium that we used for zebrafish embryo

testing (0.853 M). Overall, these observations imply that the fraction of TiO₂ NPs that is available for uptake via the water phase is extremely low. Subsequently assuming that zebrafish embryos are exposed via the water phase only, well explains the observed absence of toxicity.

4.2. Translational Modelling

4 The highest predictive power was obtained when using either the minimal or the effective diameter as a dose metric. Due to the shapes of the particles, the smallest diameter can be much smaller at a certain amount of particles per volume, compared to a spherical particle. Various studies^{18,31} report that surface to volume ratio and total surface area¹⁶ are proper dose metrics for various nanomaterials. Our results did not confirm these general findings, as surface to volume ratio was found not to be the best predictor of toxicity across NPs and as use of the total surface area actually yielded the lowest predictive power. This lack of correlation between surface area and responses was also seen by Wittmaack (2007)³². Instead, other dose metrics, including the number of particles and joint length (product of number of particles and mean size) were found to be more suited to this study³². It should be noted that our study included a variety of differently shaped NPs and, thus, offers a larger variety of surface areas for analysis, while other studies¹⁸ covered spherical NPs only.

4.3. Toxicity Prediction

Our linear regression models were found to be good predictors for the toxicity of the metallic NPs Ag, Cu, Ni, and ZnO. Therefore, these models were used to calculate the effect levels for novel metallic NPs for which no adverse responses were observed even at the highest concentrations tested. In the suspensions used for toxicity testing of zebrafish embryos, no higher actual concentrations than 20.7 mg/L TiO₂ NP for the nanobipyramids and 50.9 mg/L TiO₂ NP for the nanospheres could be obtained. Based upon the model using the minimal particle diameter, all LC₅₀ values for these TiO₂ NPs are predicted to exceed 200.6 mg/L TiO₂ NP, which is a concentration that is far above the maximum test concentration that we could achieve in the zebrafish medium employed in our study. Subsequently, these predictions nicely confirm the observed lack of effects.

The underlying reason as to why we were not able to observe any adverse effects in the case of testing of TiO₂ NPs could be related to the fact that the mechanism of toxicity of TiO₂ NPs, being stable metallic materials that do not release ions, differs from the mechanisms of toxicity of the labile metallic NPs tested in our study: Ag NPs, Cu NPs, Ni NPs, and ZnO NPs. The models developed for the labile metallic NPs are based on (acute) embryo mortality, whereas as stated previously, effects of TiO₂ NPs were reported only after long-term exposure only^{25,29}, and restricted to the effects on gene expression^{26,27} and reproduction^{28,29}, rather than morphological and lethal effects. To determine sub-lethal responses, we performed a light-dark challenge test on top of the TiO₂ NP exposure + UV illumination. As discussed above, UV illumination generally enhances the reactivity of TiO₂, hence, enlarging the potential toxicity. Moreover, the light-dark challenge test allows determining sub-lethal stress on stress responses. In our experiment, these additional assessments did not induce the responses that were observed by other researchers^{25,29}.

5. Conclusions

Fish embryo toxicity tests form an integral part of hazard identification within environmental risk assessment. To account for NP-specific issues to address in hazard testing of NPs, such as the availability of low amounts of testing material, novel experimental toxicity testing strategies are required. Our results show that modifications of the experimental setup assists in the development of testing approaches that allow applying smaller quantities of material. Toxicity was shown to be best described using the minimal particle diameter as a dose metric. A translational model could be developed on the basis of this dose metric that allows the prediction of effects for soluble metallic NPs. It is noteworthy that it is still a challenge to develop translational models for stable NPs that do not dissolve slowly. Given their low bioavailability, testing of stable NPs remains a challenge. Overall, it is to be concluded that translational modelling can assist in extrapolating the effects of non-stable metallic NPs towards effect prediction of stable NPs.

Supplementary Materials

The following materials are available online at www.mdpi.com/link; **Figure S1**. Toxicity of 50 nm Cu NPs in 24- and 96-well plates; **Figure S2**. Behavioral performance in the light-dark challenge test; **Figure S3**. Example of light-dark challenge test

recording; **Table S1.** Formulas for calculating the surface area and volume of NPs for different shapes; **Table S2.** Size, surface to volume ratio, and Zeta-potentials for each NP tested; **Table S3.** Overview of LC₅₀ and EC₅₀ values calculated for Ag NPs and TiO₂ NPs, as well as the size and surface/volume ratio of the NPs; **Table S4.** Predicted particle number values and LC₅₀ values for TiO₂ nanospheres and nanobipyramids; **Table S5.** Overview of highest measured concentration, actual 50% effect concentrations, and predicted LC₅₀ values.

Acknowledgments

The authors would like to thank Wouter J. Veneman for his assistance during the experiments. We also thank Jos J.M. van Brussel for performing the ICP-OES (Inductive Coupled Plasma- Optical Emission Spectrometry) measurements. The staff of the ZF facility of the Cell Observatory are thanked for providing the experimental working facilities. Part of the work was performed within the framework of the EU-sponsored FP7 project “FutureNanoNeeds”, grant agreement number 604602. Martina G. Vijver, Marinda van Pomeroy, and Nadja R. Brun were funded by NWO-VIDI 864.13.010, granted to Martina G. Vijver.

References

- (1) Werner, M.; Fecht, H.-J. *The nano-micro interface: Bridging the micro and nano worlds*, 2nd ed.; Van de Voorde, M., Ed.; Wiley-VCH Verlag GmbH: Weinheim, Germany, 2015.
- (2) Handy, R. D.; van den Brink, N.; Chappell, M.; Mühling, M.; Behra, R.; Dušinská, M.; Simpson, P.; Ahtiainen, J.; Jha, A. N.; Seiter, J.; et al. Practical considerations for conducting ecotoxicity test methods with manufactured nanomaterials: what have we learnt so far? *Ecotoxicology* 2012, 21 (4), 933–972.
- (3) Shaw, B. J.; Liddle, C. C.; Windeatt, K. M.; Handy, R. D. A critical evaluation of the fish early-life stage toxicity test for engineered nanomaterials: experimental modifications and recommendations. *Arch. Toxicol.* 2016, 90 (Published online), 1–31.
- (4) The Organisation for Economic Co-operation and Development (OECD). Test No. 236: Fish Embryo Acute Toxicity (FET) Test; Paris, France, 2013.
- (5) Zhang, G.; Yang, Z.; Lu, W.; Zhang, R.; Huang, Q.; Tian, M.; Li, L.; Liang, D.; Li, C. Influence of anchoring ligands and particle size on the colloidal stability and in vivo biodistribution of polyethylene glycol-coated gold nanoparticles in tumor-xenografted mice. *Biomaterials* 2009, 30 (10), 1928–1936.
- (6) Oberdörster, G.; Oberdörster, E.; Oberdörster, J. Nanotoxicology: an emerging discipline evolving from studies of ultrafine particles. *Environ. Health Perspect.* 2005, 113 (7), 823–839.
- (7) Rushton, E. K.; Jiang, J.; Leonard, S. S.; Eberly, S.; Castranova, V.; Biswas, P.; Elder, A.; Han, X.; Gelein, R.; Finkelstein, J.; et al. Concept of assessing nanoparticle

hazards considering nanoparticle dosimetric and chemical/biological response metrics. *J. Toxicol. Environ. Health. A* 2010, 73 (April 2015), 445–461.

(8) Gajewicz, A.; Jagiello, K.; Cronin, M. T. D.; Leszczynski, J.; Puzyn, T. Addressing a bottle neck for regulation of nanomaterials: quantitative read-across (Nano-QRA) algorithm for cases when only limited data is available. *Environ. Sci. Nano* 2017, 4 (2), 346–358.

(9) Kar, S.; Gajewicz, A.; Roy, K.; Leszczynski, J.; Puzyn, T. Extrapolating between toxicity endpoints of metal oxide nanoparticles: Predicting toxicity to *Escherichia coli* and human keratinocyte cell line (HaCaT) with Nano-QTTR. *Ecotoxicol. Environ. Saf.* 2016, 126, 238–244.

(10) Hua, J.; Vijver, M. G.; Ahmad, F.; Richardson, M. K.; Peijnenburg, W. J. G. M. Toxicity of different-sized copper nano- and submicron particles and their shed copper ions to zebrafish embryos. *Environ. Toxicol. Chem.* 2014, 33 (8), 1774–1782.

(11) Lin, S.; Zhao, Y.; Xia, T.; Meng, H.; Ji, Z.; Liu, R.; George, S.; Xiong, S.; Wang, X.; Zhang, H.; et al. High content screening in zebrafish speeds up hazard ranking of transition metal oxide nanoparticles. *ACS Nano* 2011, 5 (9), 7284–7295.

(12) Chen, G.; Vijver, M. G.; Peijnenburg, W. J. G. M. Summary and analysis of the currently existing literature data on metal-based nanoparticles published for selected aquatic organisms: Applicability for toxicity prediction by (Q)SARs. *Altern. to Lab. Anim.* 2015, 43, 221–240.

(13) Griffitt, R. J.; Lavelle, C. M.; Kane, A. S.; Denslow, N. D.; Barber, D. S. Chronic nanoparticulate silver exposure results in tissue accumulation and transcriptomic changes in zebrafish. *Aquat. Toxicol.* 2013, 130–131, 192–200.

(14) Oberdörster, G.; Maynard, A.; Donaldson, K.; Castranova, V.; Fitzpatrick, J.; Ausman, K.; Carter, J.; Karn, B.; Kreyling, W.; Lai, D.; et al. Principles for characterizing the potential human health effects from exposure to nanomaterials: elements of a screening strategy. *Part. Fibre Toxicol.* 2005, 2, 8.

(15) Hua, J.; Vijver, M. G.; Richardson, M. K.; Ahmad, F.; Peijnenburg, W. J. G. M. Particle-specific toxic effects of differently shaped zinc oxide nanoparticles to zebrafish embryos (*Danio rerio*). *Environ. Toxicol. Chem.* 2014, 33 (12), 2859–2868.

(16) Ma, H.; Diamond, S. A. Phototoxicity of TiO₂ nanoparticles to zebrafish (*Danio rerio*) is dependent on life stage. *Environ. Toxicol. Chem.* 2013, 32 (9), 2139–2143.

(17) Bliss, C. I. The toxicity of poisons applied jointly. *Ann. Appl. Biol.* 1939, 26 (June), 585–615.

(18) Oberdörster, G.; Oberdörster, E.; Oberdörster, J. Concepts of Nanoparticle Dose Metric and Response Metric. *Env. Heal. Perspect* 2007, 115 (6), 290–294.

(19) Zhu, M.; Nie, G.; Meng, H.; Xia, T. Physicochemical properties determine nanomaterial cellular uptake, transport, and fate. *Acc. Chem. Res.* 2013, 46 (3), 622–631.

(20) Delmaar, C. J. E.; Peijnenburg, W. J. G. M.; Oomen, A. G.; Chen, J.; de Jong, W. H.;

Sips, A. J. a M.; Wang, Z.; Park, M. V. D. Z. A practical approach to determine dose metrics for nanomaterials. *Environ. Toxicol. Chem.* 2015, 34 (5), 1015–1022.

(21) Verschoor, A.; Harper, S.; Delmaar, C. J. E.; Park, M. V. D. Z.; Sips, A. J. A. M.; Vijver, M. G.; Peijnenburg, W. J. G. M. Systematic selection of a dose metric for metal oxide nanoparticles. *Environ. Sci. Technol.* No. Submitted.

(22) Cunningham, S.; Brennan-Fournet, M. E.; Ledwith, D.; Byrnes, L.; Joshi, L. Effect of nanoparticle stabilization and physicochemical properties on exposure outcome: Acute toxicity of silver nanoparticle preparations in zebrafish (*Danio rerio*). *Environ. Sci. Technol.* 2013, 47 (8), 3883–3892.

(23) Bar-Ilan, O.; Albrecht, R. M.; Fako, V. E.; Furgeson, D. Y. Toxicity assessments of multisized gold and silver nanoparticles in zebrafish embryos. *Small* 2009, 5, 1897–1910.

(24) Bohnsack, J. P.; Assemi, S.; Miller, J. D.; Furgeson, D. Y. The primacy of physicochemical characterization of nanomaterials for reliable toxicity assessment: A review of the zebrafish nanotoxicology model. In *Methods in Molecular Biology, Nanotoxicity*; 2012; Vol. 926, pp 261–316.

(25) Faria, M.; Navas, J. M.; Soares, A. M. V. M.; Barata, C. Oxidative stress effects of titanium dioxide nanoparticle aggregates in zebrafish embryos. *Sci. Total Environ.* 2014, 470–471, 379–389.

(26) Yeo, M.-K.; Kim, H.-E. Gene expression in zebrafish embryos following exposure to TiO₂ nanoparticles. *Mol. Cell. Toxicol.* 2010, 6 (1), 97–104.

(27) Park, H.-G.; Yeo, M.-K. Comparison of gene expression changes induced by exposure to Ag, Cu-TiO₂, and TiO₂ nanoparticles in zebrafish embryos. *Mol. Cell. Toxicol.* 2013, 9 (2), 129–139.

(28) Ramsden, C. S.; Henry, T. B.; Handy, R. D. Sub-lethal effects of titanium dioxide nanoparticles on the physiology and reproduction of zebrafish. *Aquat. Toxicol.* 2013, 126, 404–413.

(29) Wang, J.; Zhu, X.; Zhang, X.; Zhao, Z.; Liu, H.; George, R.; Wilson-Rawls, J.; Chang, Y.; Chen, Y. Disruption of zebrafish (*Danio rerio*) reproduction upon chronic exposure to TiO₂ nanoparticles. *Chemosphere* 2011, 83 (4), 461–467.

(30) Keller, A. A.; Wang, H.; Zhou, D.; Lenihan, H. S.; Cherr, G.; Cardinale, B. J.; Miller, R.; Ji, Z. Stability and aggregation of metal oxide nanoparticles in natural aqueous matrices. *Environ. Sci. Technol.* 2010, 44 (6), 1962–1967.

(31) Bar-Ilan, O.; Chuang, C. C.; Schwahn, D. J.; Yang, S.; Joshi, S.; Pedersen, J. A.; Hamers, R. J.; Peterson, R. E.; Heideman, W. TiO₂ nanoparticle exposure and illumination during zebrafish development: mortality at parts per billion concentrations. *Environ. Sci. Technol.* 2013, 47 (9), 4726–4733.

(32) Wittmaack, K. In search of the most relevant parameter for quantifying lung inflammatory response to nanoparticle exposure: Particle number, surface area, or what? *Environ. Health Perspect.* 2007, 115 (2), 187–194.



Fluorescence image of ZF embryos exposed to 25nm green fluorescent polystyrene NPs

Chapter 5

The impacts of interactions between TiO₂ nanoparticles and differently dissolving nanoparticles on mixture toxicity

5

M. van Pomeran¹, W.J.G.M. Peijnenburg^{1,2}, M.G. Vijver¹.

¹ Institute of Environmental Sciences (CML), Leiden University, 2300 RA, Leiden, The Netherlands,

² National Institute of Public Health and the Environment, Center for the Safety of Substances and Products, 3720 BA, Bilthoven, The Netherlands.

In preparation

Abstract

With the increasing numbers of products on the market that contain mixtures of nanoparticles, the necessity to understand the toxicity of these mixtures becomes progressively important. With TiO₂ nanoparticles being used in various nanoparticle mixtures, it is important to gain more insight into the role of TiO₂ nanoparticles in mixture toxicity.

In this study, we aim to understand the joint effects of soluble NPs with non-reactive NPs based on the fate of the nanoparticles. By focusing on the co-agglomeration behavior and the adsorption of ions to the TiO₂ nanoparticles, we aim to distinguish the process with the highest contribution to the mixture toxicity.

In our experimental study, co-aggregation as well as adsorption of free ions to TiO₂ nanoparticles occurred to a limited extent. Moreover, the adsorption capacity of TiO₂ nanoparticles was found to be limited, indicating that the concentration, as typically used in toxicity tests, of TiO₂ nanoparticles in the mixtures was not sufficient to induce visible effects on mixture toxicity other than additivity. Thus, it is still unclear what the joint impact is that TiO₂ NPs have on soluble and non-reactive nanoparticles, as there is still a need to confirm or reject multiple hypotheses concerning the importance of co-agglomeration and adsorption of ions to TiO₂ nanoparticles.

1. Introduction

With the increase of nanotechnology, the use of nanomaterials in products has increased as well. Whereas at first only nanomaterials consisting of one type of nanoparticles (NPs) were used, current products commonly contain mixtures of NPs. For example, titanium dioxide nanoparticles (TiO_2 NPs; exhibiting photocatalytic properties under ultraviolet light) are often combined with silver NPs (Ag NPs) in order to enhance the antimicrobial effect of the Ag NPs¹. Another example are sunscreens: both TiO_2 NPs and zinc oxide (ZnO) NPs are effective ultraviolet light (UV) blockers that do not penetrate the skin², yet these NPs together show enhanced UV blocking capacity³. With the use or disposal of products containing mixtures of NPs, the mixtures will eventually be released into the environment. With TiO_2 NPs being used in a large variety of mixtures, it is important to gain more insight into the effects of TiO_2 NPs within the toxicity of mixtures of NPs in the environment.

Co-exposure of biota to two or more compounds may lead to either additive, antagonistic, or synergistic effects^{4,5}. For TiO_2 NPs, not only additivity in mixtures has been found, but they can also have antagonistic effects and reduce the toxicity of compounds. Being used as an oxidation agent in Waste Water Treatment Plants, it breaks down organic compounds under UV radiation⁶. Furthermore, TiO_2 NPs appear to have an antagonistic effect on the toxicity of other nanoparticles⁷. In co-exposure, TiO_2 NPs reduced the toxicity of ZnO and CuO to algal cells⁷. Since TiO_2 is known to agglomerate quickly and subsequently settle efficiently⁸, this sedimentation process may cause other nanoparticles to be trapped in large aggregates typically formed after emission of TiO_2 NPs, after which the particles are no longer bioavailable to pelagic organisms. On the other hand, adsorption of ions to TiO_2 NPs may also occur, reducing the amount of free ions and therewith decreasing the effective ionic concentration.

Whether nanoparticles in the environment induce toxicity depends on many factors, such as chemical factors that influence the fate of particles, but also the presence of other NPs. The toxicity of nanoparticles is highly dependent on the fate of the particles, which in turn is influenced by numerous factors and properties, including the size, composition, surface charge, concentration and coating of the particle (Vijver et al, in press ES nano). In addition, NPs have a tendency to agglomerate at higher concentrations, which subsequently alters the bioavailable dose⁹. Nanotoxicology is complicated even further by the fact that effects are not necessarily linearly related to dose¹⁰. Besides, the presence of multiple NPs in the environment may lead to mixture interactions.

As we have seen in previous examples⁷, TiO₂ NPs are capable of influencing the fate of other NPs when co-exposed. In this study, we aimed to understand the influence of TiO₂ NPs on the toxicity of other NPs, considering their influence on the fate of the other NPs. Building upon the knowledge obtained in previous work¹¹, where TiO₂ reduced the toxicity of ZnO to zebrafish embryos, we ask the question whether the toxicity reducing capacity of TiO₂ NPs can be ascribed by enhancement of the aggregation/agglomeration and subsequent sedimentation of the co-exposed NPs or whether this capacity can be ascribed to reduction of the ion concentrations in suspension due to ion sorption to TiO₂ NPs. To unravel these hypotheses, we exposed zebrafish embryos to mixtures of TiO₂ NPs and a chemically inert NP (represented by polystyrene particles) as well as to TiO₂ NPs and a slowly dissolving NP (represented by silver particles).

Secondly, we aim to focus on the dissolution behavior of the non-stable ZnO particles. The question we asked is whether the toxicity-reducing capacity of TiO₂ NPs is stronger when the dissolution of the non-stable particle is higher. It can be hypothesized that if the most dominant way of reducing toxicity is via the reduction of the concentration of free ions in suspension, the overall reduction in toxicity is higher when there are more free ions to be removed from the exposure medium. For this question, we manipulated the dissolution and aggregation/agglomeration behavior of zinc nanoparticles by adding a coating (hydrophobic and hydrophilic) to the particles.

2. Materials and Methods

2.1 Preparation of particle suspensions

Elongated Ag rods with a nominal size of 50 nm × 0.6-12 μm suspended in H₂O were purchased from Fraunhofer ISC (Würzburg, Germany). Spherical TiO₂ NPs with a nominal size of 20 nm and ZnO nanosticks with a nominal size of 43 nm were obtained as powder from Io-Li-Tec nanomaterials (Heilbronn, Germany). Hydrophobic ZnO NPs were obtained in powder from the JRC repository (JRC NM01101a). Fluorescent polystyrene nanoparticles (PS NPs), internally dyed with Firefli™ Fluorescent Green (468/508nm), of size 25 nm suspended in H₂O were purchased from ThermoFisher Scientific (Catalog number R25; Waltham, USA).

Exposure suspensions were prepared either by adding the purchased stock suspensions to egg water (60 μg/ml Instant Ocean Sea Salt, Sera GmbH, Heinsberg,

Germany) or by weighing dry powdered TiO₂ or ZnO particles into egg water. Thereafter, stock suspensions were diluted to obtain the desired concentrations. Zn²⁺ solutions were obtained by adding zinc nitrate (Sigma Aldrich, Zwijndrecht, The Netherlands) to egg water. The hydrophilic ZnO NPs were obtained by preparing a stock suspension in a 10 mg/L PVP (polyvinylpyrrolidone) solution. Immediately before exposure, the solutions were freshly prepared and sonicated for 10 min using an ultrasonic water bath (45kWh or 60W; USC200T, VWR, Amsterdam, The Netherlands).

2.2 Physicochemical characterization

Transmission electron microscopy (TEM; JEOL 1010, JEOL Ltd., Tokyo, Japan) was used directly after preparation (T0) to characterize the size and morphology of the particles in egg water. Additionally, a TEM image was obtained after 24 hours of incubation in egg water (T24). Using dynamic light scattering (DLS) assessments (Zetasizer Nano-ZS instrument; Malvern Instruments Ltd, Malvern, UK), the size distribution and zeta-potential of the particle suspensions in egg water at 0 h, 1h and 24 h were assessed.

Using atomic absorption spectroscopy (AAS; Perkin Elmer 1100B, Waltham, MA, USA), the actual total concentration of dissolved Ag ions as well as the total Ag concentration (Ag NP total) in egg water were analyzed. The same analysis was performed for the differently coated ZnO NPs. For this purpose, freshly prepared dispersions were measured at time point $t = 0$ h and after equilibration at $t = 1$ h and $t = 24$ h. The concentration of dissolved ions was obtained by sampling the supernatant after centrifugation at 5000× g for 30 min to remove the nanoparticle fraction and ultimately determine the soluble fraction in the suspension. After preparation, samples were stored in 1M HCl (CAS 7647-01-0, Sigma Aldrich, Zwijndrecht, The Netherlands) in order to digest the sample for measurement.

2.3 Experimental setup

2.3.1 Zebrafish husbandry

Zebrafish were handled as described by animal welfare regulations and maintained according to standard protocols (<http://ZFIN.org>). Adult zebrafish were maintained at 25 ± 0.5 °C in a 14 h light : 10 h dark cycle. Fertilized zebrafish eggs were obtained from an AB/TL wild-type zebrafish.

2.3.2 Set up

The tested mixtures were representing combinations of nanoparticles that show a high dissolution rate compared to those that are relatively non-reactive (Table 1).

Table 1. Overview of the different mixture setups.

NP	Nominal dose (mg/L or x time dilution)	Type of stability	Dose of TiO ₂ NPs (mg/L)
PS NP	0; 25; 32,5; 40; 47,5; 55	Non-reactive: No dissolution or aggregation/agglomeration	0; 0.25; 1; 2.5; 4; 10; 40
Ag NP	0; 30x; 100x; 300x; 1000x; 3000x	Non stable: High dissolution of Ag	0; 2.5; 4; 10; 25; 40
ZnO NP uncoated	0; 2; 4; 8; 16; 32; 64	Non stable: High dissolution of Zn and aggregation/agglomeration	0; 1.5; 3; 6; 12; 24
ZnO NP hydrophilic coated	0; 2; 4; 8; 16; 32; 64	Non stable: Dissolution of Zn, limited aggregation/agglomeration	0; 1.5; 3; 6; 12; 24
ZnO NP hydrophobic coated	0; 2; 4; 8; 16; 32; 64	Hardly reactive: Low dissolution, high aggregation/agglomeration potency	0; 1.5; 3; 6; 12; 24

2.3.3 Toxicity assessment of zebrafish embryo life stages to different mixtures

2.3.2.1 Toxicity tests with free-swimming embryos

Free swimming embryo larvae (3dpf) were selected for this experiment, since this life stage has shown to be the most sensitive¹². Per group, ten zebrafish embryos were exposed in 24-well plates and an exposure regime of 48 hours was maintained (see approach as described in Van Pomerén et al., (2017)⁸). Particle suspensions and egg water were renewed every 24 hours. At the final day of the experiment, the embryos

were screened for survival and malformations. Temperature was maintained at 28 ± 0.8 °C during the experiments.

2.3.2.2 Toxicity test on the hatching success of embryos

As zinc is known to influence the hatching of zebrafish embryos¹³, we aimed to include this feature as a more sensitive sub-lethal endpoint. For that reason, we adapted the exposure period from 4 hpf till 72 hpf. The remainder of the experimental setup was comparable to the previous mentioned setup, with the addition of hatching success as an extra sub-lethal endpoint.

For all non-stable NPs, the relative contribution to toxicity of particles and ions was calculated as explained in Van Pomerén et al. (2017)⁸.

2.4 Statistical analysis

Significance ($p < 0,05$) for effects on survival, hatching success and malformations among the different treatments was tested using a one way ANOVA using the SPSS 23 software package. Results are given as mean \pm standard deviation (SD).

3. Results

3.1 Physico-chemical characterization of polystyrene, silver and titanium dioxide particles

TEM images showing the aggregation/agglomeration state of silver + TiO₂ NPs and polystyrene + TiO₂ NPs are provided in Figure 1. Over time, silver + TiO₂ NPs form intertwined clusters, with TiO₂ NPs accumulating at the tips of the elongated Ag nanorods (Figure 1, b). Remarkably, polystyrene does not form (large) aggregates/agglomerates with TiO₂ NPs, also not over time (Figure 1, c and d). This same trend is nicely visible when considering the hydrodynamic sizes of the samples (Table S1 and S2). The silver + TiO₂ NP mixture rapidly forms aggregates/agglomerates that increase in size over time (Table S1). Most of these aggregates/agglomerates settle out of the suspension, as can be deduced from the decreasing total concentrations as measured by AAS (Table S5). Yet the addition of TiO₂ NPs does only marginal affect the decrease of the total concentration of silver in suspension. In contrast, the polystyrene

+ TiO₂ NP mixture shows two individual peaks as measured by DLS: one peak representing the single polystyrene particles, and one peak representing the agglomerating TiO₂ NPs (Table S2).

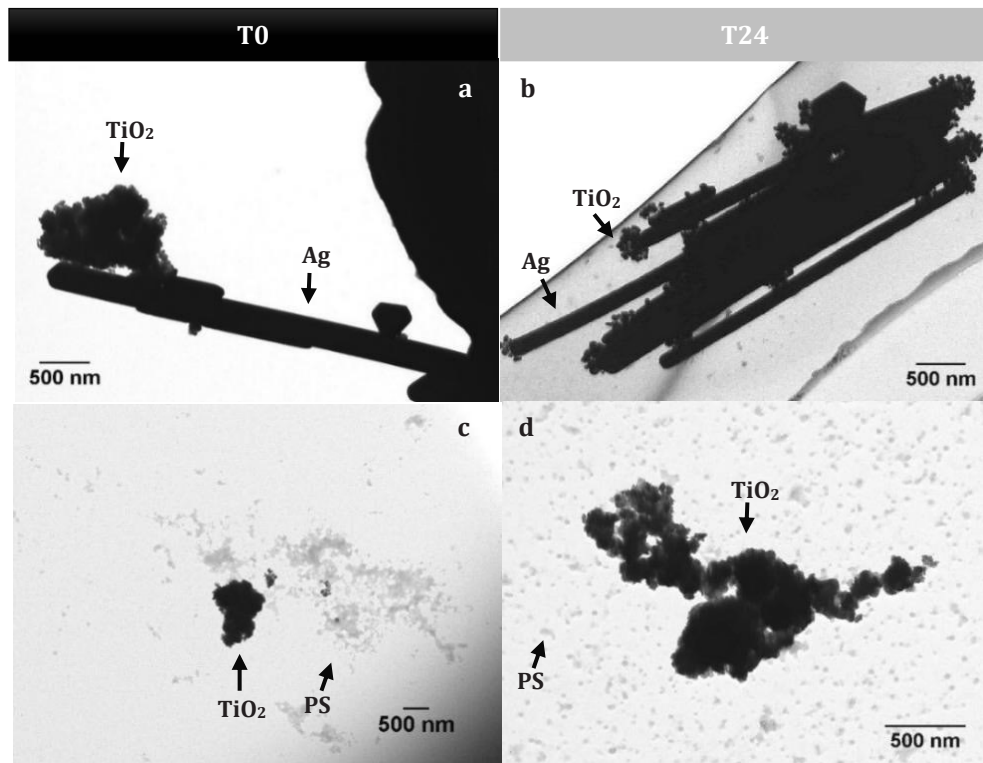


Figure 1. TEM images of Ag NPs (a, b) and PS NPs (c, d) in mixture with TiO₂ NPs, at both T0 (a, c) and T24 (b, d).

Considering the zeta potential of the mixtures (Table S3 and S4), we see indeed that the silver mixture is prone to agglomeration (zeta potential lies in between -30 and 30 mV; Table S3). In contrast, the polystyrene mixture is relatively stable, since the zeta potentials range from -25 till -35 mV (Table S4), even though the TiO₂ NPs still form aggregates/agglomerates (Table S2).

3.2 Physico-chemical characterization of differently coated zinc and titanium dioxide particles

Similar to the PS and Ag NP mixtures, Figure 2 shows TEM images of the aggregation/agglomeration state of the TiO₂ NP mixtures with differently coated ZnO NPs. All differently coated ZnO NPs form aggregates/agglomerates with TiO₂ NPs, the size of which increases over time (Figure 2). Morphologically, the aggregates/agglomerates of uncoated ZnO NPs (Figure 2, a and b) and the hydrophobic coated ZnO NPs (Figure 2, e and f) are relatively comparable. However, the hydrophilic coated particles (Figure 2, c and d) form aggregates/agglomerates with a much more open structure: there is more space around the particles. Evaluating the aggregate/agglomerate sizes obtained via the DLS measurements (Tables S6, S7 and S8) as well as the sedimentation as measured as decrease in total concentration (Table S9), it is to be concluded that only little differences are observable between the different coatings. Additionally, very little effect of the addition of TiO₂ NPs has been observed on the total concentration in suspension as well as on the amount of free ions (Table S9). When testing the sorption capability of TiO₂ NPs for Zn ions (Table S10), only minor differences were observed in the amount of free ions when TiO₂ NPs were added. This indicates that the sorption capacity is relatively low and explains why almost similar ion concentrations were observed in the different combinations of TiO₂ NPs and (coated) ZnO NPs.

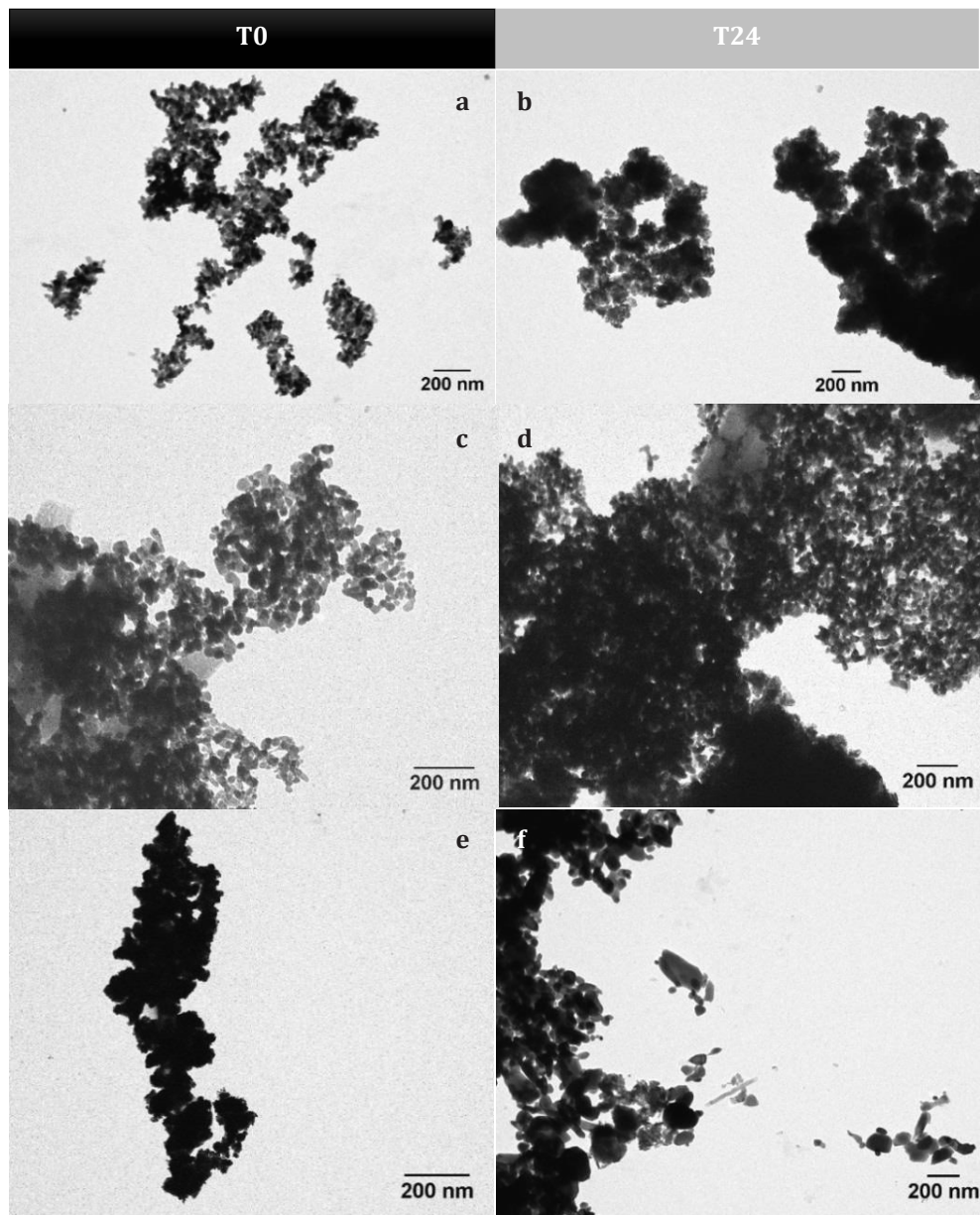


Figure 2. TEM images of ZnO nanoparticles with different coatings in mixture with TiO_2 NPs, at both T0 (a,c,e) and T24 (b,d,f). The coatings were: uncoated (a,b), hydrophylic coated (c,d) and hydrophobic coated (e,f).

3.3 Mixture toxicity of titanium dioxide with stable and non-stable particles

In Figures 3 and 4, the survival of zebrafish embryos is shown after 48h of exposure to suspensions of a mixture of TiO₂ NPs and polystyrene (Figure 3) or Ag (Figure 4) NPs. For both mixtures, the organisms were exposed from 3 dpf till 5 dpf. While both particles show a clear effect on survival of the organism, the addition of non-toxic⁸ TiO₂ NPs was found not to significantly affect the toxicity of any of the particles. When further assessing the LC₅₀ values for each treatment (Table 1 and 2), no statistically significant differences or patterns could be observed. Other endpoints such as malformations (Table S11) did not show any pattern linked to the addition of increasing concentrations of TiO₂ NPs either.

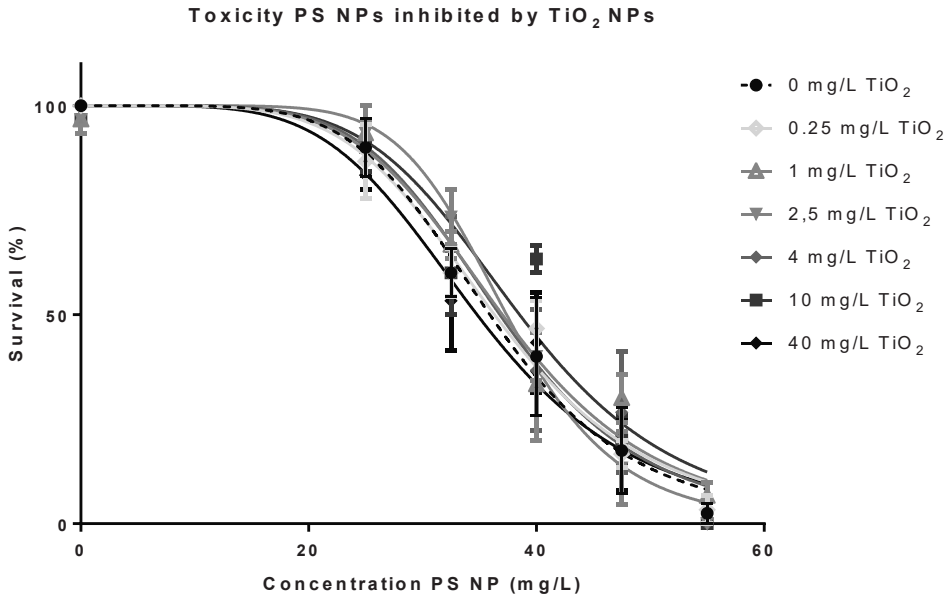


Figure 3. Survival of zebrafish embryos after exposure to PS NPs in combination with different concentrations TiO₂ NPs after exposure from 3 dpf till 5 dpf.

Table 1. *LC₅₀ values of polystyrene NPs with different concentrations TiO₂ NPs added. SE = Standard Error*

Particle	TiO ₂ (mg/L)	LC ₅₀ value (mg/L)	+ SE
Polystyrene	0	35,9	1,3
	0,25	36,3	1,0
	1	37,0	1,2
	2,5	37,4	0,8
	4	36,8	1,4
	10	38,5	1,5
	40	34,8	1,4

For the Ag NPs, we calculated the relative contribution of the ions (NP_{ion}) and the particles (NP_{particle}) to the overall toxicity observed. As can be seen in Table 2, the relative contribution did not show large differences as well, indicating that the addition of TiO₂ to the exposure medium containing either PS or Ag NPs induced only additive toxicity, although minor effects that were not observable in this test cannot be excluded.

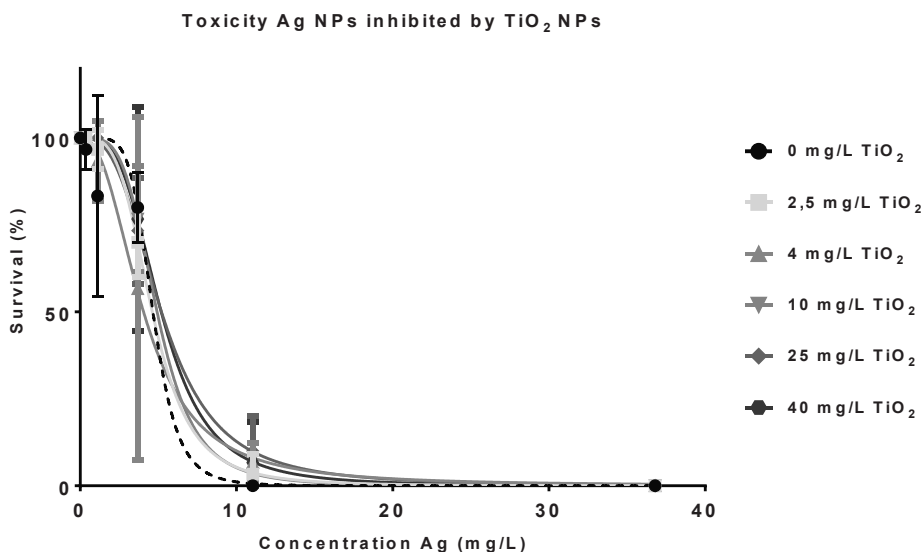
**Figure 4.** *Survival of zebrafish embryos after exposure to Ag NPs in combination with different concentrations TiO₂ NPs after exposure from 3 dpf till 5 dpf.*

Table 2. *LC₅₀ values of Ag NPs with different concentrations TiO₂ NPs added.*

Particle	TiO ₂ (mg/L)	LC ₅₀ value (mg/L)	+ SE	Relative contribution (%)	
				NP _{ion}	NP _{particle}
Silver	0	4,7	2,1	79,6	20,4
	2,5	4,6	0,2	79,6	20,4
	4	4,1	0,7	79,6	20,4
	10	4,9	0,4	79,6	20,4
	25	5,2	0,3	79,6	20,4
	40	5,2	0,7	79,6	20,4

3.4 Mixture toxicity of titanium dioxide with differently coated particles

Figure 5 shows the survival and hatching success of zebrafish embryos after 3 days of exposure to differently coated ZnO NPs. As is apparent from the graph, no full dose-response models could be drawn since the survival rate at this time point has not reached 0 % for any of the coating types and shows large variation (Figure 5). Hatching success provides a more robust endpoint.

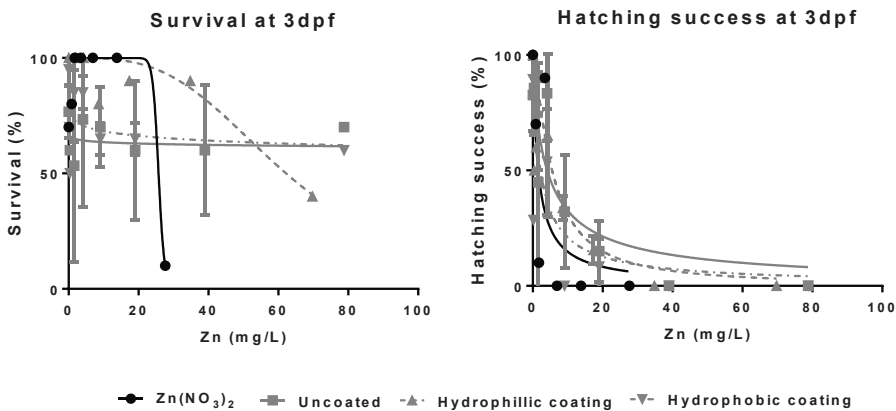


Figure 5. *Survival and Hatching success of 3 day old zebrafish embryos after exposure to differently coated ZnO NPs.*

When comparing the EC₅₀ of the different coatings, no clear difference could be observed (Table 3). Also apparent, is that the relative contribution of the ions is 100% for each of the coating types.

Table 3. EC₅₀ values of the hatching success of 3 dpf zebrafish embryos exposed to zinc ions and differently coated ZnO NPs.

Coating	EC ₅₀ value		Relative contribution (%)	
	(mg/L)	+ SE	NP ^{ion}	NP ^{particle}
Zn ²⁺	1,6	1,3	100	-
Uncoated	4,1	1,8	100,1	-0,1
Hydrophilic	7,6	0,4	100,2	-0,2
Hydrophobic	2,1	0,7	100,1	-0,1

For each different coating type, we assessed the effect of additional TiO₂ NPs in the medium. Looking at the most robust endpoint, hatching success, no clear effect could be observed (Figure 6). When we assessed the effect on the survival of the embryos, the variation in the data was found to be too large to see any pattern (Figure S1). Additionally, the relative contribution of the ions on the hatching success remained approximately 100% for each treatment (Table S12).

Hatching success at 3 dpf

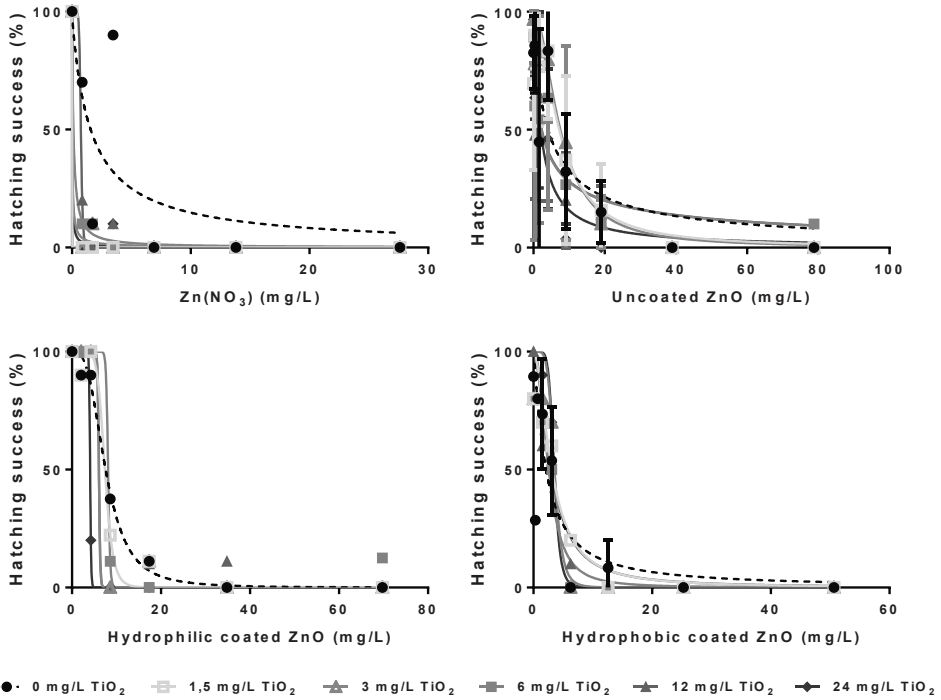


Figure 6. Hatching success of zebrafish embryos at 3 dpf after exposure to a zinc-ion control ($Zn(NO_3)_2$; a) or differently coated ZnO NPs (b,c,d) in combination with different concentrations of TiO_2 NPs.

4. Discussion

In this study, we aimed to understand the influence of TiO₂ NPs on the toxicity of other NPs, considering the influence of TiO₂ NPs on the fate of the other NPs. In order to tackle this aim, we formulated two research questions. Firstly, we asked the question whether the reducing capacity of TiO₂ NPs can be ascribed by enhancement of the aggregation/agglomeration and subsequent sedimentation of the co-exposed NPs or ascribed to reduction of the ion concentrations in suspension due to ion sorption to TiO₂ NPs. Secondly, the question we asked is whether the toxicity-reducing capacity of TiO₂ NPs is related to the dissolution behavior of non-stable particles.

5 Answering the first research question, we observed no interactive effects between PS NPs and TiO₂ NPs when assessing the fate of the particles (Table S3). The PS NPs were stable in the suspension, and no interactions with the added TiO₂ NPs were detected. The absence of interactions between the particles was also reflected in the toxicity experiments, as the toxicity of PS NPs was not affected by addition of TiO₂ NPs (Figure 3). A similar pattern was observed for the mixtures of silver NPs and TiO₂ NPs (Figure 4). Although there were indications of co-agglomeration based on TEM pictures and DLS measurements (Figure 1, Table S1), no clear effects of addition of TiO₂ NPs were observed on the total Ag concentration nor on the ion concentration in suspension (Table S5). Thus there were either no interactions (PS NPs mixtures) or the interactive effects were too small to be detected in our experimental design (as is the case for the Ag NPs mixtures).

For the second research question addressed in this study, we focused on the dissolution behavior of NPs and the subsequent effect on toxicity of mixtures of TiO₂ and ZnO NPs. By adding a hydrophobic or hydrophilic coating to the particles, we aimed to influence the dissolution behavior of the particles. Although the dissolution rate differed slightly after 1 hour of incubation, the total concentration and the percentage of ions in the suspension were similar at T24 (Table S9) in all mixtures. Due to the high dissolution rate of all differently coated NPs, the ionic form of Zn dominated the toxicity (Table 3). Most probably, this also explains why there was only a minor difference observable between the toxicity of the differently coated ZnO NPs. In addition it is to be noted that contradictory data concerning the effect of adding a coating to NPs are reported in literature. Coating NPs with PVP (which was in our study used as hydrophilic coating) was shown to reduce the toxicity of both Ag and ZnO NPs^{14,15}, yet Species Sensitivity Distribution modeling showed that a PVP coating increased the toxicity of Ag NPs¹⁶. For the hydrophobic coating used in our study the same pattern

was observed: decreased¹⁷ as well as increased¹⁸ toxicity has been reported, and also no impacts on the toxicity compared to bare ZnO particles were reported¹⁹. These contradictory findings suggest that other chemical and environmental factors may play a much larger role in the effectiveness of coatings than previously thought.

As we have built our research questions upon the knowledge obtained from previous work¹¹, we wondered why we were not able to repeat the previous results. Whereas we observed high dissolution rates of the ZnO NPs, study of Hua et al (2014)¹¹ reported much lower rates of dissolution. This resulted in a relative contribution to toxicity of up to 38% for the ions, whereas we observed that toxicity was completely due to the presence of Zn²⁺-ions formed in suspension. Upon comparing the experimental design, we noticed that the embryo media used differed significantly. Whereas the previous study reported a concentration of Instant Ocean of 210 mg/L, the egg water in our study contained 60 mg/L Instant Ocean. This difference in salt concentration may probably influence the equilibrium between ZnO NPs and Zn ions, shifting the equilibrium to the particulate form upon increasing salt concentration. Since in *in vitro* experiments, the reduction of ZnO NP toxicity by TiO₂ NPs was ascribed to the reduction of the concentration of Zn ions²⁰, this shift towards the particle form may be crucial. As we have observed that TiO₂ NPs can adsorb only limited amounts of ions, the added amount of TiO₂ NPs in our experiments is probably not sufficient to observe reducing effects on the toxicity of the co-exposed NP. In contrast, the high salt concentration may saturate the TiO₂ NPs, which makes them unable to adsorb Zn²⁺-ions. This suggests that the observed reduction of toxicity in the study of Hua et al. (2014)¹¹ can be ascribed to the co-agglomeration of ZnO NPs with TiO₂ NPs. Since the observed toxicity in our experiment was fully due to the presence of Zn²⁺-ions formed in suspension, it is not possible to confirm this hypothesis.

In our study, we observed that only limited interactive effects occurred in our experimental setups, whereas we expected to observe stronger interactions. For future research, it is worthwhile to explore which environmental factors have an influence on mixture interactions. Knowing which factors are driving mixture interactions may not only give an indication at which natural locations certain interactions may occur, but may also contribute to properly understanding and modeling mixture toxicity.

In conclusion, all of our tested mixture combinations resulted in additive responses. Based on previous studies, antagonistic effects were expected, but antagonistic interactions were not visible in zebrafish embryo responses nor was the

fate of the NPs in the aquatic exposure medium modified upon addition of TiO₂ NPs. Co-agglomeration with stable PS NPs was not observed, whereas the Ag and the differently coated ZnO NPs showed some co-agglomeration. This suggests that adsorption of free ions to TiO₂ NPs has the highest contribution to the mixture impacts. Yet, given the high dissolution rates observed in our experiments, the adsorption capacity of the added TiO₂ NPs was not sufficient to diminish ion exposure. Conversely, reduction in toxicity ascribed to co-agglomeration could not be confirmed, since the observed toxicity was due to the ionic form of Zn. This means that there is still no conclusion to be drawn regarding the impact of TiO₂ NPs on the toxicity of slowly dissolving nanoparticles.

5

Acknowledgements

The authors would like to thank Julia Mars for her contribution during the experiments. The staff of the ZF facility of the Cell Observatory is thanked for providing the experimental work environment. Marinda van Pomeran and Martina G. Vijver were funded by NWO-VIDI 864.13.010 granted to Martina G. Vijver.

Supplementary Materials

Tables

S1 Hydrodynamic size distribution (nM) + standard deviation of Ag and TiO₂ NPs in eggwater

		0x diluted		100x			300x			1000x			Ag
		0 h	1 h	0 h	1 h	24 h	0 h	1 h	24 h	0 h	1 h	24 h	
0 mg/L TiO ₂	Peak 1			0,0	0,0	128,2	91,6	251,6	157,3	0,0	10,3	239,5	
				±	±	±	±	±	±	±	±	±	
	Peak 2			0,0	0,0	51,8	104,1	97,6	30,7	0,0	17,8	70,6	
						4,2	0,0	21,4	0,0	0,0	0,0	0,0	0,0
						7,4	0,0	37,0	0,0	0,0	0,0	0,0	
2,5 mg/L TiO ₂	Peak 1	289,0 ± 38,1	303,5	648,7	450,0	110,8	427,1	329,8	262,3	350,8	304,1	286,3	
			±	±	±	±	±	±	±	±	±	±	
	Peak 2		91,6	46,2	36,4	59,3	34,2	39,4	23,3	95,1	137,2	96,3	
							0,0	0,0	0,0	151,4	0,0	0,0	17,22
						0,0	0,0	0,0	262,2	0,0	0,0	29,8	
4 mg/L TiO ₂	Peak 1	470,0 ± 21,6	450,1	635,1	386,8	132,7	295,9	336,6	164,4	276,2	134,5	207,0	
			±	±	±	±	±	±	±	±	±	±	
	Peak 2		35,8	33,8	16,1	7,9	13,6	117,0	20,3	26,2	27,7	31,8	
							0,0	0,0	0,0	0,0	0,0	0,0	0,0
						0,0	0,0	0,0	0,0	0,0	0,0	0,0	
10 mg/L TiO ₂	Peak 1	467,7 ± 42,4	530,3	639,8	409,4	194,0	310,0	344,6	197,3	136,8	334,3	134,9	
			±1	±	±	±	±	±	±	±	±	±	
	Peak 2		6,1	56,3	38,4	17,4	96,3	14,0	5,9	134,4	189,1	17,1	
							0,0	0,0	0,0	0,0	0,0	0,0	0,0
						0,0	0,0	0,0	0,0	0,0	0,0	0,0	

S2 Size distribution (nM) + standard deviation of PS and TiO₂ NPs in eggwater

		10 mg/L			25 mg/L			40 mg/L			PS	
		0 h	1 h	24 h	0 h	1 h	24 h	0 h	1 h	24 h		
0 mg/L TiO ₂	Peak 1	25,9	29,7	28,8	27,0	28,5	28,3	28,0	29,3	29,7		
		±	±	±	±	±	±	±	±	±		
		0,6	0,8	0,5	0,2	1,0	0,4	0,3	0,4	0,5		
	Peak 2	0,0	3210,7	0,0	0,0	0,0	0,0	0,0	0,0	0,0	0,0	
		±	±	±	±	±	±	±	±	±	±	
		0,0	2780,9	0,0	0,0	0,0	0,0	0,0	0,0	0,0	0,0	
	Peak 3	0,0	0,0	0,0	0,0	0,0	0,0	0,0	0,0	0,0	0,0	
		±	±	±	±	±	±	±	±	±	±	
		0,0	0,0	0,0	0,0	0,0	0,0	0,0	0,0	0,0	0,0	
2,5 mg/L TiO ₂	Peak 1	338,2	94,2	27,1	19,3	22,6	26,7	23,5	23,6	27,9		
		±	±	±	±	±	±	±	±	±		
		142,7	125,7	1,2	2,3	0,4	0,7	0,4	1,6	0,7		
	Peak 2	20,5	122,0	464,8	130,9	206,8	299,4	368,7	232,7	1625,0		
		±	±	±	±	±	±	±	±	±		
		0,5	114,7	164,5	46,1	66,9	72,3	67,4	157,8	2814,8		
	Peak 3	26,5	0,0	5217,0	0,0	0,0	0,0	0,0	0,0	0,0		
		±	±	±	±	±	±	±	±	±		
		45,9	0,0	151,5	0,0	0,0	0,0	0,0	0,0	0,0		
4 mg/L TiO ₂	Peak 1	252,4	411,5	25,2	72,4	349,8	27,1	24,5	26,9	30,1		
		±	±	±	±	±	±	±	±	±		
		109,8	140,3	1,2	91,3	122,4	0,4	0,7	0,1	1,2		
	Peak 2	20,0	24,8	178,4	115,0	23,1	369,5	377,9	467,4	2094,0		
		±	±	±	±	±	±	±	±	±		
		4,6	5,4	83,8	101,4	1,1	103,9	32,4	39,6	1172,6		
	Peak 3	0,0	0,0	0,0	0,0	0,0	1795,7	0,0	3609,3	1551,0		
		±	±	±	±	±	±	±	±	±		
		0,0	0,0	0,0	0,0	0,0	3110,2	0,0	3125,8	2686,4		
10 mg/L TiO ₂	Peak 1	269,0	403,1	25,2	269,5	533,7	28,5	506,5	618,0	28,3		
		±	±	±	±	±	±	±	±	±		
		32,4	32,2	1,4	52,5	50,4	0,4	38,5	32,7	0,6		
	Peak 2	13,5	18,4	168,9	19,7	27,2	224,8	24,6	26,8	297,1		
		±	±	±	±	±	±	±	±	±		
		1,5	1,7	34,3	1,7	1,0	45,8	0,5	1,1	48,8		
	Peak 3	0,0	0,0	0,0	0,0	0,0	1799,0	0,0	1844,0	1808,3		
		±	±	±	±	±	±	±	±	±		
		0,0	0,0	0,0	0,0	0,0	3116,0	0,0	3193,9	3132,1		

S3 Zeta potential (mV) + standard error of Ag and TiO₂ NPs in eggwater

	0x			100x			300x			1000x			Ag	
	0 h	1 h	24 h	0 h	1 h	24 h	0 h	1 h	24 h	0 h	1 h	24 h	1 h	24 h
0 mg/L TiO ₂			-7,6 ± 2,9			-31,6 ± 2,0			-22,4 ± 0,7			-15,5 ± 1,1		-17,0 ± 3,0
2,5 mg/L TiO ₂	16,8 ± 0,3	8,2 ± 0,9	-27,0 ± 1,0	-25,4 ± 1,3	-20,1 ± 0,5	-18,7 ± 0,8	-18,5 ± 0,6	-19,4 ± 0,8	-19,4 ± 1,1	-18,9 ± 0,8	-20,4 ± 1,2	-22,0 ± 0,8	-19,8 ± 0,9	-22,9 ± 0,7
4 mg/L TiO ₂	19,8 ± 0,4	7,8 ± 0,4	-26,6 ± 1,5	-25 ± 0,4	-20,5 ± 1,8	-17,7 ± 1,2	-18,5 ± 0,1	-20,6 ± 0,4	-17,7 ± 1,5	-19,8 ± 0,9	-22,0 ± 0,8	-19,8 ± 0,7	-19,8 ± 0,7	-22,9 ± 0,7
10 mg/L TiO ₂	20,2 ± 1,0	12,5 ± 0,8	-26,4 ± 1,1	-26,4 ± 0,5	-22,1 ± 0,7	-17,8 ± 0,8	-20,1 ± 0,8	-20,5 ± 0,6	-18,4 ± 0,7	-19,8 ± 0,7	-22,9 ± 0,7	-19,8 ± 0,7	-19,8 ± 0,7	-22,9 ± 0,7

S4 Zeta potential (mV) + standard error of PS and TiO₂ NPs in eggwater

	10 mg/L			25 mg/L			40 mg/L			PS	
	0 h	1 h	24 h	0 h	1 h	24 h	0 h	1 h	24 h	1 h	24 h
0 mg/L TiO ₂	-21,1 ± 2,8	-22,3 ± 2,3	-24,3 ± 1,7	-26,3 ± 2,0	-27,7 ± 0,4	-24,4 ± 4,7	-29,2 ± 1,0	-31,1 ± 1,0	-30,2 ± 1,4		
2,5 mg/L TiO ₂	-25,9 ± 0,4	-25,5 ± 2,7	-25,8 ± 2,8	-30,5 ± 0,2	-29,8 ± 0,1	-30,1 ± 1,0	-32,1 ± 0,6	-32,9 ± 0,2	-30,6 ± 0,3		
4 mg/L TiO ₂	-25,3 ± 1,8	-23,6 ± 1,2	-26,2 ± 0,7	-33,3 ± 1,1	-31,4 ± 0,5	-29,6 ± 1,2	-34,4 ± 1,4	-33,3 ± 0,2	-32,3 ± 0,8		
10 mg/L TiO ₂	-30,4 ± 1,3	-27,9 ± 0,7	-27,1 ± 1,0	-33,3 ± 0,6	-31,7 ± 0,2	-31,6 ± 0,3	-34,3 ± 0,4	-35,1 ± 0,4	-33,1 ± 0,3		

S5 Actual concentrations of silver in mixtures of Ag NPs with TiO₂ NPs in eggwater

ions	0h										1h										24h									
											TiO ₂ (mg/L)																			
	0	2,5	4	10	10	0	2,5	4	10	10	0	2,5	4	10	10	0	2,5	4	10	10	0	2,5	4	10	10					
100x	0,07	0,04	0,05	0,06	0,06	0,04	0,04	0,06	0,06	0,06	0,02	0,03	0,03	0,03	0,03	0,04	0,04	0,06	0,06	0,06	0,02	0,03	0,03	0,03	0,03					
300x	0,02	0,03	0,00	0,15	0,15	0,02	0,03	0,03	0,03	0,03	0,04	0,04	0,03	0,03	0,03	0,04	0,04	0,03	0,03	0,03	0,04	0,04	0,03	0,03	0,03					
1000x	0,23	0,16	0,22	0,19	0,19	0,02	0,01	0,02	0,03	0,03	0,05	0,05	0,05	0,05	0,05	0,05	0,05	0,05	0,05	0,05	0,05	0,05	0,05	0,05	0,05					
Total	52,48	55,52	54,08	61,12	61,12	2,50	2,36	2,53	2,50	2,50	0,11	0,07	0,04	0,06	0,06	0,11	0,07	0,04	0,06	0,06	0,11	0,07	0,04	0,06	0,06					
Dilution	300x	8,35	7,65	10,85	9,85	2,01	1,93	2,07	2,05	2,05	0,15	0,11	0,05	0,05	0,05	0,15	0,11	0,05	0,05	0,05	0,15	0,11	0,05	0,05	0,05					
1000x	2,40	2,34	2,38	2,74	2,74	1,39	1,77	1,42	1,48	1,48	0,18	0,10	0,12	0,12	0,12	0,18	0,10	0,12	0,12	0,12	0,18	0,10	0,12	0,12	0,12					
% ions	100x	0,13	0,08	0,10	0,09	1,44	1,78	2,22	2,32	2,32	20,75	40,00	50,00	34,38	34,38	20,75	40,00	50,00	34,38	34,38	20,75	40,00	50,00	34,38	34,38					
300x	0,28	0,37	0,01	1,54	1,54	1,00	1,45	1,35	1,66	1,66	25,00	9,36	61,54	64,00	64,00	25,00	9,36	61,54	64,00	64,00	25,00	9,36	61,54	64,00	64,00					
1000x	9,43	4,37	9,14	6,78	6,78	1,15	0,79	1,26	1,75	1,75	27,17	48,08	42,37	40,98	40,98	27,17	48,08	42,37	40,98	40,98	27,17	48,08	42,37	40,98	40,98					

S6 Hydrodynamic size distribution (nm) and zeta potential (mV) of uncoated ZnO and TiO₂ NPs in eggwaterSize distribution (nm) + standard error of uncoated ZnO and TiO₂ NPs in eggwater

	0 mg/L ZnO				2 mg/L ZnO				32 mg/L ZnO			
	0 h	1 h	24 h	0 h	1 h	24 h	0 h	1 h	24 h	0 h	1 h	24 h
0 mg/L TiO ₂					716 ± 261	906 ± 529	467 ± 33	1463 ± 221	1006 ± 43	842 ± 196		
1,5 mg/L TiO ₂	2723 ± 498	1800 ± 335	1161 ± 418	1530 ± 237	1617 ± 282	632 ± 17	871 ± 60	2016 ± 361	1018 ± 341			
24 mg/L TiO ₂	690 ± 52	683 ± 22	263 ± 8	697 ± 17	675 ± 21	278 ± 15	2643 ± 1210	1828 ± 388	1126 ± 446			

Zeta potential (mV) + standard error of uncoated ZnO and TiO₂ NPs in eggwater

	0 mg/L ZnO				2 mg/L ZnO				32 mg/L ZnO			
	0 h	1 h	24 h	0 h	1 h	24 h	0 h	1 h	24 h	0 h	1 h	24 h
0 mg/L TiO ₂					-21 ± 8	-25 ± 3	-16 ± 1	-6 ± 2	-21 ± 1	-21 ± 0		
1,5 mg/L TiO ₂	-4 ± 4	-24 ± 1	-25 ± 1	-19 ± 0	-22 ± 3	-23 ± 1	6 ± 3	-22 ± 1	-21 ± 1			
24 mg/L TiO ₂	-15 ± 1	-19 ± 1	-25 ± 1	-14 ± 0	-19 ± 1	-23 ± 0	0 ± 1	-23 ± 1	-22 ± 0			

S7 Hydrodynamic size distribution (nm) and zeta potential (mV) of hydrophobic coated ZnO and TiO₂ NPs in eggwaterSize distribution (nm) + standard error of hydrophobic coated ZnO and TiO₂ NPs in eggwater

	0 mg/L ZnO			2 mg/L ZnO			32 mg/L ZnO		
	0 h	1 h	24 h	0 h	1 h	24 h	0 h	1 h	24 h
0 mg/L TiO ₂				2158 ± 153	1187 ± 598	911 ± 336	746 ± 54	951 ± 118	914 ± 193
1,5 mg/L TiO ₂	2723 ± 498	1800 ± 335	1161 ± 418	996 ± 232	1313 ± 187	937 ± 197	792 ± 82	747 ± 58	589 ± 80
24 mg/L TiO ₂	690 ± 52	683 ± 22	263 ± 8	797 ± 49	804 ± 83	248 ± 9	1059 ± 25	1089 ± 5	499 ± 61

Zeta potential (mV) + standard error of hydrophobic coated ZnO and TiO₂ NPs in eggwater

	0 mg/L ZnO			2 mg/L ZnO			32 mg/L ZnO		
	0 h	1 h	24 h	0 h	1 h	24 h	0 h	1 h	24 h
0 mg/L TiO ₂				-7 ± 5	-11 ± 3	-7 ± 3	-13 ± 2	-14 ± 1	-19 ± 5
1,5 mg/L TiO ₂	-4 ± 4	-24 ± 1	-25 ± 1	-10 ± 7	-26 ± 2	-9 ± 3	5 ± 2	-18 ± 0	-22 ± 4
24 mg/L TiO ₂	-15 ± 1	-19 ± 1	-25 ± 1	-17 ± 3	-22 ± 1	-24 ± 1	3 ± 2	-12 ± 0	-21 ± 1

S8 Hydrodynamic size distribution (nm) and zeta potential (mV) of hydrophilic coated ZnO NPs and TiO₂ NPs in eggwaterSize distribution (nm) + standard error of hydrophilic coated ZnO and TiO₂ NPs in eggwater

	0 mg/L ZnO			2 mg/L ZnO			32 mg/L ZnO		
	0 h	1 h	24 h	0 h	1 h	24 h	0 h	1 h	24 h
0 mg/L TiO ₂				1020 ± 380	1567 ± 1319	2544 ± 1947	2650 ± 1724	995 ± 229	1220 ± 153
1,5 mg/L TiO ₂	2723 ± 498	1800 ± 335	1161 ± 418	2226 ± 278	1534 ± 45	1985 ± 213	1660 ± 159	1264 ± 281	1176 ± 215
24 mg/L TiO ₂	690 ± 52	683 ± 22	263 ± 8	750 ± 113	816 ± 81	316 ± 13	1463 ± 164	1096 ± 165	379 ± 34

Zeta potential (mV) + standard error of hydrophilic coated ZnO and TiO₂ NPs in eggwater

	0 mg/L ZnO			2 mg/L ZnO			32 mg/L ZnO		
	0 h	1 h	24 h	0 h	1 h	24 h	0 h	1 h	24 h
0 mg/L TiO ₂				-9 ± 2	-12 ± 3	-9 ± 3	7 ± 0	-16 ± 2	-17 ± 1
1,5 mg/L TiO ₂	-4 ± 4	-24 ± 1	-25 ± 1	-17 ± 3	-26 ± 3	-4 ± 2	-2 ± 1	-18 ± 2	-20 ± 0
24 mg/L TiO ₂	-15 ± 1	-19 ± 1	-25 ± 1	-24 ± 3	-28 ± 3	-27 ± 1	-15 ± 1	-20 ± 1	-11 ± 5

S9. Actual concentrations of hydrophilic coated ZnO NPs

	Actual concentrations of hydrophilic coated ZnO NPs											
	0 h				1 h				24 h			
	0	1,5	6	24	0	1,5	6	24	0	1,5	6	24
	TiO ₂ (mg/L)											
2	0,48	0,53	0,52	0,49	0,39	0,50	0,52	0,50	0,65	0,90	0,88	0,84
8	1,25	1,29	1,15	0,92	1,39	1,43	1,41	1,18	2,17	2,32	0,61	1,67
32	1,65	1,76	1,67	1,53	2,24	2,06	1,48	1,95	3,51	3,58	2,09	2,60
ions	2	1,13	1,08	1,02	0,39	0,43	0,43	0,41	0,37	0,74	0,69	0,61
	8	4,19	4,16	4,06	1,23	1,37	1,32	1,32	1,87	1,94	1,79	1,42
	32	17,25	17,53	17,07	4,38	4,57	2,81	3,66	2,96	3,06	2,14	2,15
Total	2	42,54	48,70	51,10	48,48	114,84	119,35	120,00	177,32	121,13	127,68	137,34
	8	29,77	30,98	27,89	22,76	104,62	107,26	89,20	116,25	120,00	0,00	117,05
% ions	32	9,58	10,06	9,45	8,94	45,00	52,78	53,12	118,58	117,25	97,70	121,30

S9. Actual concentrations of hydrophobic coated ZnO NPs

	1 h										24 h																
	0 h					1 h					24 h																
	0	1,5	6	24	0	1,5	6	24	0	1,5	6	24	0	1,5	6	24											
	TiO ₂ (mg/L)																										
ions	2	1,05	1,04	0,96	0,76	1,09	1,08	1,02	0,86	1,15	1,10	1,00	0,77	8	1,79	1,83	1,71	1,68	1,57	1,76	1,92	1,90	2,93	2,72	2,67	2,37	
	32	1,92	1,90	2,06	1,95	2,38	2,46	2,77	2,84	3,70	3,78	3,99	3,56	2	1,16	1,17	1,16	1,16	1,15	1,10	1,09	1,04	1,18	1,13	1,03	0,78	
Total	8	4,41	4,33	4,35	4,34	4,09	4,09	3,96	3,64	2,94	2,81	2,60	2,46	32	18,06	18,07	17,95	18,03	16,17	15,09	15,08	13,62	3,77	3,92	4,06	3,65	
	2	90,14	88,52	82,69	65,30	94,65	98,22	92,84	82,97	97,38	97,27	97,55	99,28	8	40,63	42,39	39,23	38,71	38,36	43,15	48,41	52,31	99,52	96,52	102,69	96,02	
% ions	32	10,62	10,53	11,47	10,79	14,72	16,33	18,38	20,86	98,14	96,43	98,28	97,32														

ZnO (mg/L)

S10 Actual concentrations of Zn ions with and without TiO₂ after 1-hour incubation in eggwater

Nominal concentration Zn ions (mg/L)	TiO ₂		Difference
	0 mg/L	6 mg/L	
3	2,548	2,518	0,03
1,8	1,552	1,540	0,012
0,9	0,776	0,758	0,018
0,3	0,262	0,258	0,004
0,1	0,100	0,096	0,004

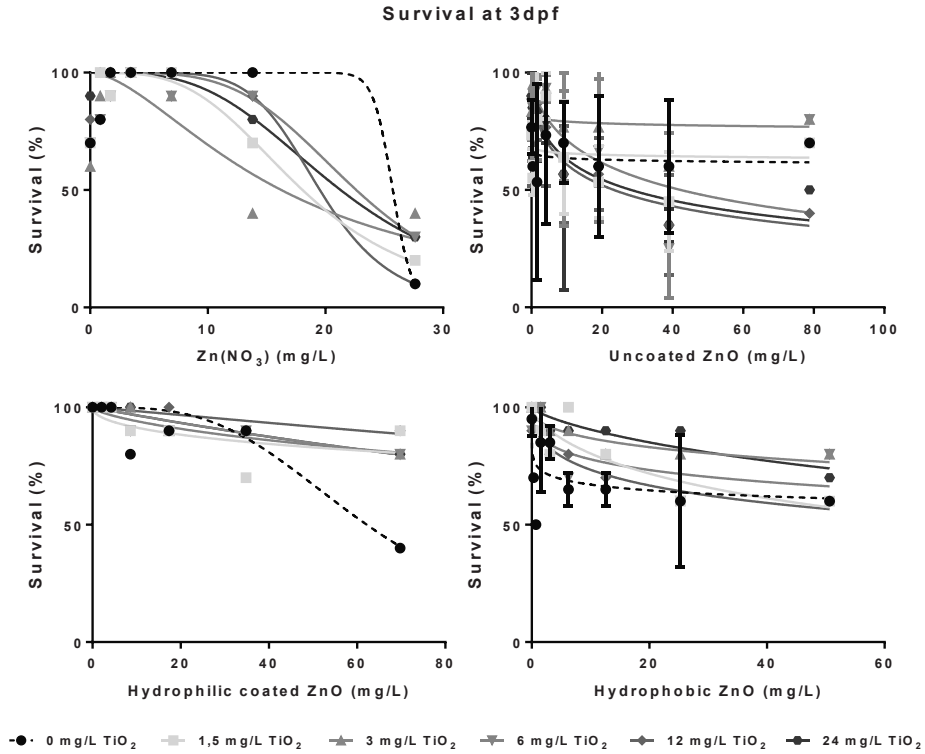
S11 EC₅₀ values of Ag NPs with different concentrations of TiO₂ NPs added

Endpoint	TiO ₂ (mg/L)	EC ₅₀ value (mg/L)	+ SE
Malformations	0	2,2	0,7
	2,5	4,6	1,3
	4	7,1	8,7
	10	3,0	0,6
	25	3,4	0,5
	40	2,7	0,4
Non-inflated swimbladder	0	0,7	0,2
	2,5	0,7	0,2
	4	0,8	0,6
	10	0,8	0,1
	25	1,0	0,1
	40	1,4	0,2

S12 EC₅₀ values of differently coated ZnO NPs with different concentrations of TiO₂ NPs added and the relative contribution of ions and particles

Coating	TiO ₂ (mg/L)	EC ₅₀ value (mg/L)	+ SD	Relative contribution (%)	
				NP ^{ion}	NP ^{particle}
Uncoated	0	4,1	1,8	100,1	-0,1
	1,5	7,2	1,9	99,8	0,2
	3	7,6	1,4	99,8	0,2
	6	2,2	1,6	100,5	-0,5
	12	2,3	1,4	100,3	-0,3
	24	2,0	0,6	100,4	-0,4
Hydrophilic	0	7,6	0,4	100,2	-0,2
	1,5	7,4	1,3	100,2	-0,2
	3	6,1	10839,0	100,2	-0,2
	6	~ 8,12	10315442	#VALUE!	#VALUE!
	12	6,1	12332,0	100,2	-0,2
	24	4,07900	0,0	100,4	-0,4
Hydrophobic	0	2,1	0,7	100,1	-0,1
	1,5	3,1	0,6	100,0	0,0
	3	3,6	0,5	100,0	0,0
	6	2,56	0,42	100,1	-0,1
	12	2,97	0,66	100,0	0,0
	24	3,5	0,5	100,0	0,0

Figure



S1 Survival of zebrafish embryos at 3 dpf after exposure to a zinc-ion control ($\text{Zn}(\text{NO}_3)_2$; a) or differently coated ZnO NPs (b,c,d) in combination with different concentrations of TiO_2 NPs.

References

- (1) Wilke, C. M.; Wunderlich, B.; Gaillard, J. F.; Gray, K. A. Synergistic bacterial stress results from exposure to nano-Ag and nano-TiO₂ mixtures under light in environmental media. *Environ. Sci. Technol.* **2018**, *52* (5), 3185–3194.
- (2) Leite-Silva, V. R.; Liu, D. C.; Sanchez, W. Y.; Studier, H.; Mohammed, Y. H.; Holmes, A.; Becker, W.; Grice, J. E.; Benson, H. A.; Roberts, M. S. Effect of flexing and massage on in vivo human skin penetration and toxicity of zinc oxide nanoparticles. *Nanomedicine* **2016**, *11* (10), 1193–1205.
- (3) Sajid, M.; Ilyas, M.; Basheer, C.; Tariq, M.; Daud, M.; Baig, N.; Shehzad, F. Impact of nanoparticles on human and environment: review of toxicity factors, exposures, control strategies, and future prospects. *Environ. Sci. Pollut. Res.* **2015**, *22* (6), 4122–4143.
- (4) Altenburger, R.; Backhaus, T.; Boedeker, W.; Faust, M.; Scholze, M. Simplifying complexity: Mixture toxicity assessment in the last 20 years. *Environ. Toxicol. Chem.* **2013**, *32* (8), 1685–1687.
- (5) Klaine, S. J.; Alvarez, P. J. J.; Batley, G. E.; Fernandes, T. F.; Handy, R. D.; Lyon, D. Y.; Mahendra, S.; McLaughlin, M. J.; Lead, J. R. Nanomaterials in the environment: behaviour, fate, bioavailability, and effects. *Environ. Toxicol. Chem.* **2008**, *27* (9), 1825.
- (6) Chong, M. N.; Jin, B.; Chow, C. W. K.; Saint, C. Recent developments in photocatalytic water treatment technology: A review. *Water Res.* **2010**, *44* (10), 2997–3027.
- (7) Ko, K.-S.; Koh, D.-C.; Kong, I. Toxicity Evaluation of Individual and Mixtures of Nanoparticles Based on Algal Chlorophyll Content and Cell Count. *Materials (Basel)*. **2018**, *11* (1), 121.
- (8) van Pomeran, M.; Peijnenburg, W.; Brun, N.; Vijver, M. A novel experimental and modelling strategy for nanoparticle toxicity testing enabling the use of small quantities. *Int. J. Environ. Res. Public Health* **2017**, *14* (11), 1348.
- (9) Suttiponparnit, K.; Jiang, J.; Sahu, M.; Suvachittanont, S.; Charinpanitkul, T.; Biswas, P. Role of Surface Area, Primary Particle Size, and Crystal Phase on Titanium Dioxide Nanoparticle Dispersion Properties. *Nanoscale Res. Lett.* **2011**, *6* (1), 1–8.
- (10) Auffan, M.; Rose, J.; Proux, O.; Borschneck, D.; Masion, A.; Chaurand, P.; Hazemann, J.-L.; Chaneac, C.; Jolivet, J.-P.; Wiesner, M. R.; et al. Enhanced Adsorption of Arsenic onto Maghemite Nanoparticles: As(III) as a Probe of the Surface Structure and Heterogeneity. *Langmuir* **2008**, *24* (7), 3215–3222.
- (11) Hua, J.; Peijnenburg, W. J. G. M.; Vijver, M. G. TiO₂ nanoparticles reduce the effects of ZnO nanoparticles and Zn ions on zebrafish embryos (*Danio rerio*). *NanoImpact* **2016**, *2*, 45–53.
- (12) van Pomeran, M.; Brun, N. R.; Peijnenburg, W. J. G. M.; Vijver, M. G. Exploring uptake and biodistribution of polystyrene (nano) particles in zebrafish embryos at different developmental stages. *Aquat. Toxicol.* **2017**, *190* (June), 40–45.

- (13) Hua, J.; Vijver, M. G.; Richardson, M. K.; Ahmad, F.; Peijnenburg, W. J. G. M. Particle-specific toxic effects of differently shaped zinc oxide nanoparticles to zebrafish embryos (*Danio rerio*). *Environ. Toxicol. Chem.* **2014**, *33* (12), 2859–2868.
- (14) Poynton, H. C.; Lazorchak, J. M.; Impellitteri, C. A.; Blalock, B. J.; Rogers, K.; Allen, H. J.; Loguinov, A.; Heckman, J. L.; Govindasmaw, S. Toxicogenomic responses of nanotoxicity in *Daphnia magna* exposed to silver nitrate and coated silver nanoparticles. *Environ. Sci. Technol.* **2012**, *46* (11), 6288–6296.
- (15) Bonfanti, P.; Moschini, E.; Saibene, M.; Bacchetta, R.; Rettighieri, L.; Calabri, L.; Colombo, A.; Mantecca, P. Do nanoparticle physico-chemical properties and developmental exposure window influence nano ZnO embryotoxicity in *Xenopus laevis*? *Int. J. Environ. Res. Public Health* **2015**, *12* (8), 8828–8848.
- (16) Chen, G.; Peijnenburg, W. J. G. M.; Xiao, Y.; Vijver, M. G. Developing species sensitivity distributions for metallic nanomaterials considering the characteristics of nanomaterials, experimental conditions, and different types of endpoints. *Food Chem. Toxicol.* **2018**, *112*, 563–570.
- (17) Bermejo-Nogales, A.; Fernández-Cruz, M. L.; Navas, J. M. Fish cell lines as a tool for the ecotoxicity assessment and ranking of engineered nanomaterials. *Regul. Toxicol. Pharmacol.* **2017**, *90*, 297–307.
- (18) Farcas, L.; Andón, F. T.; Di Cristo, L.; Rotoli, B. M.; Bussolati, O.; Bergamaschi, E.; Mech, A.; Hartmann, N. B.; Rasmussen, K.; Riego-Sintes, J.; et al. Comprehensive in vitro toxicity testing of a panel of representative oxide nanomaterials: First steps towards an intelligent testing strategy. *PLoS One* **2015**, *10* (5), 1–34.
- (19) Li, X.; Fang, X.; Ding, Y.; Li, J.; Cao, Y. Toxicity of ZnO nanoparticles (NPs) with or without hydrophobic surface coating to THP-1 macrophages: interactions with BSA or oleate-BSA. *Toxicol. Mech. Methods* **2018**, *28* (7), 520–528.
- (20) Kathawala, M. H.; Ng, K. W.; Loo, S. C. J. TiO₂ nanoparticles alleviate toxicity by reducing free Zn²⁺ ion in human primary epidermal keratinocytes exposed to ZnO nanoparticles. *J. Nanoparticle Res.* **2015**, *17* (6), 263.

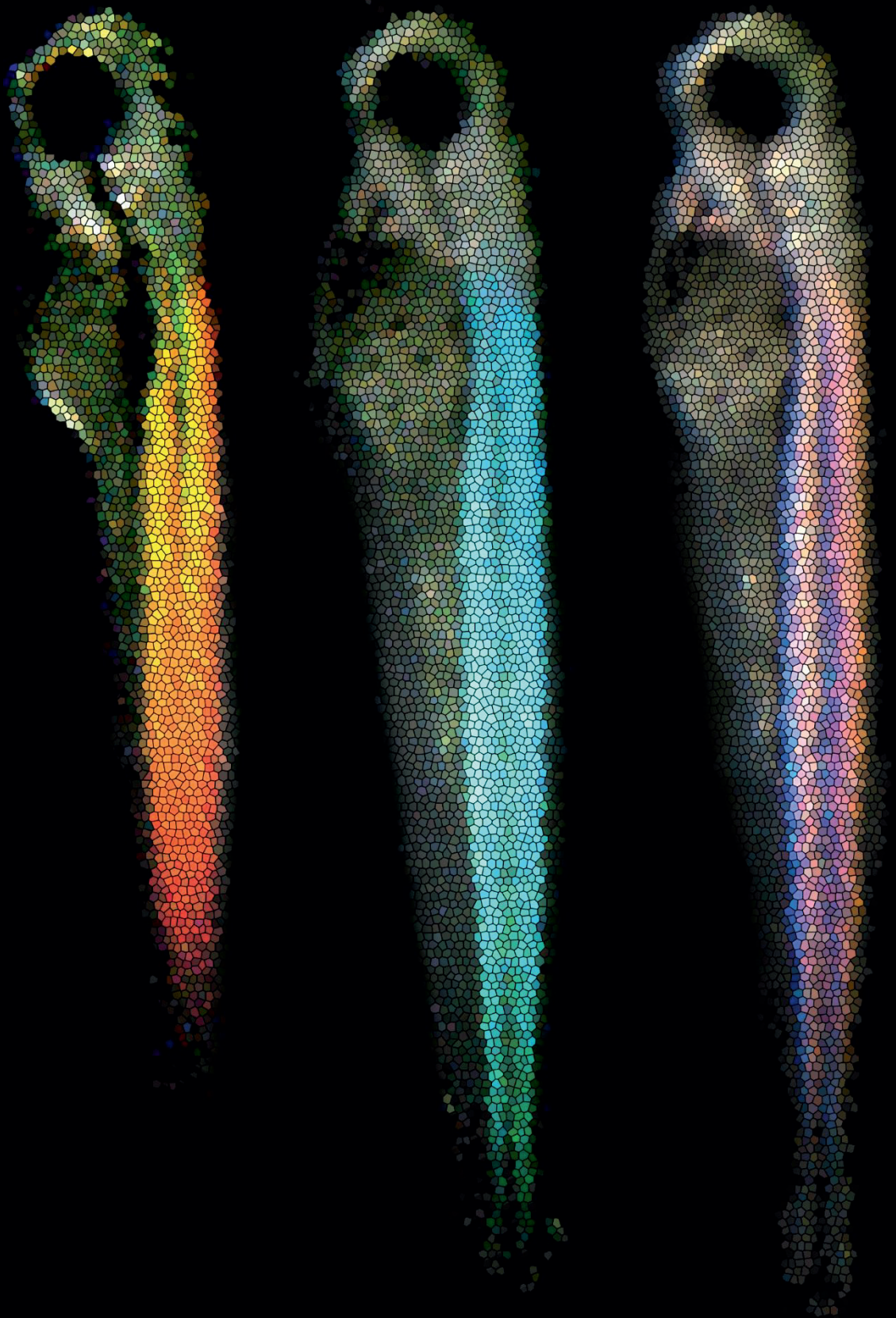


Image of control ZF embryos illuminated under different angles

Chapter 6

Discussion

Safe by design Nanoparticles

Nanomaterials have proven their advantage in both consumer products as well as in the medical world. However, our understanding of the (unwarranted and wanted) toxicity of these materials is limited. Despite the tremendous advantages that nanomaterials provide for both the manufacturing industry as well as the pharmaceutical industry, we have started to realize that we need to take care of the safety for environment and health. To fulfill this need, the idea of ‘safe by design’ nanoparticles (NPs) was introduced: building NPs that fulfil the wishes of the manufacturer/developer and that are at the same time the safest option¹. Typically, there are two strategies for ‘safe by design’ nanoparticles: reduce the hazard of the particle, or reduce the exposure to the particle by limiting the release into the environment². In this thesis, we focus on the hazard assessment of the particles. To prepare a hazard assessment, we need to figure out what particle characteristics can influence the toxicity of NPs. By providing manufacturers with detailed information on hazard, as derived from relevant parameters, they can make educated decisions. Ideally, this whole selection process for the safest NP should already occur during the Research and Development (R&D) phase. During this phase, generally only limited amounts are produced since the process is yet still small-scaled and costly. Since standardized OECD (standard Organization for Economic Co-operation and Development) tests typically require vast amounts of materials, testing during the R&D phase under the currently standardized methodologies is usually impossible. To contribute to the tackling of this hurdle, we modified the OECD ZebraFish Embryo Test (ZFET) in order to test small quantities (Figure 1; **Chapter 4**). With this, we made a first step towards more ‘safe by design’ NPs.

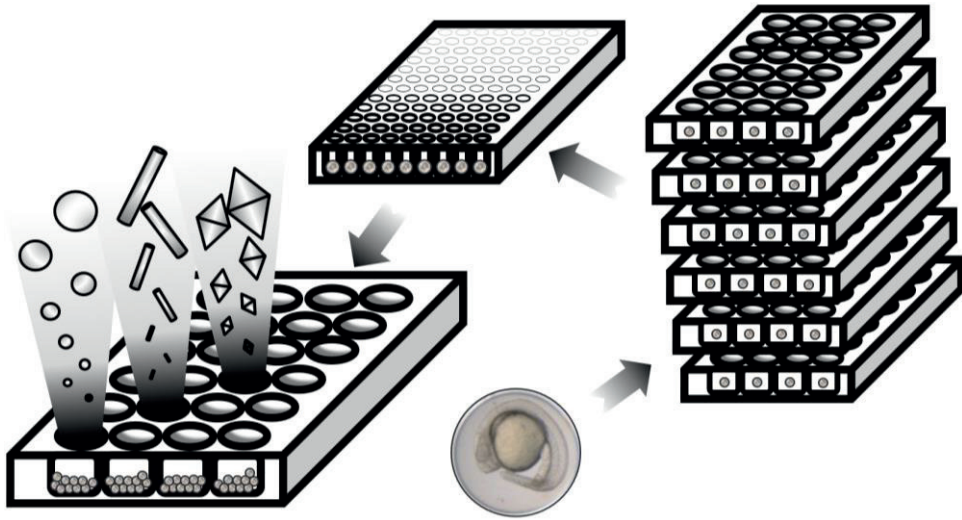


Figure 1. Schematic overview of the standard OECD Zebrafish Embryo Test (top right), the adjusted version proposed by Hua et al (2014; top left) and the method proposed in **Chapter 4** (bottom left). The OECD test demands one 24-well plate per test-concentration with one individual per well (and 40 ml per tested concentration), the method proposed in Hua et al (2014) uses sixteen wells of a 96 well plate per test-concentration (again with one individual and uses 4 ml per concentration) and our method as described in **Chapter 4** exposes one well with 10 individuals per test-concentration (and 2 ml per concentration).

The effect of single particles

In order to evaluate toxicity, the most standard way is to perform a dose-response test. By using a defined range of concentrations, the toxicity of a particular compound can for instance be addressed as a lethal or effect dose where 50% of the population responds to the exposure (LC₅₀ and EC₅₀, respectively). Knowing that NPs differ from soluble molecules, this approach might not be sufficient for all particles. It has to be borne in mind that single particles may induce more or other effects than expected from the concentration tested as compared to dissolved chemicals: if one soluble particle is capable of penetrating the organism and can shed of ions over there, toxicity is induced in a different way (different mode of action) and possibly at a lower concentration than what would have been expected from previous knowledge from the molecular-form. This indicates that NP toxicity is not always as strongly correlated with concentration as is the toxicity of dissolved chemicals³.

Nanotoxicology: a mixture of ions and particles

Although nanoparticles can be made out of a large variety of materials, a large portion of the manufactured NPs consists of metallic nanoparticles. Most of these metallic NPs (except for e.g. gold and titanium dioxide) have one feature in common: they show dissolution behavior (i.e. non-stable particles). This dissolution behavior adds another dimension to the understanding of the NP toxicity, since now the suspension does not only include particles but also ions⁴. This mixture of particles and ions makes it also important to know the toxic effects of the ions alone: by knowing the ion-toxicity, the relative contribution of both the ions and subsequently the particles can be modeled (**Chapter 4, Chapter 5**). Since the dissolution behavior differs per specific core material as well as the characteristics of the particle, it is important to measure the dissolution of the NPs in the test medium in order to address the actual particle effect rather than the ion effect.

General aims

Since we have adjusted the standard toxicity tests in order to work with small amounts of materials, we are in a position to focus on defining the most important factors determining toxicity. In this thesis, the overall aim was to get more insights in the effect of nanoparticle characteristics on the biodistribution and the subsequent toxicity in zebrafish embryos. As with any exposure, there is a difference between the nominal exposure and the effective exposure. Questions that arose were: Are the particles taken up in the organism, or do they only adsorb to the outside of the organism? And if they are taken up, where do they go to into the organism? For that reason, we investigated the effect of size (**Chapter 2**) and shape (**Chapter 3**) on the biodistribution of NPs in zebrafish embryos. On top of that, we investigated what the effect of shape is on short-term toxicity of zebrafish embryos (**Chapter 4**). In **Chapter 4**, we went even deeper into the topic of shape related toxicity. We asked ourselves the question: does the shape of particles induce a specific pattern in toxicity, irrespective of the core material? With this knowledge, we aim to predict the toxicity of a new shape, based on the information we have from other shapes. As a final step, we aimed to focus more on the interaction effects on the fate of nanoparticles in mixtures. Knowing that the dissolution behavior is important with regard to the overall toxicity of the particle suspension, we wondered what will happen when we add a stable nanoparticle to the suspension. The nanoparticles added, may interact with the dissolving particle (**Chapter 5**)?

Biodistribution and accumulation

Short-term experiments do not always give definite answers in toxicity assays (hence environmentally relevant concentrations may not induce short-term effects), but knowing where particles accumulate may give an indication of where effects will occur on the long term. Therefore, accumulation can also be classified as a sub-lethal effect. By locating where particles accumulate, so which target organs the NPs have, we can obtain a sub-lethal endpoint that gives an indication of where effects eventually may occur and what type of long-term endpoint will be affected. For this reason, a large part of this thesis focusses on the biodistribution of particles: in which organ(s) do they accumulate?

Knowing the biodistribution patterns of particles does not only give an idea about the possible long-term implications of NPs for that particular organism, but also provides a predictive tool for assessing the impacts of nanoparticles in the environment. Particle build-up in particular organs may result in effects once a threshold has been reached, or when the organ is overloaded with particles and is unable to perform its function. In order to evidence accumulation of nanomaterials, the uptake rate of the particle should be higher than the elimination rate. For that reason, it is important also to include the clearance capacity in the toxicity assessments. Unfortunately, it was not feasible within our experiments to include both an exposure period as well as a clearance period. However, the capability of organisms to clear certain particles influences the long-term toxicity of these particles. When particles are cleared within a short period of time, then the overall toxicity will be low, especially when the exposure was only for a short duration. In contrast, when the organisms cannot clear the particles, the internal concentration will continue to increase over time. Not only will the exposure concentration increase over time, causing much more toxicity after a longer period of exposure than expected, this build-up of particles will also have environmental consequences. The absence of clearance classifies the particles as persistent, causing them to transfer through the food chain and in some cases even to build-up along the food chain (biomagnification). Whereas the small (test) organisms may not perceive any toxic effects, the top predator may.

Factors influencing biodistribution and the subsequent effects

In this thesis, we focused on the two particle characteristics that are known to influence cellular uptake: size and shape^{5,6}. As we saw in **Chapter 2**, size not only influences the

uptake, but also the biodistribution of particles. Whilst 50nm particles were able to distribute to the eye, 250nm particles remained in the gut system and adsorbed to the skin. This indicates that there is a size limit in between 50 and 250nm above which the particles become too large to be taken up by cells and subsequently by the organism. If the particles have reached this size (or beyond), then the toxicity will most likely decrease significantly: toxicity can now only be induced by hindering the organism (adsorption) or by release of ions from the NPs. In addition, also the shape of the particle influences the biodistribution. In **Chapter 3**, we saw the particles flowing through the blood vessels, after which they were removed via the mononuclear phagocyte system (MPS). Although all shapes were found in the same clearance organs, the ratio in which they were found over these organs differed. This indicates that some shapes are better in evading the immune system than others, prolonging their circulation time in the organism and therewith enabling themselves to reach other organs in higher quantities.

Based on our knowledge on how size (**Chapter 2**) and shape (**Chapter 3**) influences the biodistribution of particles, we aimed to assess the importance of these characteristics for NP toxicity (**Chapter 4**). By subtracting the effects induced by the ionic form from the total observed toxicity, we obtained the effect induced by the shape of the particle. Each differently shaped particle gave a different toxicity, which we tried to explain by different parameters. The parameter that explained the shift in toxicity the best was the minimal diameter of the particle: the smallest diameter that can be found on the particle. This is in line with our earlier findings that demonstrated that size is an important driver determining the efficiency of uptake of NPs (**Chapter 2**). To illustrate this: a rod with the same volume as a spherical particle will have a smaller diameter. Therefore, the rod might penetrate the membrane of a cell easier than its equally weighted spherical counterpart might. When particles can penetrate the membrane easier, the uptake in the organism will occur faster, which will lead to a higher internal concentration and thus higher internal exposure concentration within the same period.

However, not only the minimal diameter influences the toxicity of the particles. While looking at the data generated for Ag NPs, we see that some data points (each representing another shape) deviate more from the modeled line than others do (Figure 3c, **Chapter 4**). Whereas the possibility to penetrate is mostly dictated by the minimal diameter of the particle, sharp edges of the particles may also contribute to higher penetration rates. Since it is quite difficult to express this feature in a specific (numeric)

characteristic, we were not able to add this characteristic/dose-metric to our comparison. Nevertheless, it would be interesting to group particles in categories ranging from 'very sharp' to 'blunt' and see how these groups are distributed in Figure 3c (**Chapter 4**). When the categories that lie close to 'very sharp' show the largest deviation from the model line, then this feature (as observable via TEM imaging) can be taken into account when predicting toxicity. On the other hand, particles with sharp edges might also show higher dissolution rates (which can be verified via chemical measurements). Our model is based on the particle-toxicity, so the toxicity of the material itself (induced by the released ions) is extracted. When the dissolution rate increases, the relative contribution of the particle might decrease, resulting in a lower suspension toxicity (so a higher LC_{50} value). The same might be true for other characteristics of the nanoparticles (e.g. coatings), which may influence the dissolution rate of the particles. Additionally, the shape may influence the mode of action of the particle, influencing the slope of the dose-response curve and therewith the relative contributions at different concentrations. Whereas at low concentrations the ions contribute the most to the total toxicity of the NP, at higher concentration the particle effect may have much more impact in a relative sense.

Using this knowledge on the effect of size and shape on the uptake and biodistribution of particles, we aimed to contribute to the knowledge needed to obtain 'safe by design' nanoparticles. With the knowledge that the size influences the uptake efficiency of particles (**Chapter 2**), it might be ideal to produce particles that are around 250nm and therewith limiting the amount of particles taken up in the organism. However, this may result in particles being too big for the purpose of the manufacturer. In those cases, it is recommended to use particles that are as big as possible, while remaining within the useful range of the manufacturer. The same is true for the shape of the particle. As we saw that sharp edges of particles influences their uptake (**Chapter 3**) and toxicity (**Chapter 4**), the safest choice would be for the particles to have the bluntest shape: spherical. However, sometimes the shape determines the functionality of the particle for the manufacturer. Therefore, the best option would be to opt for the bluntest shape that still provides the desired functionality. In general, based upon the knowledge we obtained, the particle most suited for the label 'safe by design' would be the largest and bluntest particle of the possible options suited for the manufacturer.

The pace of technological innovations gives increased applicability

6

In order to be able to visualize particles, they either need to be dyed/labeled, need to have optimal optical properties or need to be measured by using highly specialized equipment. Each of these requirements brings its own restrictions. For instance, the dye or label of the particle should not get detached; otherwise, it is impossible to know whether one is imaging the particles or the detached dye/label. Additionally, attaching a label to a particle may influence its behavior inside the organism, resulting in a different biodistribution pattern as compared to the bare particle. To continue, optimal optical properties are sparse among the full range of nanoparticles. This limits the amount of testable NPs significantly. In order to visualize the full range of available NPs, highly specialized equipment is needed. Unfortunately, this type of equipment is not always within reach, restricting researchers to the previous two options. Luckily, technology develops with an astonishing pace. Where we started to investigate the use of the two-photon confocal laser microscope at the beginning of this PhD project, only able to distinguish injected nanoparticles in the 3 cell-layers thick tailfin, we are able to fully visualize and track injected particles inside the whole organism (**Chapter 3**) just 3 years later. Where most technologies are currently able to visualize clusters of particles, future technologies will enable researchers to track single particles inside living organisms. Development of faster microscopes with higher resolution, such as light-sheet microscopes, will further increase our knowledge on the biodistribution of particles in living organisms. Probably within even shorter time window, methods like single-particle ICP-MS will make it possible to routinely measure very low amounts of particles in different organs, giving a quantitative image of the biodistribution. The largest benefit of all these new technologies is that we can gain more knowledge on single, non-modified particles.

Key events and AOPs

Knowledge on mode of action, or in mechanistic pathways ‘mechanisms of action’, of nanoparticles informs us on how the particles induce toxicity. In order to describe this mode of action, ‘key events’ are being formulated: measurable endpoints that are specifically linked to exposure⁷. Using these key events, Adverse Outcome Pathways (AOPs) can be built⁸. Within these AOPs, a chain of events is described that eventually results in the adverse effects observed in the organism. For instance, a disturbance at the molecular level might eventually lead to effects on the growth or survival of organisms⁹. With the knowledge obtained in this thesis on the biodistribution of

nanoparticles, building blocks were formed for further research and the eventually development of AOPs. For instance, the knowledge which size is small enough for uptake provides a first step in an AOP. This will answer the question whether there is actual internal exposure.

Although we have obtained a glimpse of what can be important for developing key events and subsequent AOPs, there is still a lot of lacking knowledge. Most of our knowledge is built upon experiments with stable particles, especially concerning biodistribution. Yet, the dissolution behavior of particles plays also an important role in their toxicity. It is key to understand which characteristics of the particles influence the dissolution behavior, and how this subsequently influences the toxicity. Looking more into the effect of coatings may be an important aspect here, as well as how multi-exposures (mixtures of different NPs) influence the particle. As seen in **chapter 5** the relationships between NPs in co-exposure are then not always easy to explain. Obtaining more information about which characteristics influences the fate of the mixture and therewith the toxicity, showed to be a relative unexplored field.

Read across from zebrafish embryos to humans

When comparing zebrafish to humans, they have proven to be a relative good non-mammalian model organism. From all the human genes, roughly 70% has an identifiable counter gene in the zebrafish model¹⁰. Not only is the zebrafish model fully sequenced and annotated, the zebrafish offers a wide repertoire of genetic, molecular and cellular manipulation tools¹¹. These tools are used to answer various biomedical and toxicological research questions, such as within research on cancer and ecotoxicology¹². Additionally, due to the high conservancy between the molecular pathways, the development and internal structure of the zebrafish and mammalian species, the zebrafish provides a strong screening model in between cell/tissue cultures and higher animal models. For these reasons, knowledge obtained and the emergence of AOPs based upon zebrafish data can be used for the read-across from zebrafish to humans. During the exposures in **Chapter 2**, we noticed that the exposure route to a high extent determines the uptake of particles. Although the uptake of single particles cannot be excluded, no clear biodistribution pattern was observed until the mouth of the embryo opened at three days old. This indicates that (at least for the particles we tested) the addition of the intestine lining exposure route results in a much higher uptake than solely via the epidermal exposure route. Moreover, since the uptake via the

skin was limited, performing solely *in vitro* studies on dermal cell cultures might underestimate the uptake efficiency/capacity of particles. Due to these underestimations, particles may appear to be safe (for dermal exposure), while their uptake occurs somewhere else. Determining the most likely location for uptake will provide a more realistic view on the hazard of exposure.

In **Chapter 3**, we concluded that the shape of the particle influenced the ratio in which the particles were distributed over three organs related to toxicant clearance. These same organs have been found to accumulate NPs in humans¹³, indicating that the same clearance processes (the MPS) are present in both zebrafish and humans. However, there are many more organs where particles can distribute to when the particles have escaped the immune system. Within cancer research, there has been a large emphasis on which particle shape is capable of evading the immune system in order to reach the highest accumulation rate of particles in tumors¹⁴. Since tumors are often tissues that demand high oxygen levels and usually contain relatively high amounts in capillary vessels, it is clear why tumors accumulate large quantities of NPs: large quantities of blood pass through this tissue over time, accelerating the accumulation of particles. However, healthy organisms in the environment do not contain tumor tissue. So the question remains: where do these particles go to when there is no tumor tissue present? And more specifically, how is the accumulation in other tissue/organs that are physiologically similar to tumor tissue (i.e. high in capillary vessels)? The brain is an organ that consumes a lot of oxygen and has therefore a high amount of capillary vessels. Obviously, it is unwarranted that NPs accumulate in our brain, where they might interfere with neurological and biological processes or even change the structure. The blood-brain barrier is effective in preventing most molecules from entering the brain. Important to know, is that molecules pass membranes via active uptake. In contrast, we do not know for sure which particles can cross the membrane barrier via passive diffusion. Particles that cross membranes via passive uptake are much more likely able to cross the blood-brain barrier. Fairly small particles can enter the brain¹⁵, but perhaps also particles with sharp edges. This relatively unexplored field may be of high interest, especially concerning long-term effects.

Long-term testing and other experimental applications

Within this thesis, we have obtained more insights in the factors that are important for the uptake and biodistribution of particles. Ideally, this type of test will substitute long-

term tests, saving a lot of time, money and expensive materials. However, in order to make short-term tests a full substitute for long-term testing, it is important to understand the uptake and depuration efficiency, as stressed before. Without this knowledge, it is unsure whether the observed accumulation over short-term will lead to long-term effects. So, besides including an analysis of the depuration efficiency in the experiment, it should be validated whether the accumulation and biodistribution of nanoparticles is a genuine predictor of long-term effects and which endpoints are the best to predict. Furthermore, imaging techniques might be also interesting for other types of experiments. By using sensitive imaging techniques, it will be possible to examine the embryos for that have been taken up (internalized particles). Currently, it is impossible to distinguish quantitatively between internalized particles and particles that adhere to the outside of the organism. The benefit of imaging techniques is that they will enable researchers to distinguish between internal and external particles.

Ultimately, building detailed AOPs on the knowledge obtained via improved biodistribution patterns will provide a more comprehensive view of the actual hazards posed by NPs. Using these AOPs, we will have a more refined knowledge of the toxic effects on both the environment and on humans.

References

- (1) Savolainen, K.; Backman, U.; Brouwer, D.; Fadeel, B.; Fernandes, T.; Kuhlbusch, T.; Landsiedel, R.; Lynch, I.; Pyllkkänen, L. *Nanosafety in Europe 2015-2025 : Towards Safe and Sustainable Nanomaterials and Nanotechnology Innovations Nanosafety in Europe Towards Safe and Sustainable Nanomaterials and Nanotechnology Innovations*; 2013.
- (2) Kraegeloh, A.; Suarez-Merino, B.; Sluijters, T.; Micheletti, C. Implementation of Safe-by-Design for Nanomaterial Development and Safe Innovation: Why We Need a Comprehensive Approach. *Nanomaterials* **2018**, *8* (4), 239.
- (3) Browning, L. M.; Lee, K. J.; Huang, T.; Nallathamby, P. D.; Lowman, J. E.; Nancy Xu, X.-H. Random walk of single gold nanoparticles in zebrafish embryos leading to stochastic toxic effects on embryonic developments. *Nanoscale* **2009**, *1* (1), 138.
- (4) Deng, H.; Zhang, Y.; Yu, H. Nanoparticles considered as mixtures for toxicological research. *J. Environ. Sci. Heal. - Part C Environ. Carcinog. Ecotoxicol. Rev.* **2018**, *36* (1), 1–20.
- (5) Dasgupta, S.; Auth, T.; Gompper, G. Shape and orientation matter for the cellular uptake of nonspherical particles. *Nano Lett.* **2014**, *14*, 687–693.
- (6) Zhu, M.; Nie, G.; Meng, H.; Xia, T. Physicochemical properties determine nanomaterial cellular uptake, transport, and fate. *Acc. Chem. Res.* **2013**, *46* (3), 622–631.

- (7) The Organisation for Economic Co-operation and Development (OECD). Users' handbook supplement to the guidance for developing and assessing AOPs. *Cartogr. Perspect.* **2014**, No. 75, 1.
- (8) Ankley, G. T.; Bennett, R. S.; Erickson, R. J.; Hoff, D. J.; Hornung, M. W.; Johnson, R. D.; Mount, D. R.; Nichols, J. W.; Russom, C. L.; Schmieder, P. K.; et al. Adverse outcome pathways: a conceptual framework to support ecotoxicology research and risk assessment. *Environ. Toxicol. Chem.* **2010**, *29* (3), 730–741.
- (9) Brun, N. R.; Peijnenburg, W. J. G. M.; van Pomeran, M.; Vijver, M. G. Implementing the current knowledge of uptake and effects of nanoparticles in an adverse outcome pathway (AOP) framework. In *Ecotoxicology - Perspectives on Key Issues*; 2018; pp 145–169.
- (10) Howe, K.; Clark, M. D.; Torroja, C. F.; Torrance, J.; Berthelot, C.; Muffato, M.; Collins, J. E.; Humphray, S.; McLaren, K.; Matthews, L.; et al. The zebrafish reference genome sequence and its relationship to the human genome. *Nature* **2013**, *496* (7446), 498–503.
- (11) Strähle, U.; Bally-Cuif, L.; Kelsh, R.; Beis, D.; Mione, M.; Panula, P.; Figueras, A.; Gothilf, Y.; Brösamle, C.; Geisler, R.; et al. EuFishBioMed (COST Action BM0804): A European network to promote the use of small fishes in biomedical research. *Zebrafish* **2012**, *9* (2), 90–93.
- (12) Veneman, W. J.; Spaink, H. P.; Brun, N. R.; Bosker, T.; Vijver, M. G. Pathway analysis of systemic transcriptome responses to injected polystyrene particles in zebra fish larvae. *Aquat. Toxicol.* **2017**, *190* (June), 112–120.
- (13) Heringa, M. B.; Peters, R. J. B.; Bleys, R. L. A. W.; van der Lee, M. K.; Tromp, P. C.; van Kesteren, P. C. E.; van Eijkeren, J. C. H.; Undas, A. K.; Oomen, A. G.; Bouwmeester, H. Detection of titanium particles in human liver and spleen and possible health implications. *Part. Fibre Toxicol.* **2018**, *15* (1), 15.
- (14) Truong, N. P.; Whittaker, M. R.; Mak, C. W.; Davis, T. P. The importance of nanoparticle shape in cancer drug delivery. *Expert Opin. Drug Deliv.* **2015**, *12* (1), 1–14.
- (15) Ramsden, C. S.; Smith, T. J.; Shaw, B. J.; Handy, R. D. Dietary exposure to titanium dioxide nanoparticles in rainbow trout, (*Oncorhynchus mykiss*): No effect on growth, but subtle biochemical disturbances in the brain. *Ecotoxicology* **2009**, *18*, 939–951.



Fluorescence overlay image of 25nm green fluorescent polystyrene nanoparticles in the intestine and gall bladder of a zebrafish embryo

Summary

Nanoparticles (NPs) can be produced in a variety of sizes and shapes. Each little detail of these characteristics may influence the toxicity of the NPs. This thesis aims to gather more information about the importance of the size and shape of a particle on its toxicity. I not only focused at standard apical endpoints like lethality and mobility, but also aimed to gain more insight in the effective exposure of embryos to NPs. By focusing on the uptake and biodistribution of NPs, it can be examined where particles end up in the organism after short-term exposure and where long-term effects may be expected to occur. As a final step, it was aimed to focus on the interactions nanoparticles experience in mixtures that are determinative of their fate. Being aware that the dissolution behavior of NPs is important with regard to the overall toxicity of the particle suspension, I wondered what would happen when a stable nanoparticle is added to different NP suspensions.

In **Chapter 2**, the aim was to investigate the effect of particle size on the uptake of the NPs, combined with an assessment of how the uptake route affects the uptake of NPs into the organism. It was found that only the small particles (≤ 50 nm) were able to penetrate the zebrafish embryos, spread through the body and eventually accumulate in specific organs and tissues such as the eyes. Particles larger than 50 nm were predominantly adsorbed onto the intestinal tract and outer epidermis of zebrafish embryos. Embryos exposed to particles via both epidermis and intestine showed the highest uptake and they eventually accumulated particles in their eyes, whereas uptake of particles via the chorion and epidermis resulted in marginal uptake.

In **Chapter 3**, the effect of particle shape on NP biodistribution was assessed. By assessing both the trafficking of the particles as well as the immune response of the embryo, it was possible to observe a shape-dependent trafficking of the particles, which resulted in a different distribution of the particles over the target organs. The differences across the distribution patterns indicate that the particles behave slightly different, although they eventually reach the same target organs – yet in different ratios. Macrophages were found to take up Au NPs from the body fluid, to be transferred into the veins and to be transported to digestive organs for clearance. The trafficking of the particles in the macrophages indicates that the particles are removed via the mononuclear phagocytic system. The different ratios in which the particles are distributed over the target organs, indicate that shape influences the behavior and eventually the toxicity of particles.

Testing nanomaterials may imply working with small amounts of materials. In order to be able to test NPs in low quantities, an adaptation to the standardized zebrafish embryo test was proposed in **Chapter 4**. Using this method, a variety of differently shaped NPs was tested. With the data generated, in combination with existing data, it was aimed to determine the best dose-metric to describe the toxicity of NPs. Subsequently, the aim was to develop translational models for dose-response predictions for those NPs that showed low responses at the highest exposure levels possible. The modeling efforts in **Chapter 4** indicated that there is indeed an influence of shape on the toxicity, irrespective of the core-material. The parameter that explained the shift in toxicity the best was the minimal diameter of the particle: the smallest diameter that can be found on the particle.

In the study discussed in **Chapter 5**, the effect of TiO₂ NPs on the fate and toxicity of other NPs was assessed. Given the common use of multiple NPs in nanomaterials, the urgency to investigate interaction effects in mixtures of NPs has increased as well. The aim of **Chapter 5** was to investigate the joint effects of quickly dissolving NPs and chemically stable NPs based on the fate of the nanoparticles. No specific interactions between the particles were found and possible fate determining processes like co-agglomeration and adsorption of free ions were found not to be affected by addition of stable NPs.

In conclusion, it can be said that the studies in this thesis have yielded a more detailed knowledge about 1. Whether NPs adsorb or are being taken up, 2. How they distribute through the body of a zebrafish and into organs 3. Which characteristics the toxicity of NPs determine and 4. How NPs can be tested properly. This information is valuable for information for predicting long-term toxicity and for modeling efforts on predicting shape-related effects. These predictions are essential for the development of 'Safe by Design' nanoparticles, in which the planet is protected by means of preventive measures.

Samenvatting

Nanodeeltjes kunnen in verschillende groottes en vormen worden gesynthetiseerd. Minuscule veranderingen in deze kenmerken kan de toxiciteit van de nanodeeltjes beïnvloeden. Dit proefschrift heeft tot doel meer informatie te verzamelen over het belang van de grootte en vorm van een deeltje op de opname en toxiciteit. Niet alleen wordt er gekeken naar standaard lethale eindpunten, maar wordt ook meer inzicht gezocht in de sub-lethale eindpunten waaronder opname en accumulatie scharen. Door te concentreren op de opname en de biodistributie van verschillende grootte en verschillende vormen van nanodeeltjes, kan een idee gekregen worden van de deeltjes die in het organisme terechtkomen na kortdurende blootstelling en waar in het lichaam verwacht kan worden dat er eventueel effecten optreden. Als laatste stap wordt meer gefocust op de effecten van interacties tussen nanodeeltjes, met nadruk op het gedrag van nanodeeltjes in mengsels. Wetende dat het oplossingsgedrag belangrijk is met betrekking tot de totale toxiciteit van een suspensie van langzaam oplossende deeltjes, was de vraag wat er gebeurt als een inert nanodeeltje aan de suspensie toevoegt wordt.

In **Hoofdstuk 2** werd het effect van de deeltjesgrootte op de opname van nanodeeltjes onderzocht waarbij expliciet de opname route meegenomen wordt. De resultaten laten zien dat alleen de kleine deeltjes (≤ 50 nm) in de zebravis embryo's konden doordringen, zich door het lichaam verspreidden en zich uiteindelijk ophoopten in specifieke organen en weefsels. Deeltjes groter dan 50 nm werden voornamelijk geadsorbeerd aan het darmkanaal en de epidermis van zebravis embryo's. Embryo's blootgesteld aan nanodeeltjes via zowel de epidermis als de darm vertoonden de hoogste opname en uiteindelijk een zichtbare accumulatie van deeltjes door het hele lichaam en zelfs in het oog. De opname van deeltjes via het chorion en de epidermis resulteerde in een marginale verhoging van de interne gehalten.

In **Hoofdstuk 3** werd de invloed van vormen op de biodistributie van deeltjes beoordeeld. Door zowel de ophoping van de deeltjes als ook de immuunrespons van het embryo te beoordelen, kon een vorm-afhankelijk interne distributie van de deeltjes worden waarnemen. Meer concreet; de deeltjes verdeelden zich vorm afhankelijk over de doelorganen, maar wel in verschillende verhoudingen. De goud nanodeeltjes werden door macrofagen uit de lichaamsvloeistof gehaald, waarna ze via de bloedbanen naar de spijsverteringsorganen getransporteerd werden, zeer waarschijnlijk gevolgd door excretie. Het transport van de deeltjes via macrofagen geeft aan dat de deeltjes worden

verwijderd via het mononucleaire fagocytische systeem. De verschillende verhoudingen waarin de deeltjes worden verdeeld over de doelorganen, geven aan dat de deeltjesvorm het gedrag en uiteindelijk de toxiciteit van de deeltjes beïnvloedt.

Het testen van nanomaterialen kan impliceren dat er met hele kleine hoeveelheden materiaal moet worden gewerkt. Om deze deeltjes ondanks de kleine hoeveelheid materiaal toch te kunnen testen, is in **Hoofdstuk 4** een aangepaste versie van de gestandaardiseerde zebavis embryo-test voorgesteld. Met deze methode is een selectie aan nanodeeltjes getest, welke in combinatie met bestaande data gebruikt is om te bepalen wat de beste dosimetrie is om de toxiciteit van de deeltjes te beschrijven. Vervolgens werd geprobeerd translatie modellen te ontwikkelen, zodat dosis-respons voorspellingen gedaan konden worden voor nanodeeltjes die zeer weinig of geen effecten lieten zien op blootstellingsniveaus die praktisch nog haalbaar zijn om te maken. Onze modelleeractiviteiten gaven aan dat er inderdaad een invloed van deeltjesvorm op de toxiciteit is, ongeacht het kernmateriaal. De parameter die de toxiciteit het beste beschreef, was de minimale diameter van het deeltje.

Met het toenemend gebruik van meerdere nanodeeltjes in nanomaterialen is de urgentie om interactie-effecten in mengsels te onderzoeken toegenomen. De doelstelling in **Hoofdstuk 5** was om de gezamenlijke effecten van snel oplosbare nanodeeltjes met niet-reactieve nanodeeltjes te begrijpen op basis van het gedrag van de nanodeeltjes. De resultaten toonden aan dat er geen sterke interactie-effecten waren met betrekking tot het gedrag van de deeltjes (bijvoorbeeld co-agglomeratie en adsorptie van vrije ionen) wanneer stabiele nanodeeltjes toegevoegd werden.

In conclusie kan gesteld worden dat de studies in deze thesis een meer gedetailleerde kennis hebben opgeleverd over 1. Of deeltjes adsorberen danwel opname hebben, 2. Hoe ze zich door het lichaam van een zebavis bewegen en in organen ze dan komen, 3. welke kenmerken de toxiciteit van nanodeeltjes bepalen en 4. Hoe die goed te testen zijn. Deze informatie is waardevol voor het voorspellen van de lange-termijn effecten. Daarbij kan het ook zeer waardevol zijn bij het ontwikkelen van modellen voor het voorspellen van vorm gerelateerde effecten. Deze voorspellingen zijn essentieel voor de ontwikkeling van 'Safe by Design' nanodeeltjes, waarbij de planeet beschermd wordt met preventieve maatregelen.

Curriculum Vitae

Marinda van Pomeran was born in Amstelveen (the Netherlands) on July 6th 1989. In 2007 she obtained her VWO diploma from Christelijke Scholengemeenschap Buitenveldert in Amsterdam. From 2007 to 2010 she did her Bachelor studies in biology at the Vrije Universiteit (VU) in Amsterdam. Her Bachelor thesis was conducted at the department of Animal Ecology (VU Amsterdam) under the supervision of Dr. A.E. van Ommen-Kloeke and Dr. ir. T.F.M. Roelofs. She studied the toxicity of the anti-herbivory metabolite 3-Phenylpropionitrile on woodlice. After finalizing her Bachelor studies in 2010, Marinda followed the Master track "Ecology" at the Vrije Universiteit (VU) in Amsterdam. During her Masters, she wrote her literature essay on the susceptibility of different life stages of invertebrates in ecotoxicology under the supervision of Dr. ir. C.A.M. van Gestel (Animal Ecology, VU Amsterdam). She did two MSc internship projects. The first project was supervised by Dr. W. Cornwell and Prof. dr. J.H.C. Cornelissen (Systems Ecology; VU Amsterdam) where she investigated mixture effects on the flammability of plant litter. The second project was supervised by Dr. T. de Boer and Prof. dr. ir. J. Legler (Amsterdam Sustainability Institute; VU Amsterdam) and was focused on the effects of zinc on the survival and genetic responses of *Daphnia pulex*. After graduation, Marinda worked as a junior researcher at the Institute of Environmental Studies (IVM, VU Amsterdam), focusing on the effects of brominated flame-retardant on the development and survival of zebrafish embryos. In 2014, she joined the Institute of Environmental Sciences (CML, Leiden University) as a PhD-student. Her PhD-project lasted from 2014-2018, in which she focused on the impact of the size and shape of nanoparticles on their uptake, biodistribution and toxicity. Her promotors were Prof. dr. ir. M.G. Vijver and Prof. dr. W.J.G.M. Peijnenburg.

Publication list

van Pomeran, M., Peijnenburg, W. J. G. M and Vijver, M. G. 'The impacts of interactions between TiO₂ nanoparticles and differently dissolving nanoparticles on mixture toxicity.' *In preparation*

van Pomeran, M., Peijnenburg, W. J. G. M., Vlieg, R. C., van Noort, S. J. T. and Vijver, M. G. 'The biodistribution and immuno-responses of differently shaped non-modified gold particles in zebrafish embryos.' *Nanotoxicology*.

doi: 10.1080/17435390.2018.1564079

Brun, N. R., Peijnenburg, W. J. G. M., **van Pomeran, M.** and Vijver, M. G. (2018) 'Implementing the current knowledge of uptake and effects of nanoparticles in an adverse outcome pathway (AOP) framework', in *Ecotoxicology - Perspectives on Key Issues*, pp. 145–169. doi: 10.1201/b21896.

van Pomeran, M., Brun, N. R., Peijnenburg, W. J. G. M. and Vijver, M. G. (2017) 'Exploring uptake and biodistribution of polystyrene (nano)particles in zebrafish embryos at different developmental stages', *Aquatic Toxicology*, 190, pp. 40–45. doi: 10.1016/j.aquatox.2017.06.017.

van Pomeran, M., Peijnenburg, W. J. G. M., Brun, N. R. and Vijver, M. G. (2017) 'A novel experimental and modelling strategy for nanoparticle toxicity testing enabling the use of small quantities', *International Journal of Environmental Research and Public Health*, 14(11), p. 1348. doi: 10.3390/ijerph14111348.

Legradi, J., **van Pomeran, M.**, Dahlberg, A.-K. and Legler, J. (2017) 'Effects of Hydroxylated Polybrominated Diphenyl Ethers in Developing Zebrafish Are Indicative of Disruption of Oxidative Phosphorylation', *International Journal of Molecular Sciences*, 18(5), p. 970. doi: 10.3390/ijms18050970.

Zhao, W., Cornwell, W. K., **van Pomeran, M.**, van Logtestijn, R. S. P. and Cornelissen, J. H. C. (2016) 'Species mixture effects on flammability across plant phylogeny: the importance of litter particle size and the special role for non- Pinus Pinaceae', *Ecology and Evolution*, 6(22), pp. 8223–8234. doi: 10.1002/ece3.2451.

Legradi, J., el Abdellaoui, N., **van Pomeran, M.** and Legler, J. (2015) 'Comparability of behavioural assays using zebrafish larvae to assess neurotoxicity', *Environmental Science and Pollution Research*, 22(21), pp. 16277–16289. doi: 10.1007/s11356-014-3805-8.

van Ommen Kloeke, A. E. E., Jager, T., van Gestel, C. A. M., Ellers, J., **van Pomeran, M.**, Krommenhoek, T., Styriehave, B., Hansen, M. and Roelofs, D. (2012) 'Time-related survival effects of two gluconasturtiin hydrolysis products on the terrestrial isopod *Porcellio scaber*', *Chemosphere*, 89(9), pp. 1084–1090. doi: 10.1016/j.chemosphere.2012.05.074.

Acknowledgements

I would like to thank my promotors for offering me the chance of this PhD position, Martina Vijver and Willie Peijnenburg. Empowered by their trust in me, I have grown on both personal and professional level. I would like to thank them for supporting me and providing the possibilities to collaborate with other interesting researcher.

I would like to thank all the researchers, without whom I would not have been able to learn all the different techniques and methods. First of all, I would like to thank Wouter Veneman for showing me around in the lab and learning me how the microscopes worked. Secondly, I thank Gerda Lamers for the instructions on the more advanced microscopes and multiple lab-techniques. I would like to stress my appreciation for my collaboration with John van Noort, Sara Carroza and Redmar Vlieg. Due to all the work Sara and Redmar had put in their two-photon laser multi-focal microscope, we were able to write a nice article together. I really appreciated my collaboration with Martin Rücklin and Bertie Joan van Heuven, spending time and effort in trying to adapt a method for my research, for which I want to thank them. Although we did not succeed to make it work, I enjoyed learning from you. Rudo Verweij, thank you for assisting during measurements. At last, I would like to thank everyone from IBI, the fish facility and Cell Observatory for working together and facilitating. Ulrike Nehrlich, thank you for taking care of the fish and allowing me to collect my eggs in the afternoon so I could run 2 experiments on one day.

Before I started my PhD, I developed my research skills via internships and a junior researcher position. I would like to thank all my supervisors for their support during my internships (Elaine van Omme-Kloeke, Dick Roelofs, Tjalf de Jager en Juliette Legler) and literature study (Kees van Gestel). I like to thank Juliette Legler for the opportunity to work as a junior researcher. I thank Jessica Legradi for the valuable lessons on how to work with zebrafish and how to perform toxicity tests during that period.

I am grateful to my committee members for assessing my PhD thesis.

I want to thank all the supporting staff of in our department: Susanne van den Oever, Jory Sjardijn, Maarten van het Zelfde, Ester Philips, Jasper Williams and Paul de Hoog. Thanks to my colleagues from CML who assisted and helped me during my thesis: Tineke Kampen, Jing Hua, Guangchao Chen, Yinlong Xiao, Yujia Zhai, Daniel Arenas Lago, Fazel Abdolapur Monikh, Henrik Barmantlo, Bregje Brinkmann, Tom Nederstigt,

Qi Yu and all others. Special thanks go to Nadja Brun, for all the scientific discussions and input. Thank you for the nice conversations, laughs and 'fruit pauses'! Thanks to Serina van Pomeran and Tineke Kampen for being my paranymphs. I also want to thank my friends for their support.

Finally, I want to express my deep gratitude to my family and partner for their unconditioned love and support. They encouraged me to follow my dreams, supported me through good and bad times, and were always there for scientific discussion.



Leiden 2019